AN ASSESSMENT OF THE DYNAMIC PROPERTIES OF ADAPAZARI SOILS BY CYCLIC DIRECT SIMPLE SHEAR TESTS

A THESIS SUBMITTED TO
THE GRADUATE SCHOOL OF NATURAL AND APPLIED SCIENCES
OF
MIDDLE EAST TECHNICAL UNIVERSITY

BY

KAVEH HASSAN ZEHTAB

IN PARTIAL FULFILLMENT OF THE REQUIREMENTS
FOR
THE DEGREE OF MASTER OF SCIENCE
IN
ENGINEERING SCIENCES

JULY 2010

Approval of the thesis:

AN ASSESSMENT OF THE DYNAMIC PROPERTIES OF ADAPAZARI SOILS BY CYCLIC DIRECT SIMPLE SHEAR TESTS

Submitted by **KAVEH HASSAN ZEHTAB** in partial fulfillment of the requirements for the degree of **Master of Science in Engineering Sciences Department, Middle East Technical University** by,

Prof. Dr. Canan Özgen _____
Dean, Graduate School of **Natural and Applied Sciences**

Prof. Dr. Turgut Tokdemir _____
Head of Department, **Engineering Sciences**

Assist. Prof. Dr. Mustafa Tolga Yılmaz _____
Supervisor, **Engineering Sciences Dept., METU**

Examining Committee Members:

Prof. Dr. Polat Gülkan _____
Civil Engineering Dept., METU

Assist. Prof. Dr. M. Tolga Yılmaz _____
Engineering Sciences Dept., METU

Prof. Dr. B. Sadık Bakır _____
Civil Engineering Dept., METU

Assoc. Prof. Dr. Kemal Beyen _____
Civil Engineering Dept., Kocaeli University

Assist. Prof. Dr. Mustafa Kutanis _____
Civil Engineering Dept., Sakarya University

Date: July 02, 2010

I hereby declare that all information in this document has been obtained and presented in accordance with academic rules and ethical conduct. I also declare that, as required by these rules and conduct, I have fully cited and referenced all material and results that are not original to this work.

Name, Last name: Kaveh Hassan Zehtab

Signature:

ABSTRACT

AN ASSESSMENT OF THE DYNAMIC PROPERTIES OF ADAPAZARI SOILS BY CYCLIC DIRECT SIMPLE SHEAR TESTS

Hassan Zehtab, Kaveh

M.Sc., Department of Engineering Sciences

Supervisor: Assist. Prof. Dr. Mustafa Tolga Yılmaz

July 2010, 142 pages

Among the hard-hit cities during 17 August 1999 Kocaeli Earthquake (Mw 7.4), Adapazarı is known for the prominent role of site conditions in damage distribution. Since the strong ground motion during the event was recorded only on a rock site, it is necessary to estimate the response of alluvium basin before any study on the relationship between the damage and the parameters of ground motion. Therefore, a series of site and laboratory tests were done on Adapazarı soils in order to decrease the uncertainty in estimation of their dynamic properties. In downtown Adapazarı, a 118 m deep borehole was opened in the vicinity of heavily damaged buildings for sample recovery and in-situ testing. The stiffness of the soils in-situ is first investigated by standard penetration tests (SPT) and by velocity measurements with P-S suspension logging technique. Disturbed samples were recovered by core-barrel and split-barrel samplers. 18 Thin-Walled tubes were successively used for recovering undisturbed samples. A series of monotonic and cyclic direct simple shear tests were done on specimens recovered from the Thin-Walled tubes. It is concluded that the secant shear modulus and damping ratio of soils exposed to severe shaking during the 1999 event are significantly smaller than those estimated by using the empirical relationships in literature. It is also observed that the reversed-S shaped hysteresis loops are typical for cyclic response of the samples.

Keywords: Cyclic direct simple shear, P-S suspension logging, standard penetration test, dynamic soil properties, Adapazarı.

ÖZ

ADAPAZARI ZEMİNLERİNİN DİNAMİK ÖZELLİKLERİNİN DEVİRLİ DİREKT BASİT KESME DENEYİ İLE DEĞERLENDİRİLMESİ

Hassan Zehtab, Kaveh
Yüksek Lisans, Mühendislik Bilimleri Bölümü
Tez Yöneticisi: Yrd. Doç. Dr. Mustafa Tolga Yılmaz

Temmuz 2010, 142 sayfa

17 Ağustos 1999 Kocaeli Depreminde (Mw 7.4) ağır hasar gören şehirlerden Adapazarı saha koşullarının hasar dağılımı ile belirgin ilişkisi ile bilinmektedir. Kuvvetli yer hareketi kaydının sadece bir kaya sahada alınması sebebi ile, hasar ve yer hareketi parametreleri arasındaki ilişkiyi inceleyen çalışmalarda öncelikle alüvyon basenin tepkisi tahmin edilmelidir. Bu doğrultuda, Adapazarı zeminlerinin dinamik özelliklerinin tahmininde belirsizliği azaltmak için bir seri saha ve laboratuvar deneyleri gerçekleştirilmiştir. Numune alınması ve sahada deneyler gerçekleştirilebilmesi için, 118 m derinliğinde bir sondaj kuyusu Adapazarı şehir merkezinde ağır hasarlı yapıların yakınlarındaki bir sahaya vurulmuştur. Yerinde zeminlerin sertliği ilk olarak standard penetrasyon deneyi (SPT) ve P-S askıda kaydetme yöntemleri ile tecrübe edilmiştir. Karotiyer ve SPT numune alıcısı ile örselenmiş numuneler elde edilmiştir. 18 ince cidarlı numune tüpü ile örselenmemiş numuneler alınmıştır. Örselenmemiş numuneler ile laboratuvarda bir seri tekdüze ve devirli direkt basit kesme deneyi gerçekleştirilmiştir. 1999 depremindeki yer hareketine maruz kalan zeminlerin sekant kesme modulü ve sönümleme oranlarının literatürde verilen ampirik yaklaşımlara göre daha düşük değerlerde olduğu sonucuna

varılmıştır. Ters-S şeklindeki histeresis döngülerinin bu numunelerin devirli tepkisi için tipik olduğu gözlemlenmiştir.

Anahtar Kelimeler: Devirli direkt basit kesme deneyi, P-S askıda kaydetme, standard penetrasyon deneyi, dinamik zemin özellikleri, Adapazarı.

To My Family,

For your endless support and love

ACKNOWLEDGEMENTS

I would like to express my endless appreciation to my supervisor Assist. Prof. Dr. M. Tolga Yılmaz for giving me the chance, believing me and his permanent presence and support during all periods of this study. His keen look and prominent knowledge made this challenging study possible. The courage of starting this study and later on overcoming all problems wouldn't be possible without his valuable and precious guidance.

I would also like to thank coordinator of our research project Assist. Prof. Dr. Mustafa Kutanis whose leadership took this study to the place it is. His presence and help especially during fieldworks in Adapazari is deeply thanked.

I would like to thank Prof. Dr. Sadık Bakır, who supported me during this study. Working in Geomechanics laboratory of Civil Engineering Department of METU and using all facilities of that laboratory wouldn't be possible without his support and help.

My thanks and sincere appreciations go to Division of Soil Mechanics and Tunnels of Department of Technical Research, General Directorate of Highways. To Dr. Engin Mısırlı supervisor of division and to Ms. Şenda Sarıalioğlu supervisor of Geomechanics laboratory who gave me the limitless access to work in their laboratory. Working in such a laboratory equipped with the latest testing machines was the only way to finish this study on time. It should not be forgotten advises and cooperation of highly experienced technicians of this laboratory specially Mr. Turan Kaya Özbay and Mr. Ufuk Gündüztepe.

Also my respects and appreciations go to Dr Rachid Hankour, vice chairman of Geocomp corporation, to Mr. İlhan Usanmaz, chairman and Mr. Şsafak Soysal, project coordinator of CFU test company who helped me on installation and calibration of machines. Their support and feedback helped me on solving problems related to testing equipments.

This study is founded by the Scientific and Technological Research Council of Turkey (TUBITAK) under Award No. 108M303.

I have to thank my dear friend Mr. Selman Sağlam who helped me take my first steps

in Geotechnical testing. His experience and kind friendship helped me in organizing my testing procedure in the best way possible.

Special thanks go to my friend Semih Erhan whose character and great scientific profile helped me since the first moment I met him. His friendship is one of the most valuable gifts I have received.

I should thank my friends, İbrahim Aydoğdu, Serdar Çarbaş, Fuat Korkut, and Alper Akın for their friendship and encouragement during this study.

And the most special person in my life Renata Vázquez Santamaría for her love, support and patience during this study is thanked eternally.

The last but the most, there is no word to state how grateful I am to my family beside love. To my father, Mohammad Hassan Zehtab, my mother, Shahnaz Zhalehpour that I owe my all and to my sister, Negar Hassan Zehtab.

TABLE OF CONTENTS

LIST OF FIGURES

FIGURES

LIST OF TABLES

TABLES

LIST OF SYMBOLS

A_{loop}	Area of hysteresis loop
c	Viscos damping coefficient
C_1	Inside clearance ratio of Thin-Walled tube sampler
C_a	Area index of Thin-Walled tube sampler
CC	Clay content
CSR	Cyclic Stress ratio
D_1	Inside diameter of cutting edge of Thin -Walled tube sampler
D_2	Outside diameter of cutting edge of Thin -Walled tube sampler
D_3	Inside diameter of Thin-Walled tube sampler's respectivity
e	Void ratio
e_0	Initial void ratio
E_D	Dissipated energy in a cycle
$e_{in\text{-}situ}$	In-situ void ratio
e_{ps}	Before shear void ratio
f	Frequency
FC	Fines content
$F_e(e)$	Function of void ratio
F_{fr}	Total friction resistance of the apparatus and membrane to horizontal displacement
F_{max}	Maximum reaction force

F_{max}	Minimum reaction force
Gdr	Material stiffness factor
G_{max}	Maximum shear modulus
G_S	Specific gravity
G_{sec}	Secant shear modulus
$G_{sec\text{-}2nd\ cycle}$	Secant shear modulus at the second load cycle
$G_{sec\text{-}ultimate}$	Secant shear modulus at the last load cycle
K	Characteristic Coefficient for different soil classes
k_{sec}	Secant stiffness of spring
LL	Liquid limit
n	Characteristic Coefficient for different soil classes
OCR	Overconsolidation ratio
P_a	Atmospheric pressure
PI	Plasticity index
PL	Plastic limit
r_u	Excess pore pressure ratio
t	Time
$u(t)$	Nodal displacement acting on spring and dashpot
u_0	Horizontal displacement amplitude
u_{max}	Maximum horizontal displacement recorded during a cyclic test
u_{min}	Minimum horizontal displacement recorded during a cyclic test
V_S	Shear wave velocity

w_c	Water content
λ	Damping ratio
μ_p	Population mean of property measured under pressure p
γ	Shear strain
γ_c	Maximum shear stress
ρ	Density
$\sigma'_{v\ in\text{-}situ}$	In-situ effective overburden stress
σ_h	Horizontal stress
σ_m'	Mean effective stress
σ_v	Normal stress
σ_v'	Vertical effective stress
τ	Shear stress
τ_c	Maximum shear stress
τ_{cyclic}	Amplitude of cyclic stress

CHAPTER 1

INTRODUCTION

1.1 General

Among the hard-hit cities during 17 August 1999 Kocaeli Earthquake (Mw 7.4), Adapazarı is known for the prominent role of site conditions in damage distribution. Adapazarı, the central district of Sakarya province, had a population size of over 200,000 during the event. Lives of almost 2% of its population (3700 persons) were lost during the event. The distance between the surface trace of fault rupture and the central Adapazarı was about 5 km. On the other hand, The overall damage level was strikingly low in the southern parts of the city, situated over stiff and shallow soils (Figure 1.1). As a general trend, concentration of damage over the city increased rapidly to the north, underlain by the soft, thick alluvial soils, with midrise structures receiving the greatest impact [Bakir et al., 2002]. The relationships between the damage on buildings, the structural properties and the soil conditions have been topic of several research studies that aim to improve the state of earthquake engineering [e.g., Sancio et al., 2002; Bakir et al., 2005; Yakut et al., 2005].

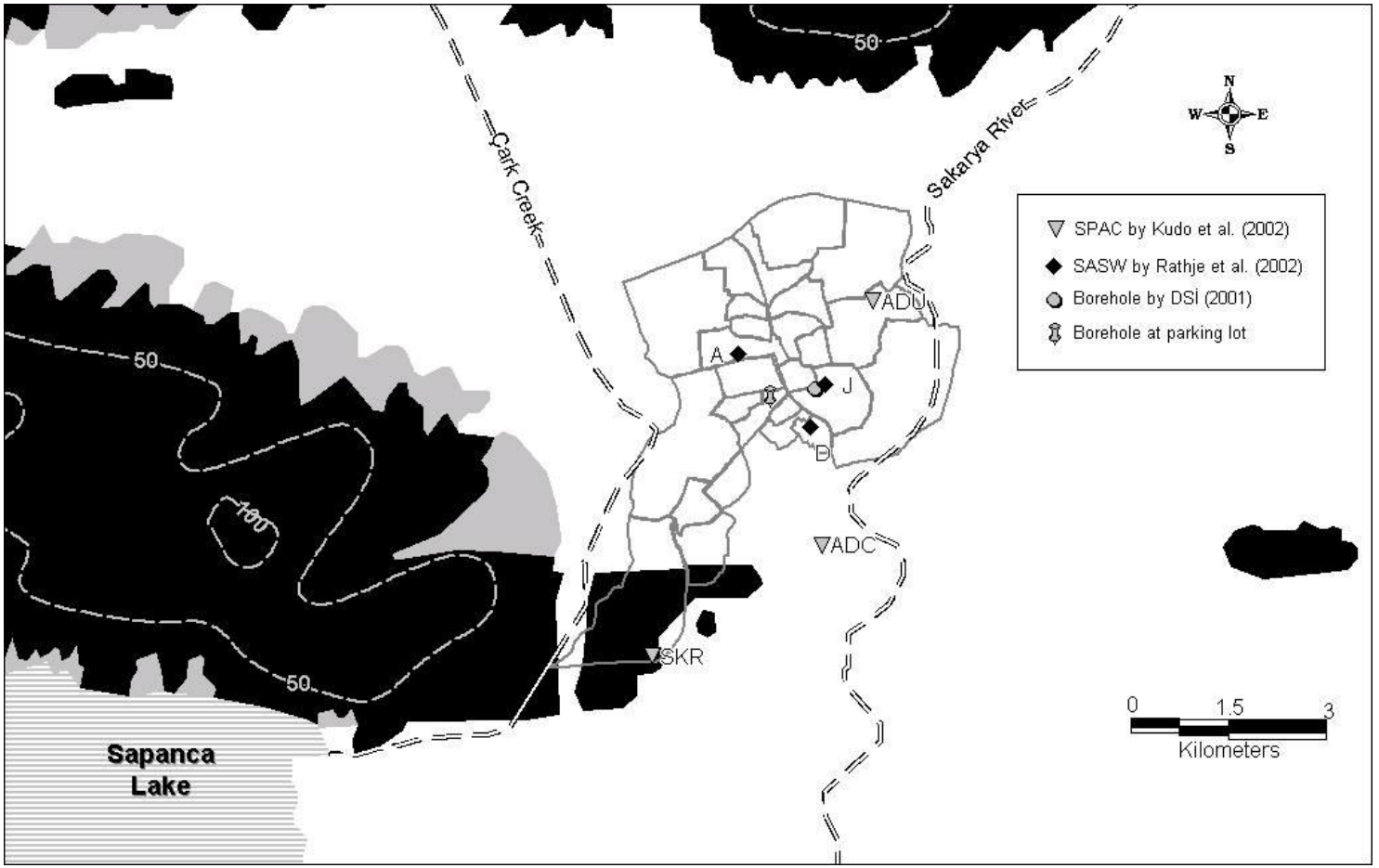

Figure 1.1 Location of downtown Adapazarı, and several site investigation studies.

Characteristics of strong ground motion on a site are dictated by properties of seismic source (e.g. amount of energy released and type of faulting), properties of path that incident seismic waves travel between source and site (e.g. distance between source and site), and site conditions (e.g. shear wave velocity of soil deposits, and topographic profile of bedrock beneath deposits) [Kramer, 1996; Darendeli, 2001; Boore, 2004; Roca et al. 2006]. Figure 1.2 demonstrates the three factors, namely the source, path and site effects governing the frequency and amplitude contents of strong ground motion on a site. Because the damage on Adapazarı was concentrated on alluvial basin, the site response was apparently responsible of the characteristics of strong ground motion imposing excessive seismic demand on structures [Bakir et al., 2002].

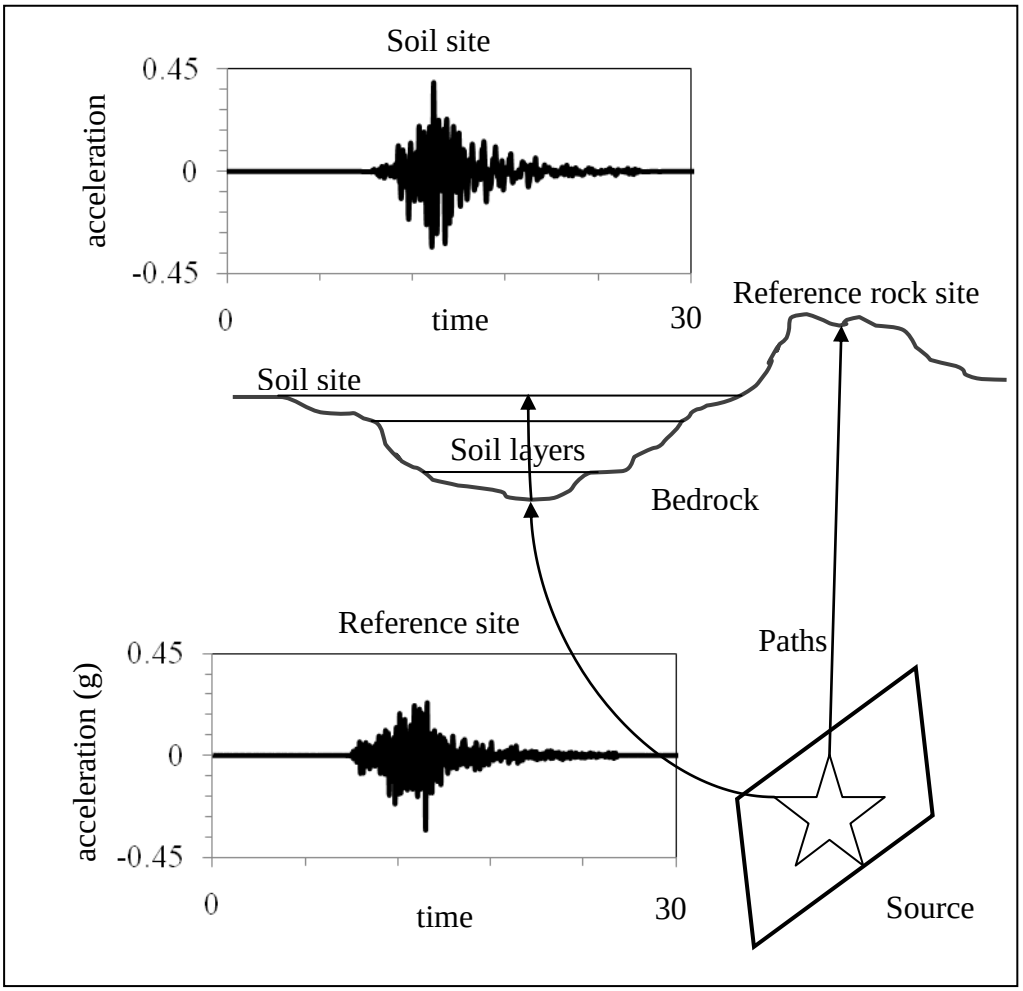

Figure 1.2 Source, path and site effects on ground motion characteristics and the difference between accelerograms on rock and soil sites.

The research project "*Development of Performance Based Design and Evaluation Methods by Comparison Earthquake Performance of the Structures in Turkey"* primarily aims to contribute for the performance based evaluation of existing buildings in Chapter 7 of the new Turkish Earthquake Design Code [GDDA, 2007], by examining the theoretical methods on estimation of the reported damage on structures, mostly located on Adapazarı basin. Since the accelerograms of 1999 event in Adapazarı are recorded on a rock site, it is crucial to estimate the characteristics of strong motion on thick alluvial deposits. This study is a part of the research project, and comprises the gathering and evaluation of geotechnical and geophysical data on a representative site downtown, which is useful for estimation of the seismic demand on structures located on the alluvial basin. A series of site and laboratory tests were done in order to decrease uncertainty in soil parameters in a site-response analysis. The soil specimens recovered from a borehole are tested by a cyclic simple shear test apparatus for assessment of dynamic properties of Adapazarı deposits. The necessity of the tests is explained in the following through a criticism of the data presented in the literature for site-response analyses of Adapazarı basin.

1.2 Literature Survey

In the following, a survey of literature is presented in order to explain briefly (i) the significance of site response in strong ground motion and the available methods for geotechnical site-response analyses, (ii) the behavior of soils during seismic loading, and (iii) data presented in literature for computation of site response in Adapazarı.

1.2.1 Geotechnical Site-Response Analysis

The site-response analysis is one of the key issues in geotechnical earthquake engineering. The effect of site conditions on strong ground motion is negligible for a "reference" rock-outcrop, so that only source and path characteristics should be studied. The modulation of frequency and amplitude contents of strong motion by site conditions can be separately formulated for a site close to the reference, through a

statistical assessment of differences between characteristics of strong ground motion recorded on similar soil sites and those on reference rock sites, or by computing dynamic response of a soil profile to strong motion prescribed for a reference site [Kramer, 1996; EPRI, 1993]. Several methods exist for a dynamic site-response analysis, each having particular advantages and disadvantages.

The applicability of any method for dynamic site-response analysis depends on the consistency between strain amplitudes encountered in soil and stress-strain (constitutive) relationships representing behavior of soil under cyclic loads. An equivalent linear method is suggested for small ($<10^{-5}$) and medium ($<10^{-3}$) amplitude range of shear strain, such that the nonlinear response of soil is not very severe [Hryciw et al., 1991]. Hence, the soil is presumed to be an elastic or visco-elastic material with parameters averaged to reflect overall stiffness and damping properties of soil through the duration of the strong excitation. The representative soil parameters are attributed to peak shear strain computed in a response analysis, the relationship between cyclic shear strain amplitudes and nonlinear response of soils observed in lab tests, and the frequency content of strong motion. The linearity assumption allows utilization of linear transformations and modal analysis technique for the solution of dynamic response problem at hand [Seed and Idris, 1970; Schnabel and Idriss, 1972; EPRI, 1993; Park and Hashash, 2004]. In contrast, an integration in time domain for tracing of nonlinear soil response is suggested for larger ($>10^{-3}$) amplitudes of shear strain in order to follow nonlinear stress-strain path accurately [Ishihara, 1996; Park and Hashash, 2004].

The geotechnical site-response analysis requires a solution of system of partial differential equations expressing the propagation of seismic waves through the soil layers with various mechanical properties. Due to the older age of deeper materials and to the confining effect of increasing overburden pressure, soil stiffness and consequently wave propagation velocity tends to increase by depth [Darendeli, 2001]. Considering Snell's law, stating that waves travelling from a higher velocity material to a lower velocity material are refracted closer to the normal to the interfaces, waves propagating upward through soft layers near earth surface will be refracted much closer to a vertical path [Kramer, 1996]. So the actually three-dimensional wave propagation problem reduces to a one-dimensional (1D) wave propagation problem for softer deposits [Idriss, 1968; Roesset, 1977; Idriss, 1990; Hryciw et al., 1991;

Kramer, 1996; Williams et al., 2000]. Since only horizontal components of strong ground motion are usually considered in seismic analysis of structures, the partial differential equation expressing the propagation of vertically incident shear-waves (S-waves) among horizontal soil layers are to be solved (Figure 1.3). The efficiency of 1D model with equivalent linear method of analysis has been statistically validated for estimation of spectral parameters on soft deposits, such as young (Holocene) lake-bed or marine sediments [EPRI, 1993; Schindler et al., 1993; Silva et al., 1998]. Nonetheless, use of 1D models for stiff sites, and actually use of any method ignoring path and source effects in a site-response analysis is not statistically beneficial with respect to the empirical approaches employing crude definition (classes) of site conditions, such as "soil" or "soft rock" [Baturay and Stewart, 2003; Boore, 2004].

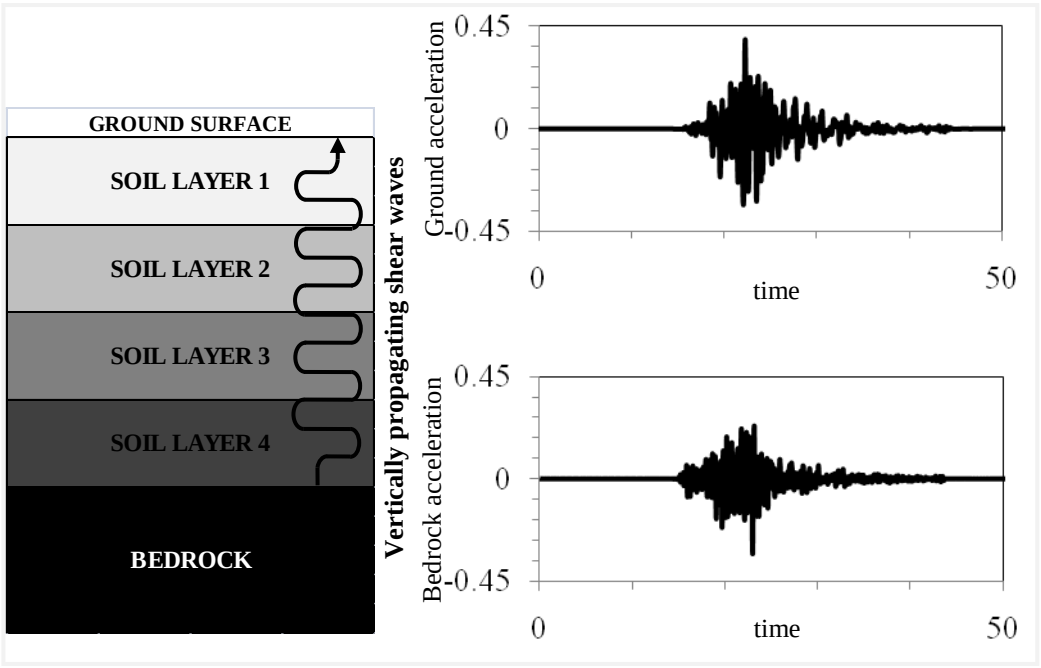

Figure 1.3 The vertical propagation of shear waves from bedrock to ground surface through soil layers.

1.2.2 Dynamic soil properties

The magnitude of nonlinearity of soil response to seismic excitation depends on several parameters such as soil type, loading amplitude, number of loading cycles, in-situ confining pressure and loading frequency. Nonlinear hysteretic soil behavior observed during cyclic loading tests in laboratory is usually summarized by plotting

degradation in secant shear modulus and a variation in damping ratio as functions of amplitude of cyclic shear strain [Seed and Idris, 1970; Hardin and Drnevich 1972; Hashash and Park, 2001]. Figure 1.4 shows typical hysteretic loop observed during a symmetric cyclic loading test: The stress-strain path begins at point A where shear stress (τ) and strain (γ) are both zero. As the load on specimen increases, the response follows the initial loading path to point B, namely the backbone curve followed during a monotonic loading test. On point B, the maximum shear stress (τ_c) and strain (γ_c) are attained, which are simply equal to amplitudes of cyclic stress or cyclic strain in a load-controlled or a displacement-controlled test respectively. The unloading stage of load cycle begins at point B. Nonetheless, the soil response does not follow the backbone curve, but the path B-C passing below it, and resulting in residual (inelastic) shear strain at point C (i.e., $\gamma \neq 0$ when $\tau = 0$). Following point C, the magnitude of shear stress increases in negative direction of loading to point D, defined as the condition that either $\tau = -\tau_c$ or $\gamma = -\gamma_c$ for a load-controlled or displacement-controlled test respectively. Afterwards load changes its direction once again such that the soil response follows the path D-E-B, and closing the first hysteretic loop. The test continues with the desired number of load cycles, so that the relationship between number of load cycles and the shape of hysteretic loop can be observed [Ishihara, 1996].

The stiffness-strain relationship can be practically expressed by reporting the variation of calculated secant shear modulus (G_{Sec}) with cyclic shear strain amplitude (γ_c) after a set of cyclic loading tests. The secant shear modulus is simply the slope of the line A-B in Figure 1.5:

$$G_{Sec} = \frac{\tau_c}{\gamma_c} \qquad [1.1]$$

The amount of dissipated energy during a load cycle is equal to the area of hysteretic loop B-D-B (A_{Loop}) in Figure 1.5. The maximum retained strain energy in a loading cycle is equal to the area of triangle A-B-F in Figure 1.5. Equivalent viscous damping ratio (λ) is the ratio of dissipated energy to maximum retained energy in a single load cycle [Kramer, 1996; Rollings et al. 1998; ASTM D 3999-91; Darendeli, 2001]:

$$\lambda = \frac{1}{4\pi} \cdot \frac{A_{Loop}}{\tau_c \gamma_c} \qquad [1.2]$$

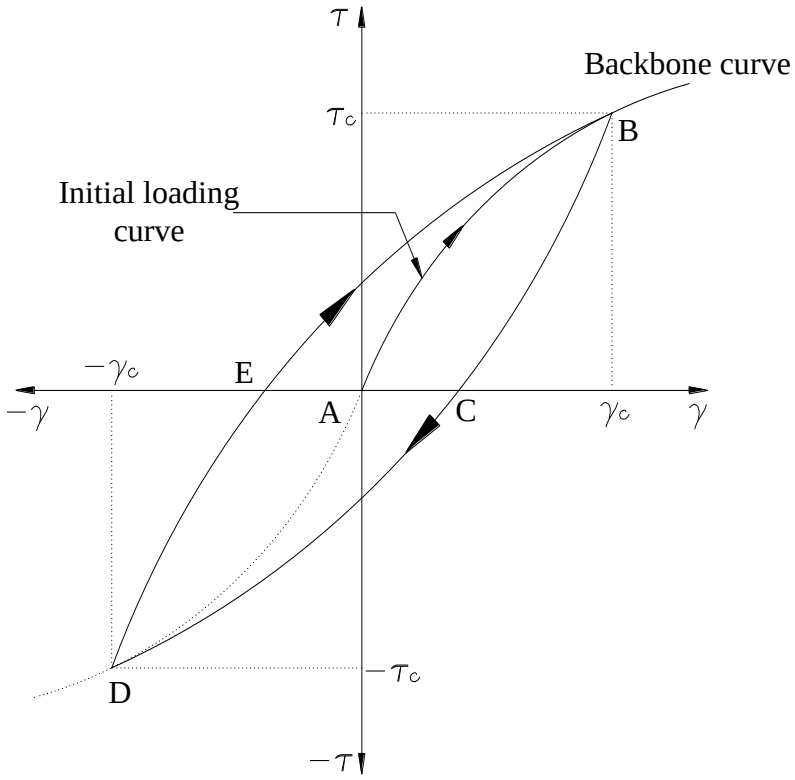

Figure 1.4 Nonlinear hysteretic soil behavior under cyclic loading.

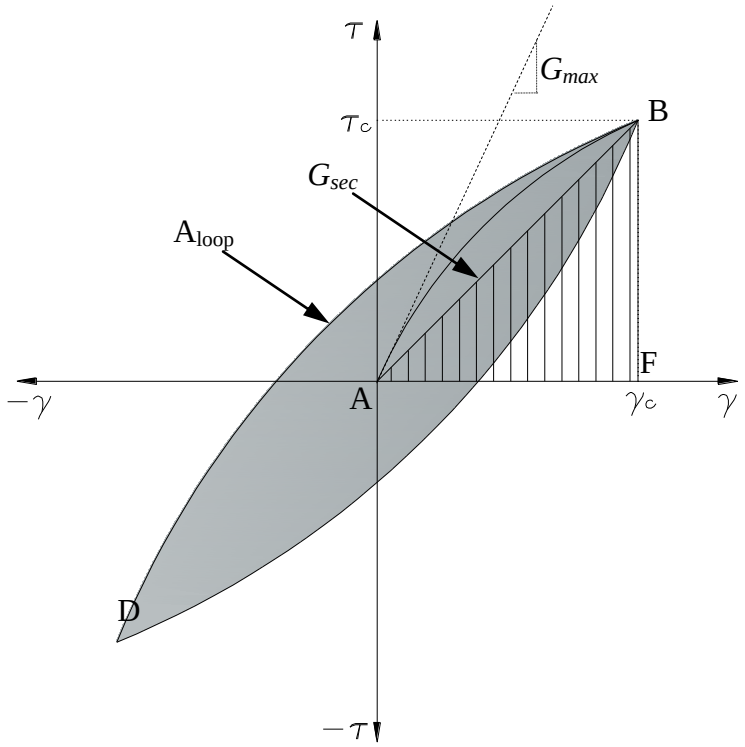

Figure 1.5 Dynamic soil properties on cyclic loading loop.

Load or deformation controlled cyclic triaxial tests are often employed so as to determine the relationship between secant shear modulus (G_{sec}), damping ratio (λ) and amplitude of cyclic shear strain (γ_C) for a wide strain range, [Kokusho, 1980; Kokusho et al., 1982; Anderson et al., 1983; Seed et al., 1986]. A widely used alternative is the resonant column test, which is particularly useful for measuring dynamic properties of specimens at extremely-small strains [EPRI, 1993].

The direct simple shear test is also another widely used test procedure (e.g., Finn et al., 1971; Ishibashi and Sherif, 1974; Peacock and Seed, 1968; and Seed and Peacock, 1971; Ladd and Edgar, 1972). The monotonic loading of specimen in a direct simple shear test procedure is well described by the code ASTM D 6528-07. In a direct simple shear test, the soil specimen is confined in a stack of rings or within a wire-reinforced membrane, and is consolidated under a vertical load exerted by a load piston. Being similar to a typical oedometer test, the stress-condition of the specimen is presumed to be similar to that in-situ. The shear stress is applied through inducing a lateral (shearing) load onto the specimen. The stresses induced by incident S-waves can be simulated by cyclic variation of lateral load. Although the shearing direction is always horizontal in the cyclic simple shear test, the stress-distribution in a simple-shear test is not uniform, since no complementary shear-stress is imposed on the vertical sites (i.e, by the stack of rings or membrane). The uniformity in stress-distribution improves by increasing the diameter/height ratio of the specimen, [Airey et al. 1985].

In order the express the severity of nonlinear response, G_{sec} has been always normalized by G_{max} in literature, the theoretical maximum value of G_{sec} that is equal to the initial tangent modulus of the backbone loading curve. Hence, the relationship between G_{sec}/G_{max} and γ_c can be employed for similar soils with different G_{max}, which is dependent on several parameters such as the confining pressure on soil in situ, and void ratio [Hardin and Black, 1969; Hardin 1978; Shibata and Soelarno, 1978; Zen et al. 1987; Jamiolkowski et al. 1991; Shibuya and Tanaka, 1996; Kawaguchi and Tanaka, 2008]. The damping ratio is usually expressed as a function of γ_c, but can also be expressed as a function of G_{sec}/G_{max} as well [Ishibashi and Zhang, 1993]. Figure 1.6 demonstrates the degradation of normalized secant shear modulus (G_{sec}/G_{max}) and increase in damping ratio (λ) with increasing cyclic strain amplitude (γ_c) [Ishibashi and Zhang, 1993].

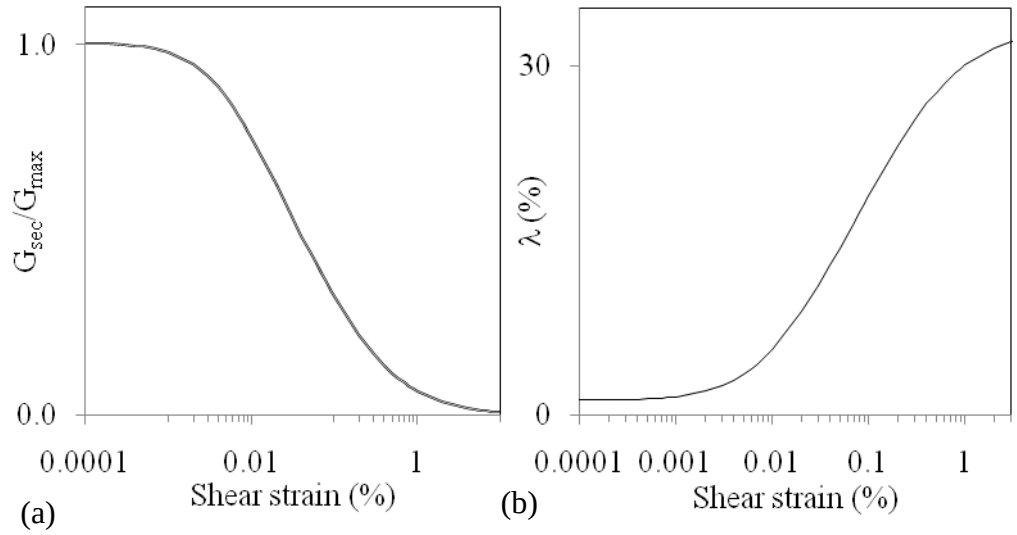

Figure 1.6 Typical curves showing (a) reduction in shear modulus, and (b) increase in damping ratio by increasing cyclic strain amplitude [Ishibashi and Zhang, 1993].

Several test results and empirical relationships are presented in literature for estimation of G_{sec}/G_{max} and λ for a given γ_c. Seed and Idriss, (1970, 1984) suggested relationships for sands and gravels and showed that the modulus reduction and damping ratio is also dependent on effective mean stress (σ_m'). The significance of σ_m' for low-plasticity soils is also verified by Kokusho, (1980) and Ishibashi and Zhang (1990) and (1993). On the other hand the influence of plasticity index (PI) on modulus degradation and damping was first noticed by Zen et al., (1978) and then by Kokusho et al. (1982). Vucetic and Dobry (1991) showed that the overconsolidation ratio (OCR) of clays is a less significant parameter than PI. Ishibashi and Zhang (1993) proposed empirical equations for estimation of G_{sec}/G_{max} and λ for a given set of σ'_m, PI, and γ_c. The most recent study on estimation of modulus reduction and damping in different types of soils was presented by Darendeli, (2001). All those studies also concluded that G_{sec}/G_{max} decrease by increasing number of load cycles.

For normalization of G_{sec}, maximum shear modulus (G_{max}) is obtained in a particular test in which the amplitude of shear strains is lower than the elastic limit. The elastic limit of shear strains is as low as 0.0001% for typical soils [Dyvik and Madshus, 1985; Doroudian and Vucetic, 1995; EPRI, 1993; Lanzo et al., 2009]. The experimental equipments designed to measure large-strain response of soils are usually incapable of performing a test with very low strain amplitudes. Therefore, either special test

devices are implemented on those equipments, such as the bender elements, or particular apparatuses are designed for performing low-strain tests, such as the resonant column [Dyvik and Madshus, 1985, EPRI, 1993]. However, any of these small-strain tests in lab can be very sensitive to the sample quality than the large-strain tests. Nonetheless, in-situ measurements of low-strain modulus of soil can avoid the complications due to sample disturbance. Hence, assuming that the soil is isotropic elastic media, another option for determination of G_{max} is to perform geophysical tests. The relationship between shear-wave velocity (V_s) and density (ρ) for an isotropic elastic media is [Richart et al., 1970]

$$G_{\max} = \rho \cdot V_S^2 \qquad [1.3]$$

There are several in-situ measurement techniques to estimate shear wave velocity in soil layers. One of the most widely used techniques is the Spectral Analysis of Surface Waves (SASW) in which the propagation of Rayleigh waves is monitored on the ground surface. Hence, no borehole is necessary for a SASW application. Uphole and downhole Seismic techniques are based on monitoring upward or downward propagation of longitudinal or shear waves in soil near a borehole. Hence, a borehole is necessary for lowering either the wave source (Uphole) or the receiver (Downhole). An alternative is the crosshole Seismic technique, in which the geophone lowered in a borehole receives waves generated by a source lowered in a second borehole. crosshole technique is useful for measuring velocity in deep strata, since the length of travel path for waves hinders the use of cheaper uphole or downhole options in deep investigations. P-S suspension logging is a feasible alternative for investigation of deep strata [Ishihara, 1996; Kramer, 1996; EPRI, 1993]. In this technique a probe consisting of a source and two receivers that are isolated from each other is suspended by a tension cable in borehole filled by a suspension fluid. The travel time of a wave between source and receiver is measured by monitoring the motion of the fluid. The weakness of the technique is the sensitivity of results to borehole quality. [EPRI, 1993].

In absence of any wave-velocity or material-stiffness measurement, G_{max} can be estimated by empirical relationships, which are functions of several soil index parameters, such as void ratio (e), OCR, PI, and liquid limit (LL); and of stress parameters, such as σ'_m, and vertical effective stress σ'_v on soil [e.g. Hardin and Black,

1969; Hardin 1978; Shibata and Soelarno, 1978; Zen et al. 1987; Jamiolkowski et al. 1991; Shibuya and Tanaka, 1996; Kawaguchi and Tanaka, 2008].

1.2.3 Significance of site response in Adapazarı

Because of its rapidly developing industry, Sakarya has been receiving large immigration and sustaining fast urbanization before the 1999 Kocaeli earthquake. Most of the residential structures in Adapazarı were non-ductile 3 to 5 story reinforced concrete buildings. Most foundations were reinforced concrete shallow mat foundations. Shallow depth of ground-water table, low load-bearing capacity of the shallow soils, and deep alluvial basin were the other remarkable characteristics of most sites in downtown Adapazarı [Bakır et al., 2002].

A strong motion station of General Directorate of Disaster Affairs, located on a stiff site of southern Adapazarı, recorded the peak EW ground acceleration as 0.4g (Figure 1.7Figure 1.8). Due to malfunction the station could not gather an accelerogram on NS direction, which is almost perpendicular to fault strike [Anderson et al., 2002]. Heavy damages and structural collapses were concentrated on downtown Adapazarı over the deep alluvial basin, and were mostly due to structural weakness of 4 to 6-story buildings in resisting strong ground motion on the basin. Hence, the concentration of heavy damage on the downtown sites, and analyses performed thereafter the 1999 event were pointing out the amplification of low frequency S-waves by deep alluvial basin under downtown [Bakır et al., 2002; Özel and Sasatani, 2004; Beyen and Erdik, 2004].

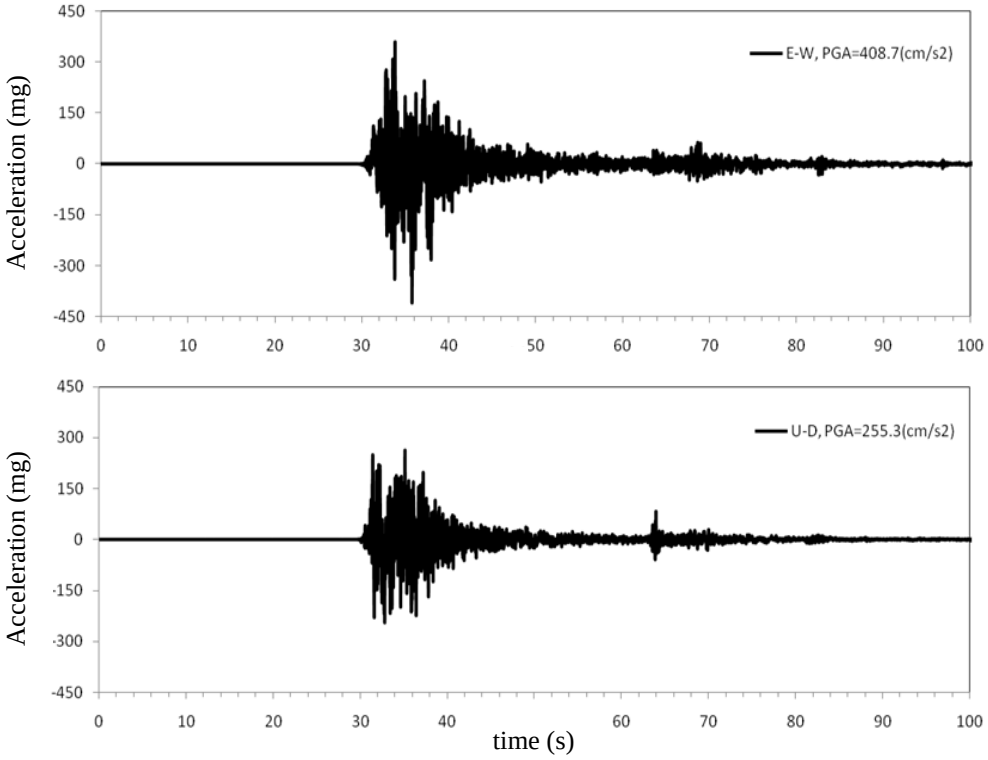

Figure 1.7 Strong motion recorded at the permanent Sakarya station during the 17 August 1999 earthquake [DAPHNE, 2009].

Downtown Adapazarı is located on a former lake bed and is between Sakarya river on the west and Çark river on the east. The two water resources are feeding the very shallow ground-water table, usually not deeper than 3 m. It has a smooth topography with an elevation of approximately 30 m. The alluvial basin is underlain by upper Cretaceous flysch bedrock in depths exceeding 300 m. The soil profile of downtown Adapazarı is mostly formed by a thick layer of fine grain soils with variable plasticity index (PI). Stiff clayey layers in deeper profiles are replaced by loose soils with low penetration resistance in shallow depths. A dense gravelly layer is encountered in the range of depths between 40 and 50 m in southern basin, but it appears at depth of about 80 m in the north [Bakır et al., 2002, Beyen and Erdik, 2004, DSI, 2001]. An idealized soil profile of downtown Adapazarı is shown in Figure 1.8.

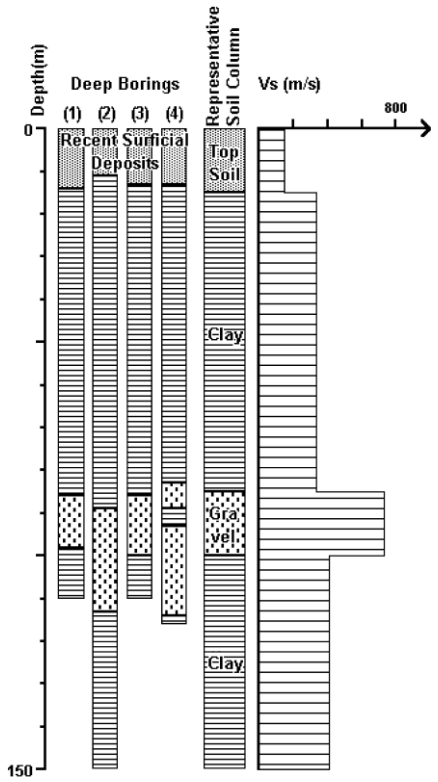

Figure 1.8 Idealized soil profile in downtown Adapazarı (Bakır et al., 2002).

Kudo et al. (2002) applied the spatial autocorrelation method (SPAC) to array data of microtemors for determination of S-wave velocity profile beneath the strong motion station (SKR) and beneath two points located on the alluvial basin (ADC and ADU in Figure 1.1). The S-wave velocity profiles presented in Table 1 show that the relatively stiff layers (V_S > 730 m/s) are located at depths exceeding 135 m beneath southern basin (i.e., near ADC) and at depths exceeding 413 m beneath sites located a few kilometers farther on northeast of downtown (i.e., near ADU). Depth to formations competent at V_S > 1500 m/s (i.e., the minimum limit for a type-A class site according to NEHRP, 2003) is estimated as 377 m and 576 m for ADC and ADU sites respectively. The S-wave velocity profiles reported by Kudo et al. are in general agreement with those estimated by Bakır et al. (2002), and Beyen and Erdik (2004): Bakır et al. (2002) estimated the depth to bedrock as a value in between 150 to 200 m based on a previous geophysical study of Sakarya University. Beyen and Erdik (2004) developed a two-dimensional model of the basin by employing those aftershock records recorded on the basin, and concluded that the depth to bedrock exceeds 300 m in central locations of the city.

Komazawa et al. (2002) investigated bedrock structure in Adapazarı using basis of Bouguer gravity anomaly. This study estimates depth to bedrock in downtown Adapazarı around 1000 meters and more. The large difference with respect to the aforementioned studies can be explained by the differences in definition of "bedrock" among these studies, such that Komazawa et al. defined the bedrock in terms of the contrast in density of formations, and stated that the definition is equivalent to V_S = 3500 m/s for bedrock.

Table 1.1 V_S profiles for ADC, ADU, and SKR sites (Kudo et al., 2002).

SKR		ADC		ADU	
Latitude(º)	Longitude(º)	Latitude(º)	Longitude(º)	Latitude(º)	Longitude(º)
40.737	30.381	40.753	30.411	40.787	30.419
Vs (m/sec)	Thickness (m)	Vs (m/sec)	Thickness (m)	Vs (m/sec)	Thickness (m)
1050	72	234	38	166	44
1500	56	441	97	331	88
2000	∞	728	242	500	281
-	-	1500	70	878	63
-	-	2000	∞	1050	100
-	-	-	-	1500	∞

The fundamental period of a central location in downtown Adapazarı, which is related to depth to bedrock, is estimated as a value around 1.5 s by Bakır et al. (2002) using spectral acceleration ratios of aftershock motions recorded in downtown Adapazarı and at stiff site (SKR), whereas it is estimated as a value between 3 and 4 s for deeper basin sites by Komazawa et al. (2002) using H/V ratios of microtremors. Fäh et al. (2004) estimated fundamental period as 2.0 s for ADC and more than 3.0 s for ADU

site by using peak H/V ratio of microtremors. The fundamental site period reported by Fäh et al. for the ADC site is not in agreement with the data provided in Table 1.1. Hence, no apparent consensus on site period of downtown Adapazarı is seen in literature.

Large spatial variability in properties of the shallow deposits is reported in literature. The deposits located in top 7 m of soil profile vary from non-plastic soils to highly plastic silty clays. Similarly, the penetration resistances of those shallow deposits, related to their shear strength, show exceptional spatial-variability. Beneath 7 m, generally stiff soils with high penetration resistance are encountered. Excessive foundation displacements were observed on shallow soils with low penetration resistances [Bakır et al., 2005; Sancio et al., 2002]. Employing downhole and uphole seismic tests, Sancio et al. reported the S-wave velocity profiles on various sites where excessive foundation displacements were observed. Besides, Rathje et al., (2002) used the method of spectral analysis of surface waves (SASW) for several sites, in order to estimate S-wave velocity profile for depths reaching 45 m. The data provided by Sancio et al., 2002 and Rathje et al., (2002), plotted in Figure 1.9, also suggests the significant spatial dependency of S-wave velocity in downtown Adapazarı.

The significant differences in site characteristics reported in literature and the significant spatial-variability of soil properties in the basin emphasize the necessity of a local site-investigation study for a reliable dynamic site-response analysis of Adapazarı basin.

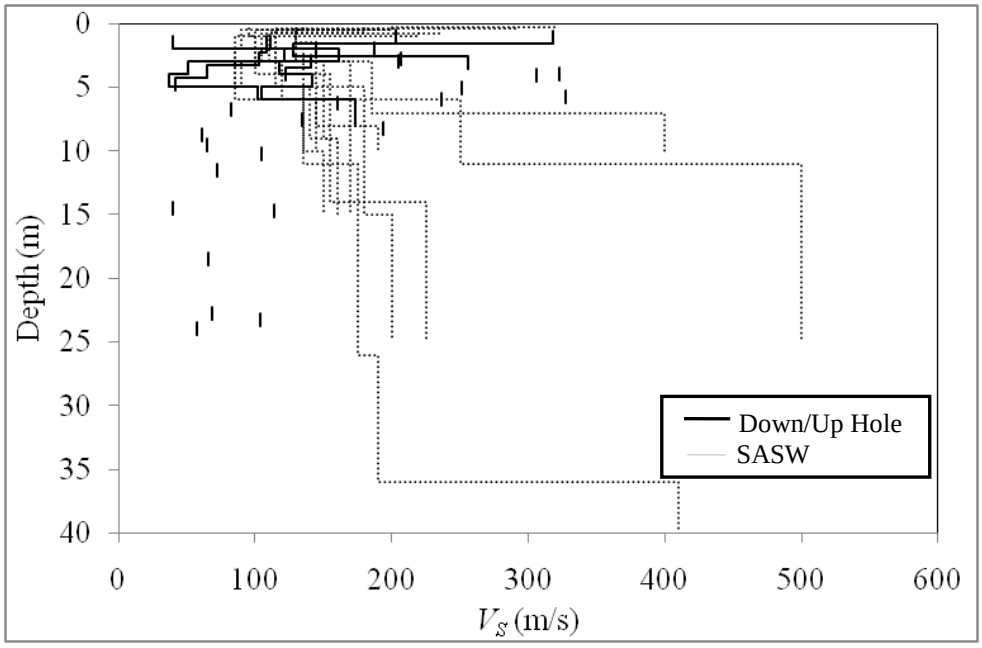

Figure 1.9 Velocity profiles of shallow deposits on several sites in Adapazarı [Sancio et al., 2002; Rathje et al., 2002]

1.2.4 Scope

In this study, a site-investigation and lab-testing program is run in order to produce geotechnical data for a more reliable dynamic response analysis of Adapazarı basin. Cyclic loading tests were done on undisturbed specimens recovered from Adapazarı, in order to investigate the dynamic properties of those deposits. In Chapter 1, a literature survey showing the necessity for a site-investigation program prior to dynamic site-response analyses of the basin is presented. In Chapter 2, the selected site for investigation, the sampling technique and results of in-situ tests are presented. In Chapter 3, the test program consisting of determination of index properties of specimens and cyclic testing of specimens is presented. Particular emphasis is put on the cyclic direct simple shear apparatus used for tests. In Chapter 4, the results of cyclic loading tests are compared with those of other studies on similar soils. Finally, the summary and conclusions of the study are presented in Chapter 5.

CHAPTER 2

SAMPLING AND IN-SITU TESTS

2.1 Introduction

Since the dynamic properties of shallow deposits can have prominent effect on the characteristics of strong ground motion, assessment of them by a series of in-situ and laboratory tests is important [EPRI, 1993]. Therefore, in order to investigate the relationship between shear modulus and strain, and to provide realistic estimates for energy dissipation capacity of soils, samples are recovered from a borehole on a selected site in Adapazarı. The undisturbed specimens are used for cyclic loading tests in lab, and both the undisturbed and disturbed specimens are used for determination of index parameters necessary for soil classification. On the other hand, since the mechanical properties of soils at very small strains can be very sensitive to limited disturbance induced during sampling, the shear-wave velocity measurements are performed in the borehole for reasonable estimations of shear moduli of soils at small strains [Gazetas, 1991]. The geophysical tests are also useful in examination of velocity profiles proposed for Adapazarı basin by other researchers.

A vacant parking lot in Pabuccular district near Yeni Cami square in downtown Adapazarı was chosen for drilling the borehole. The site is located at coordinate 40.7719ºN and 30.4009ºE (Borehole-108M303 in Figure 1.1). The reasons of choosing the parking lot are its proximity to the buildings investigated within the TUBITAK project 108M303, its central and easily accessible location, and the lack of any observations regarding excessive foundation settlements in its vicinity. The latter reason is important for the scope of the TUBITAK project with award number of 108M303, which excludes the effects of nonlinear soil-structure interaction on structural response. Besides, the site is close to area where no or very limited

excessive foundation displacements have been reported despite the severity of structural damage [Bakir et al., 2005]. Nonetheless, whenever consideration of very-loose shallow deposits is necessary for site-response analyses, the amply reported data on the shallow soils of Adapazarı, reported in Chapter 1, can be used for improving the theoretical models. Although the sole soil-profile obtained in this study may not be representative for all sites in the downtown, the geotechnical data gathered is useful for developing theoretical models whenever supplementary information on soil stratification is made available by local borings. On the other hand, the data is useful in the investigation of variability of site-response on Adapazarı through considering uncertainty in seismic excitation and variability in soil profiles shown by several deep borings in Adapazarı (e.g., Bakir et al., 2002; Beyen et al., 2003).

2.2 Drilling and sampling

Drilling and sampling operation was made by Geoteknik Co. using a D500 type drilling machine between 31.10.2009 and 21.11.2009. The drilling method was rotary wash boring. The hole diameter was 88.9 mm down to the depth of 76 m, but then the diameter was lowered to 76.2 mm because of gravels blocking the drilling apparatus. No measurements were done on actual borehole diameter during and after drilling, but attention was paid to keep it as constant as possible through the borehole. A wide hole was dug on the ground surface near the borehole as a pool for settling of particles in mud, and as a secondary water reservoir (Figure 2.1.a). Drilling mud was pumped down the drill stem to the borehole bottom, where it picks up soil cuttings and carries them to the ground surface. The mud also served to support the borehole walls. The drilling method was consistent with the procedure explained by Lowe and Zaccheo (1975).

Boring was stopped at the final depth of 118 meters. The drilling and sampling became very difficult in very dense gravelly soils encountered at depths exceeding 76 m. Hence the boring was stopped at the final depth of 118 m after the last unsuccessful attempt of sampling. First 9 meters of the borehole was supported by metal casings (Figure 2.1.b). Disturbed samples were recovered from borehole by split barrel sampler conventionally used for a Standard Penetration Test (SPT), and by core-barrel

samplers. The undisturbed samples were recovered from Thin-Walled tube samplers. The disturbed samples were only used for soil classification. Also blow-counts of SPT (SPT-N) provided supplementary information about the density or stiffness of soils encountered. The Thin-Walled tube samples were used to prepare higher quality (undisturbed) specimens for laboratory tests. The sampling procedures implicitly followed the standards ASTM D 1587-08 and ASTM D 1586-08. Detailed information on the sampling equipment presented in the following sections.

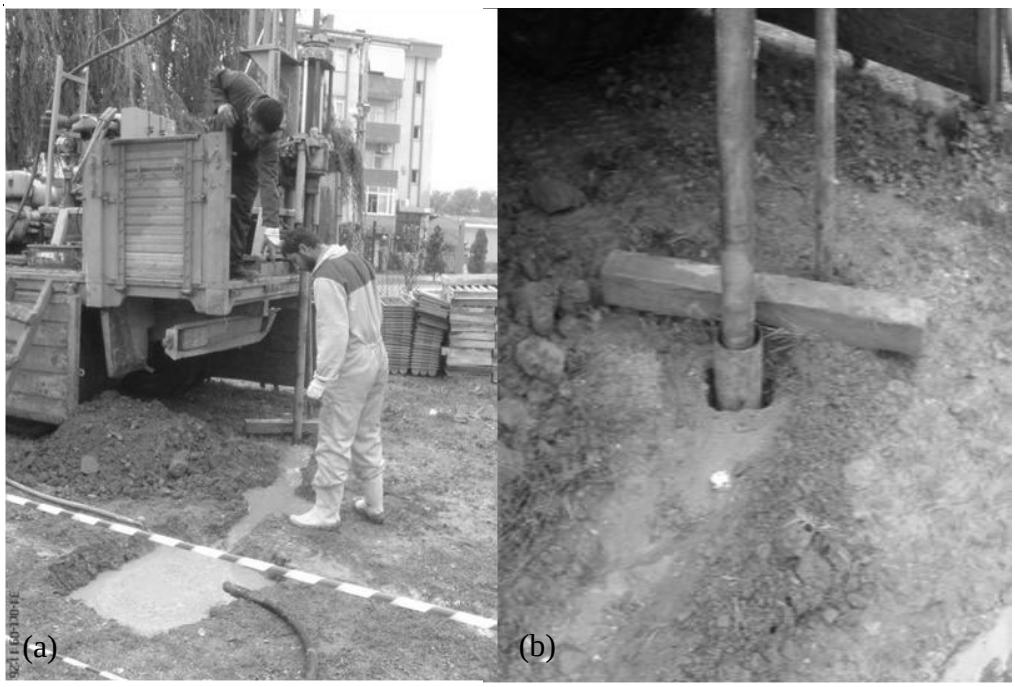

Figure 2.1 The drilling operation in Adapazarı: a) drilling machine and the secondary water reservoir near borehole; b) metal casing supporting borehole walls.

The initial objective in boring was to obtain one disturbed and one undisturbed sample per 1.5 meter through the borehole. However, no Thin-Walled tube sample could be recovered at depths exceeding 33.5 m due to the stiff soils encountered. Therefore, the Thin-Walled tube sampling method was substituted by the core-barrel sampling method for deeper layers. All disturbed samples were isolated with plastic bags in order to prevent any loss of water content. At depths exceeding 78 m, no sample could be recovered due to presence of gravelly layers blocking drilling heads and core-barrel samplers. A total number of 18 Thin-Walled tube samples, 7 core samples and 17 SPT samples were recovered. Figure 2.2 shows distribution of depth of sample recovery.

Detailed information on samples, including depth of recovery along with recovery percentage and soil classification is presented on the borehole log given in the Appendix. The details of samplers which have prominent effect on sample quality are presented in the following sections.

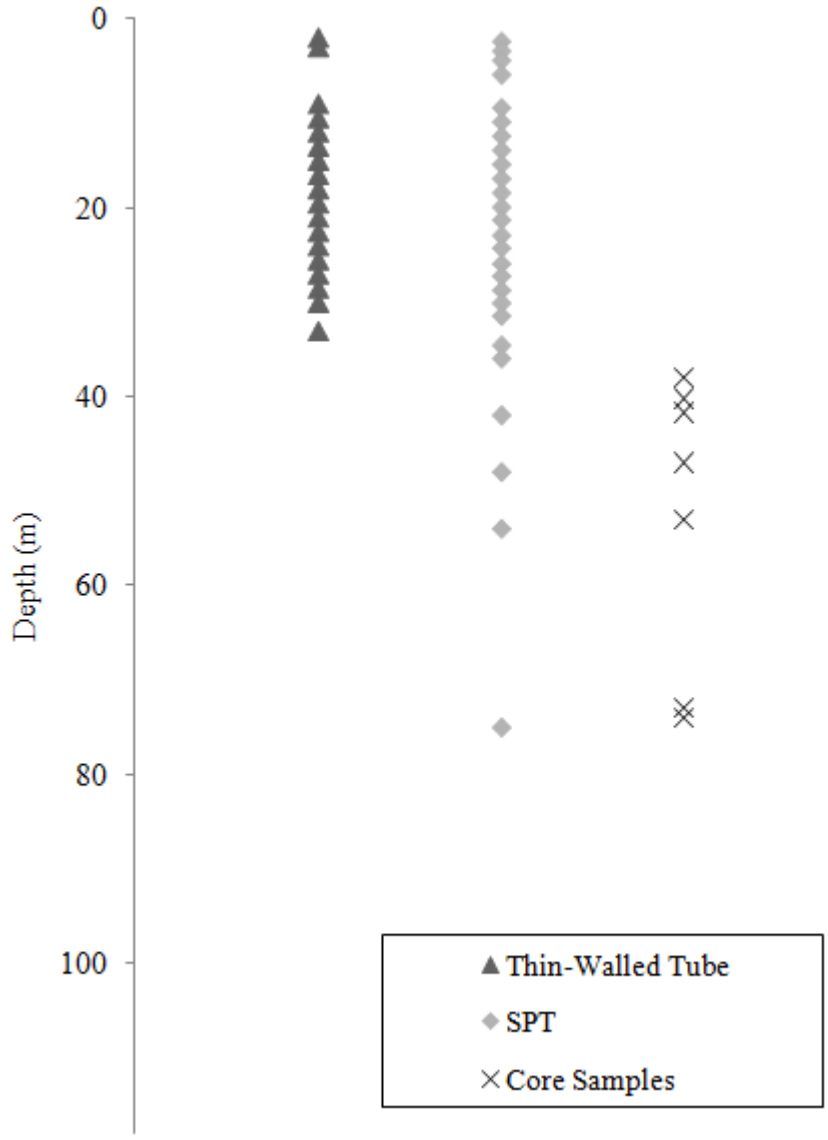

Figure 2.2 The depths of sample recovery.

2.1.1 Thin-Walled Tube Sampler

The Thin-Walled open-drive tube sampler, or 'Shelby Tubing' has been known to the widest community of geotechnical engineers since it was first introduced in USA in the late 1930s. The reason that the sampler is preferred in most applications is its simplicity in use, its ability to recover high quality samples (i.e., practically undisturbed) when used with care in soft and stiff cohesive soils, and the low probability of being damaged it possesses during operation. [USACE, 2000]. In order to provide samples of least possible disturbance to cyclic loading tests in laboratory, Thin-Walled tube samplers were ordered and manufactured following the specifications on the standards ASTM D 1587-08 and TS ENV 1997-3. According to TS ENV 1997-3, the sample quality is dependent on two indices which are dependent on their parameters: D_1, D_2, and D_3 defined as the inside diameter of cutting edge, the outside diameter of tube and the inside diameter of tube respectively (Figure 2.3). The first index is the area ratio, C_a, which is defined as

$$C_a(\%) = \frac{D_2^2 - D_1^2}{D_1^2} \times 100 \qquad [2.1]$$

The second index is the inside clearance ratio, C_1, defined as

$$C_1(\%) = \frac{D_3 - D_1}{D_1} \times 100 \qquad [2.2]$$

In order to recover samples of class A quality from soft clays, C_a should be less than 15%, C_1 should be less than 1%, D_1 should be at least 71.1 mm, and D_3 should be less than D_1+0.7. According to TS ENV 1997-3, the tube length should be less than $6 \cdot D_1$ for all soils, but somewhat longer tubes are allowable for cohesive soils.

Hence, considering that the borehole diameter is 80 mm, manufacturing of 550 mm long tubes with diameters D_1=D_3=71.2 mm, and D_2=76.2 mm are ordered, in order to recover samples as large as possible, and to keep necessary room for mounting holes at tube's ending. In that case, the length of tube's advance in soil should be 500 mm during sampling. Figure 2.3 schematically shows the Thin-Walled tubes manufactured for this study.

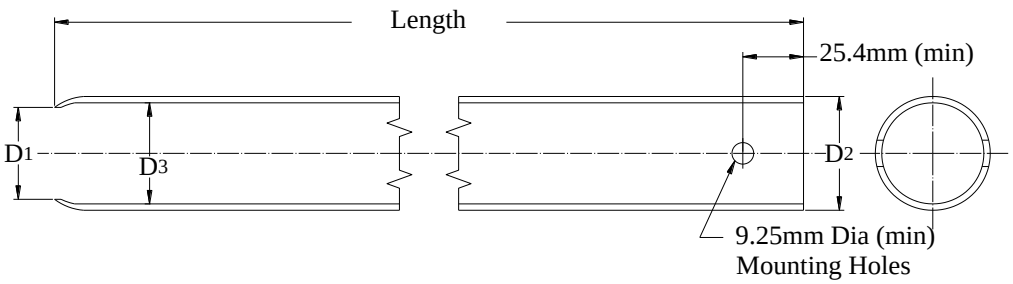

Figure 2.3 A schematic plan of the Thin-Walled tube sampler according to ASTM D 1587 – 08.

The Thin-Walled tubes were mounted to the end of drilling rods (Figure 2.4.a). Attention was paid to the lowering of the tube to the bottom of the hole in order to avoid scrapping of borehole wall by the cutting edge of sampler. After reaching to the bottom of the hole, tubes were driven into the soil by the drilling rods. When sampling procedure was finished drilling rods were detached from the drilling machine and were pulled out of the hole by a cable connected to the end of drilling rods. Then, tubes were sealed on both openings following the removal of drilling cuts remaining at the top of the sample, and the material located at the last 2 cm of recovery (Figure 2.4.b). The tubes were identified according to sample no, date of sample, and depth of sample; and they were tightly covered by plastic bags before the shipment (Figure 2.4.c).

Figure 2.4 Preparation of an undisturbed sample for shipment: a) Thin-Walled Tube sampler is mounted to drilling rod, b) upper end of a Thin-Walled Tube sampler is sealed with wax, c) Sealed and identified thin-walled tube sample is ready for shipment.

2.1.2 Split Barrel sampler (SPT samples)

In this method a Split-Barrel sampler, which is consisting of a sampler head, a Split-Barrel sampling tube, and a driving shoe, is driven to bottom of the borehole by a

hammer falling at top of the drilling rods, in order to recover disturbed samples for determination of water content and class of soils (Figure 2.5). The procedure, namely the Standard Penetration Test, SPT, follows the specifications of ASTM D 1586-08. A Donut type metal hammer with 64 kg (140 lb) weight was repeatedly dropped from 0.76m ± 25mm height. Hence, the number of hammer blows necessary for sampler penetration through 30 cm of soil on the bottom of the borehole is also reported as the results of Standard Penetration Test, or SPT-N, which is related to soil stiffness. Besides, relationships between several parameters of soils and SPT-N have been proposed in literature. SPT is generally applicable to fairly clean medium to coarse sands and fine gravels at different water contents, and to saturated cohesive soils. However, significantly biased estimates of parameters can be obtained in case SPT is applied to unsaturated fine soils and to saturated silty sands [USACE, 2000].

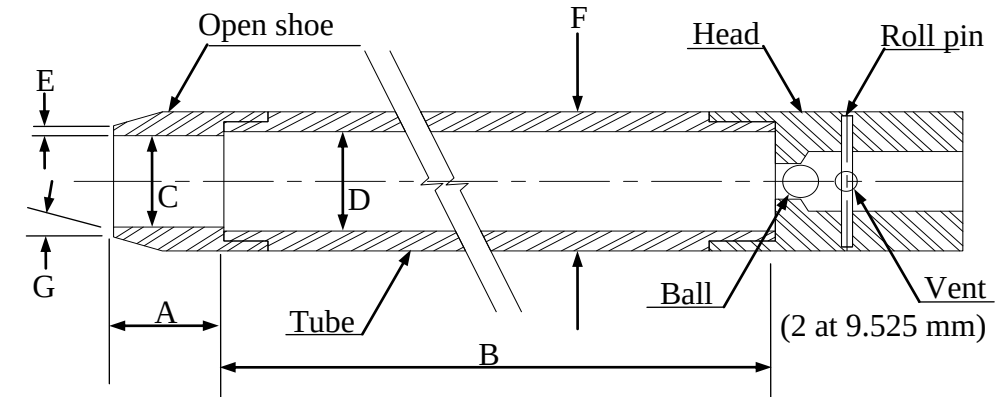

A = 25 to 50 mm
B = 0.457 to 0.762 m
C = 34.93 ± 0.13 mm
D = 38.1 ± 1.3 – 0.0 mm
E = 2.54 ± 0.25 mm
F = 50.8 ± 1.3 – 0.0 mm
G = 16.0° to 23.0°

Figure 2.5 The dimensions of split-barrel sampler used in this study.

The high variability of SPT-N is in agreement with the heterogeneity encountered in soil profile (Figure 2.7). Several disturbed samples were recovered during the standard penetration tests, which were useful for soil classification. Figure 2.6 shows a disturbed sample that is packed and identified. Detailed information on sample recoveries and SPT-N are presented on the borelog [TUBITAK, 2010] presented in Appendix A. In the borehole, loose to medium dense sands at very shallow depths are replaced by dense and very dense sands at depths between 4 and 9 m. Stiff clays and

silts are encountered below those sandy layers. Layers of fine soils successively continue to the depth of 57 m, where clayey gravel deposits first appear. The clayey gravel layer that ends at depth of 71 m makes sampling extremely difficult. Last sample is gathered from a 5 m thick stiff clay underlying the clayey gravel. Following the clayey layer borehole pass through a second clayey gravel layer between 76 and 89 m. Finally, a very stiff gravel layer was encountered between 89 m and 118 m so that the drilling is stopped at 118 m without breaching the stiff deposit.

Figure 2.6 Disturbed sample recovered during SPT.

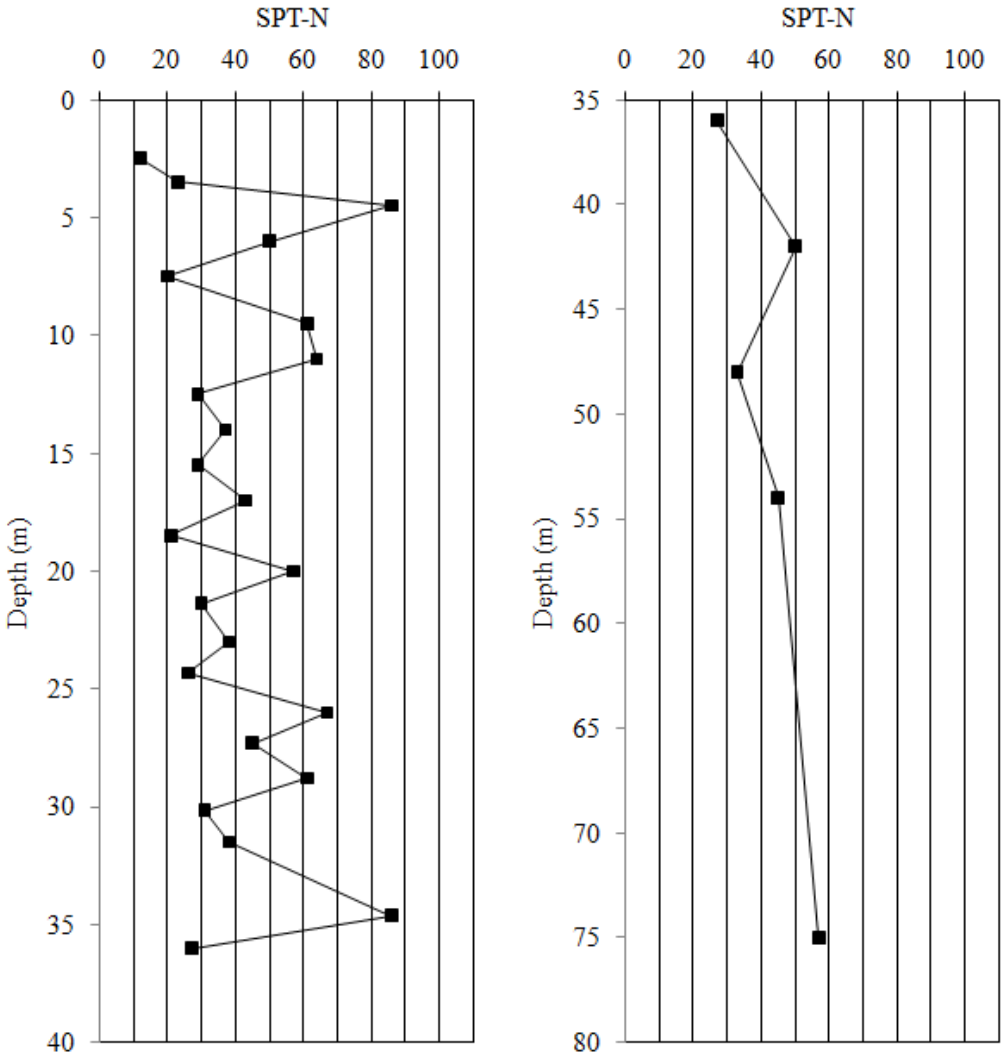

Figure 2.7 Results of standard penetration tests in the borehole.

2.1.3 Core Barrel samplers

Rotary core barrel samplers which were originally designed for sampling in rock are also able to recover samples from hard soils. In application, the drilling machine on the ground surface rotates drilling rods that are connected to a cutting bit. A downward force applied by drilling machine to drilling rods makes cutting bit advance in formations encountered. The specimen enters into the sampling tube behind the bit, as its cutting edge advances through the formations. Drilling fluid cools the bit,

removes cuttings and carries the particles to the ground surface [USACE, 2000]. A single-tube core barrel sampler recovers slightly disturbed samples that can be used for classification. Figure 2.8 shows a schematic view of a single-tube core barrel sampler. In the borehole opened in Adapazarı, the core barrel samples were recovered at depths where use of Thin-Walled tube samplers was not possible due to very stiff layers encountered. The specimens were used in lab tests only for classification of layers encountered. The depths of recovered core-barrel samples are shown in Figure 2.2. Detailed information on the core barrel samples are provided in the borelog [TUBITAK, 2010] presented in Appendix A. Figure 2.9 shows recovered sample from Adapazarı by core-barrel sampler.

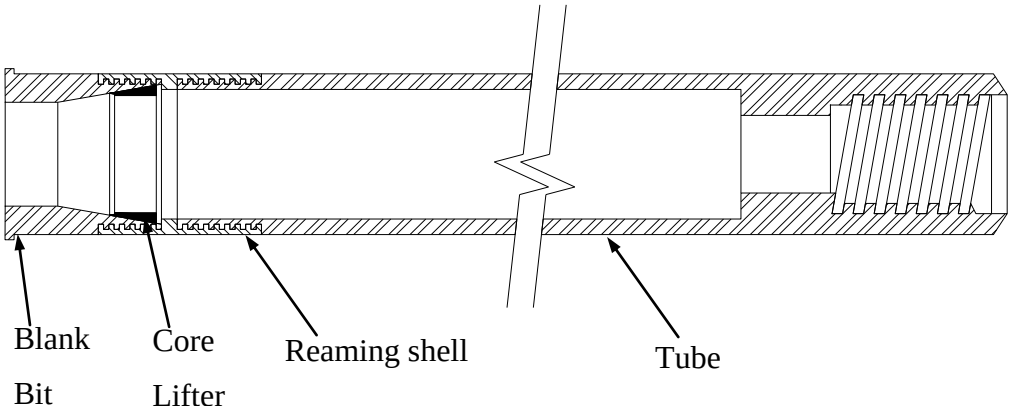

Figure 2.8 Schematic view of a single-tube core-barrel sampler according to ASTM D 2113-99.

Figure 2.9 Recovered core-barrel sample.

2.2 P-S Suspension Logging

Following the end of drilling at depth of 118 m, borehole was left to rest for a duration of 15 days before the seismic velocity measurements. A PVC pipe was placed inside borehole and metal casing was removed. The diameter of PVC pipe is 76 mm which provides the necessary space for P-S suspension logging. The PVC pipe could not be advanced to levels deeper than 76 m because of the decrease in borehole diameter in gravelly layers. The PVC pipe was filled with water afterwards. A mixture of water and cement was injected in the space between PVC pipe and borehole walls so that adequate contact between the PVC pipe and the surround borehole walls was achieved. A concrete cover with a metal cap was build on top of the borehole in order to keep the borehole sealed for 15 days (Figure 2.10). The P-S suspension logging technique has been widely in use in Japan since 1980 for soil profiles with low shear wave velocities [Tanaka et al., 1985; Ng et al., 2000]. The method is the most feasible technique in measuring shear wave velocity at depths exceeding 200 m [Ishihara, 1996; Chen and Wu, 2000; FHWA, 2008; EPRI, 1993]. This technique was successfully used on different geological backgrounds, such as the silty and clayey soil profiles of Texococo lake bed in Mexico and sediments of Ilan County in Taiwan [Mayoral et al., 2008; Kuo et al., 2009]. P-S suspension logging method provides more information on local variability in velocity profile than most other geophysical techniques [Pecker, 2007; EPRI, 1993]. The characteristics of Adapazarı soils as regards the low shear-wave velocity and heterogeneity, and the initially unknown exploration depth on the deep basin were the reasons of choosing P-S suspension logging method for measurement of shear-wave velocity in the experienced layers.

Figure 2.10 Preparation of the borehole for P-S suspension logging: a) installation of PVC pipes inside the borehole, b) the sealing of borehole.

Figure 2.11 shows a schematic diagram of P-S suspension logging. Approximately a 7 m long probe, consisting of an impulse source and two receivers that are isolated from each other by flexible cylinders, is suspended by a conductor cable in borehole filled with water. The source is located near probe's bottom. The lower biaxial geophone receiver is located 3 m above the source. The upper biaxial geophone is located 1 m above the lower geophone. The impulsive pressure generated by the source is horizontally transmitted to the soil adjacent to borehole walls by a P-wave propagating in the fluid inside the borehole. The P-wave arriving at the wall causes a horizontal displacement in the adjacent soil. The disturbance on the boundary propagates upwards with P and S-waves propagating in soil, finally resulting in disturbance on the wall section just near to the receivers. The filter (rubber) tube between the source and the receivers is necessary for reducing the amplitudes of P-waves propagating from the source to the receivers within the borehole fluid (i.e., for noise reduction). The borehole fluid transmits the P-wave generated by the disturbance on the wall to the receivers. Shear wave's travel time and therefore its velocity can be measured by monitoring motion of the fluid by geophones. Two impulses of opposite polarity are

used in order to distinguish between P- and S-wave arrivals. The digitally recorded signals of geophones then have to be analyzed by an experienced operator who picks the arrival times of both compression and shear waves at each geophone. The P- and S-wave velocities are calculated by employing the differences in arrival times between the two geophones that are 1 m apart [Ishihara, 1996; Kramer, 1996; EPRI, 1993].

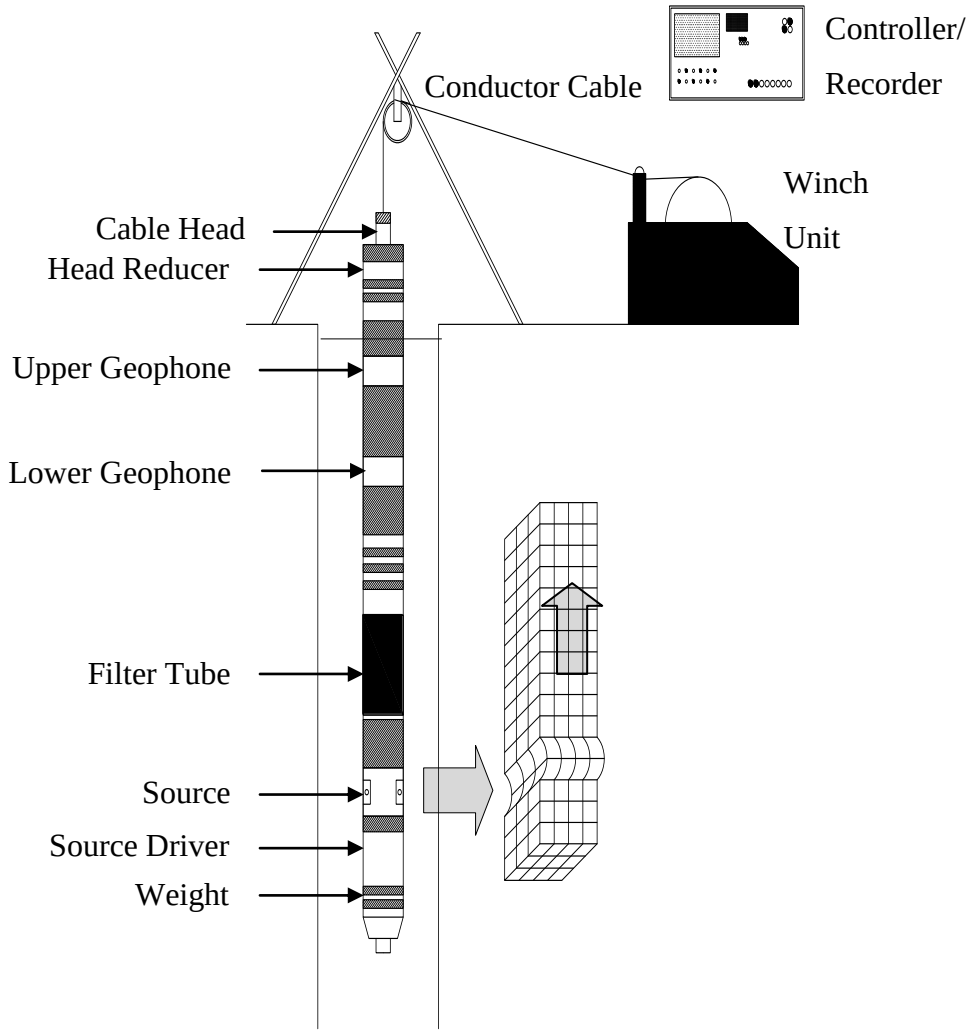

Figure 2.11 A schematic diagram of P-S suspension logging [EPRI, 1993].

Figure 2.12 shows P-S suspension logging in Adapazarı on 18.12.2009. Since the end of PVC pipe is at depth of 76 m and the distance between the source and the lower geophone is 3 m, the logging has ended at depth of 73 m. The logging interval is 0.5 m for the top 50 m of borehole, and 1 m at depths between 50 and 73 m. The S- and P-wave profiles of the site are shown in Figure 2.13 and Figure 2.14 respectively. The

sudden drop in P-wave velocity at 64 m possibly depicts the severe loss of integrity in materials located at the periphery of borehole.

Figure 2.12 The equipment and stages of P-S suspension logging in Adapazarı: a) the probe, b) the borehole with PVC pipe, c)lowering the probe inside the borehole, d) suspending the probe inside the borehole with a cable, e) the winch unit, and f) laptop used for recording and analyzing data.

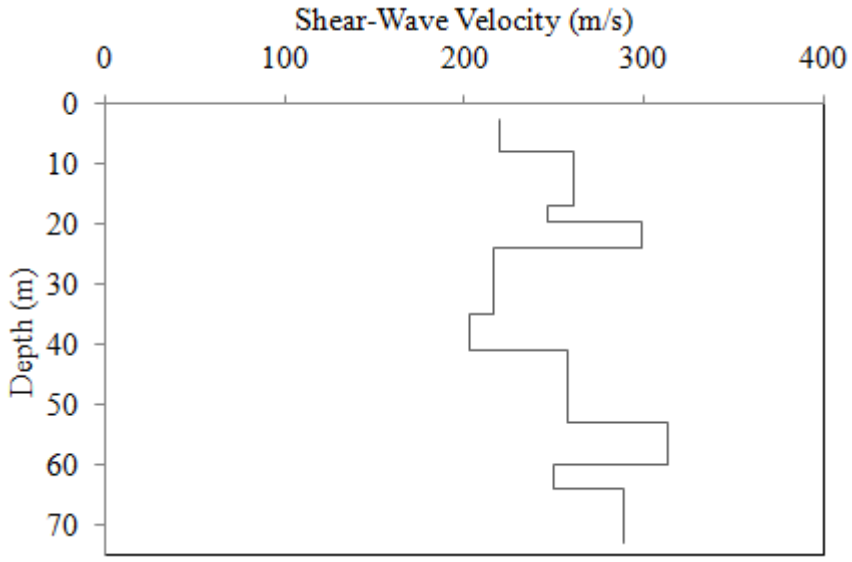

Figure 2.13 The variation of S-wave velocity through the borehole.

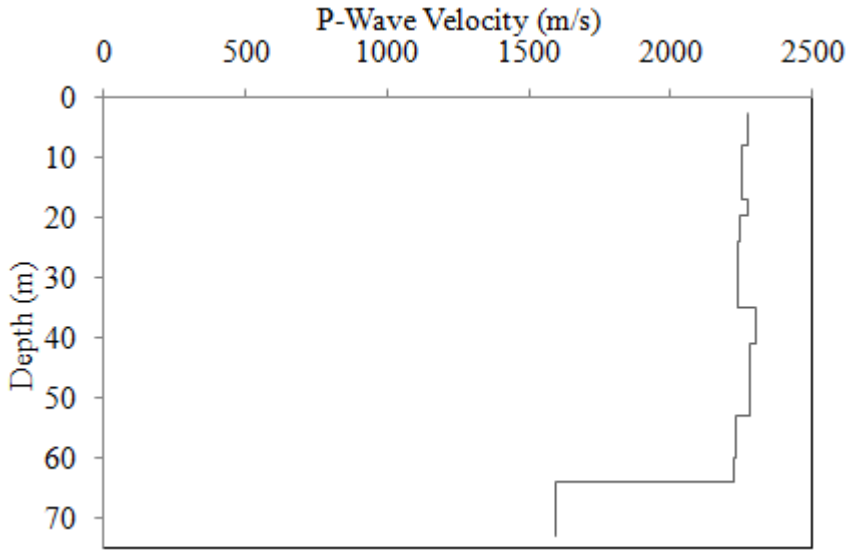

Figure 2.14 The variation of P-wave velocity through the borehole.

S-wave velocity (V_s) is compared with SPT-N in Figure 2.15. The low coefficient of determination (r^2=0.08) suggests that there is no correlation between V_s and SPT-N. However, both sets of data sets agree in that the site class is D according to the seismic site classification system of NEHRP (2003).

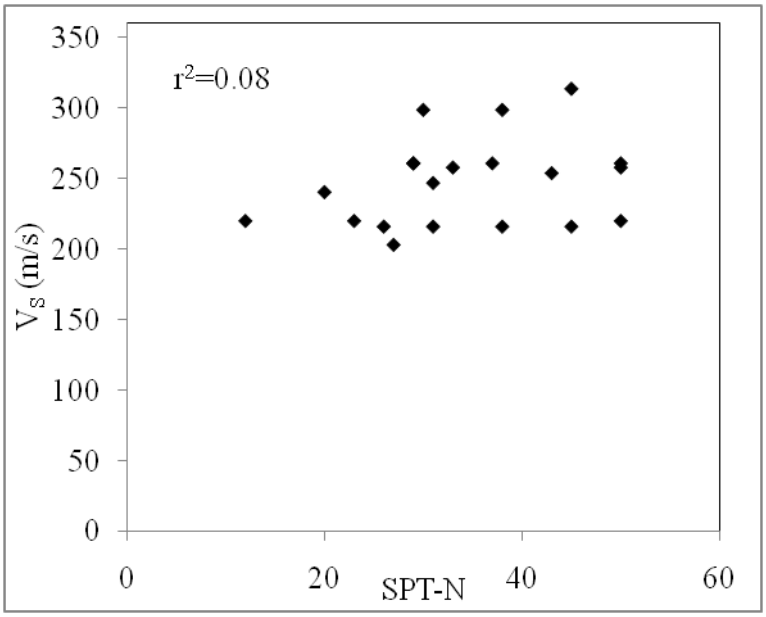

Figure 2.15 V_s versus SPT-N.

2.3 Comparisons with other studies

The log of a 200 m deep borehole opened by General Directorate of State Hydraulic Works [DSİ, 2001] near Teverler building, which is located approximately 750 m east-northeast of the parking lot (Figure 1.1), shows layering of deep deposits. The two soil profiles are compared in Table 1.1. Despite the distance between the two boreholes, the soil profile on parking lot is reasonably consistent with the borelog of DSİ. On both sites, majority of the layers shallower than 75 m consist of fine materials. The stiff gravelly layer is first encountered at the depth of 57 on parking lot, whereas stiff gravelly sand is encountered at depth of 74 m on DSİ site. The thickness of the gravelly layer is 12.70 m on DSİ borelog, whereas the lower boundary of stiff gravel was not reached at the end of boring at parking lot. The comparison of ranges of SPT-N achieved on two sites (Figure 2.16) shows that the soils experienced on parking lot are stiffer than the soils experienced near Teverler building, provided that the energy efficiency achieved in SPT is similar for both borings.

Table 2.1 Comparison of soil profile on parking lot with that on site of Teverler building.

Borelog of DSİ (2001)		**Borelog of TUBITAK (2010)**	
Depth (m)	*Description*	*Depth (m)*	*Description*
0.00 – 0.50	Artificial Fill	0.00 – 2.00	Artificial Fill
0.50 – 6.70	Silt	2.00 – 8.00	Silty Sand, Sand
6.70 – 13.00	Silt-Clay	9.00 – 11.00	Silt-Clay
13.50 –15.40	Sand	11.00 – 13.00	Sandy Silt
15.40 – 24.30	Clay	13.00 – 25.50	Silt-Clay
24.30 – 26.30	Sand	25.50 – 32.50	Silt
26.30 – 33.90	Clay		
33.90 – 42.00	Sand	32.50 – 54.00	Silt-Clay
42.00 – 74.30	Clay	54.00 – 57.00	Sand
		57.00 – 72.00	Clayey Gravel
		72.00 – 75.50	Clay
74.30 – 87.00	Gravelly Sand	78.00 – 88.50	Clayey Gravel
87.00 – 146.50	Clay	88.50 – 118.00	Gravel

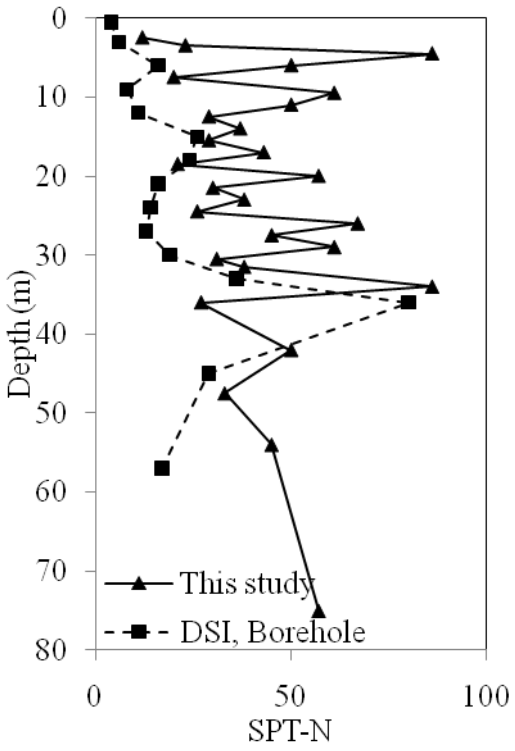

Figure 2.16 Comparison of penetration resistances experienced at parking lot and near Teverler building.

Figure 2.17 compares the shear-wave profiles reported by several studies. The parking lot is roughly located between ADC and ADU sites experienced by Kudo et al. (2002). The results of P-S suspension logging are reasonably consistent with the V_S profile given for ADC site at depths below 38 m. However, the range of V_S measured in deeper deposits of parking lot is smaller than 441 m/s, suggested by Kudo et al. as an average value for a 97 m thick soil deposit (Table 1.1). On the other hand, the range of V_S at depths exceeding 44 m is more consistent with that of ADU site. Three of the velocity profiles (PEER Sites A, D, and J in Figure 1.1) presented by Rathje et al. (2002) are also compared with the results of P-S suspension logging. However, none of the velocity profiles is consistent with the others shown in Figure 2.17.

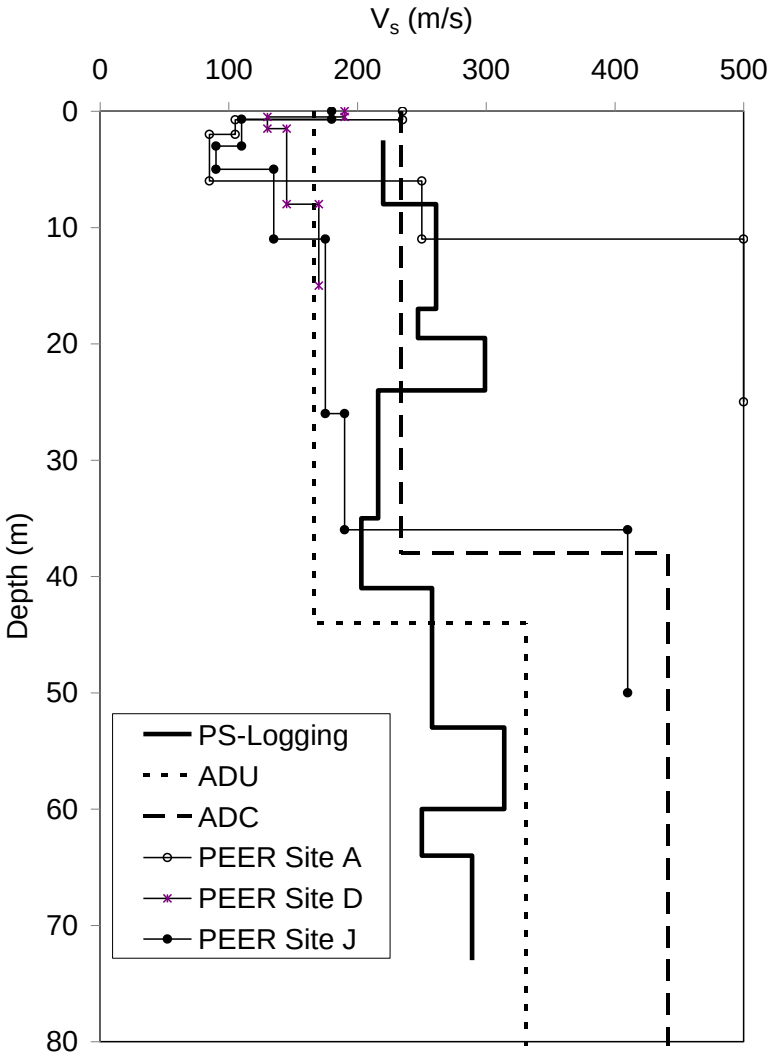

Figure 2.17 Comparison of velocity profiles reported in literature with the velocity profile on parking lot.

CHAPTER 3

CYCLIC LOADING TEST APPARATUS AND PROCEDURES

3.1 Introduction

A series of cyclic direct simple shear (CDSS) tests were run in order to construct modulus-reduction and damping curves for all undisturbed soil specimens recovered from Adapazarı. When compared to that of cyclic triaxial tests (CTX), CDSS apparently has three advantages: First, the shearing direction is similar to that of a vertically incident S-waves propagating on site [Duncan and Dunlop, 1969; Kramer, 1995]. Second, saturation of specimen is not necessary since constant-volume (undrained) soil response is achieved by instantaneous adjustments of vertical confining pressure on specimen [Taylor, 1952; Duncan and Dunlop, 1969; Airey et al., 1985; Budhu and Britto, 1987]. Third, the likelihood that a soft CDSS specimen is excessively disturbed during preparation for testing is less than that of a CTX specimen, because the height of a CDSS specimen is much less than its diameter, whereas the height of slender CTX specimens is approximately two times the diameter. The last two advantages of CDSS tests are crucial for engineering studies that have important time constraints. The CDSS test procedure is based on that of a constant-volume direct simple shear testing of soils, which has been studied extensively for half a century and is described in the standard ASTM D6528-07.

The simple shear is the test condition that only normal (σ_v) and shear (τ) stress acting on top face of a prismatic specimen is defined, whereas the displacement constraints exist for the other boundaries: The bottom face of specimen is theoretically fixed, and

the radial strain (orthogonal to the known normal stress acting on top face) on specimen is zero (Figure 3.1).

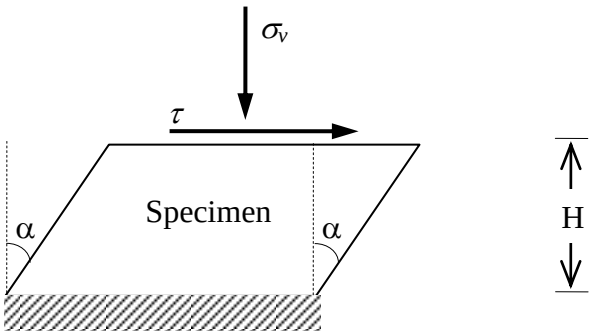

Figure 3.1 The simple shear condition, Dyvik et al., 1987.

In absence of any (horizontal) shear stress acting on top, the state of stress for the horizontally confined specimen is similar to that in an oedometer. The horizontal stress acting on top ideally imposes uniform shearing condition on a prismatic specimen. The volumetric strain is equal to the axial strain, and the volume of the specimen during shearing is proportional to its height. During a constant-volume test, the height of the prismatic specimen is constant whereas the vertical stress is variable. Hence, in a constant-volume direct simple shear test, the variation in total vertical load on top face (instead of normal stress) that yields a constant height for specimen is monitored, whereas the horizontal load on top face (instead of shear stress) is controlled. For simple calculations, it is assumed that the normal (σ_v) and shear (τ) stress on specimen is uniformly distributed. Nevertheless, the assumption is valid in the case that the diameter of specimen is considerably larger than its height [Duncan and Dunlop, 1969; Airey et al., 1985; Budhu and Britto, 1987].

The first constant-volume direct simple shear tests were run at Massachusetts Institute of Technology in 1948 [Taylor, 1953]. Kjellman [1951] employed a device with a cylindrical specimen constrained by a rubber membrane reinforced with wire rings. The wire rings ensure the specimens to be sheared uniformly in horizontal direction. The Norwegian Geotechnical Institute developed a direct simple shear device to test sensitive Norwegian quick clays that became the standard research device for direct simple shear testing [Bjerrum and Landva, 1966].

A constant-volume shearing condition was achieved by adjusting the vertical load, such that the height of laterally confined cylindrical specimen was constant (Figure 3.2.a). Besides, the change in total vertical stress during shearing is assumed to be equal to change in pore water pressure in a real undrained test. Dyvik et al., (1988) actually showed that the results of constant-volume simple shear tests agree with those of true undrained simple shear tests. An alternative to tests with wire-reinforced membrane is proposed by Roscoe (1953), and is known as the Cambridge simple shear apparatus. Instead of a cylindrical specimen, a rectangular specimen was used. Hence, the specimen could be laterally confined with rigid plates supported by hinges and sliders (Figure 3.2.b) in order to achieve simple shear conditions [Airey et al. 1985; Budhu and Britto, 1987].

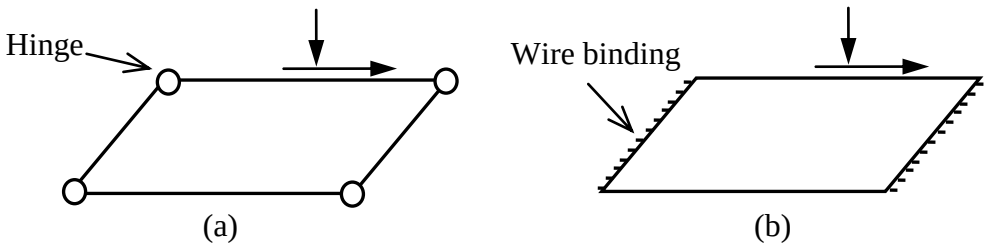

Figure 3.2 Basic mechanism of a) a Cambridge simple shear apparatus, and b) a Norwegian simple shear apparatus [Airey et al., 1985].

By installation of a cyclic load unit that can successively reverse the direction of shearing, the direct simple shear apparatus becomes a CDSS, which can be employed for determination of liquefaction susceptibility and cyclic shear strength of soils [e.g., Finn et al., 1971; Ishibashi and Sherif, 1974; Peacock and Seed, 1968; and Seed and Peacock, 1971], and for investigation of nonlinear soil response to shearing [e.g. Andersen, 1983; Anderson et al., 1983; Vucetic and Dobry, 1986; Tan and Vucetic, 1989]. Some improvements on CDSS apparatus have been proposed so that lower cyclic strain levels can be effectively tested for purpose of calculating dynamic soil characteristic [Vucetic, 1984; Doroudian and Vucetic, 1995, 1998].

Most of the CDSS apparatus used in the previous studies employ the reinforced membrane for testing. On the other hand, the apparatus used in this study employs an alternative design for achievement of simple shear condition. The design consists of a stack of aluminum rings around membrane, the use of which is allowed by ASTM

D6528-07 for direct simple testing [ASTM D6528-07]. Reinforcing the membrane externally with aluminum rings provides a cheaper substitute for wire-reinforced membrane, since only the ordinary rubber membrane is to be replaced when it is damaged during tests. The details of the apparatus are presented in the following. Baxter et al., (2002) and (2010) presented test results depicting the consistency between the two types of direct simple shear apparatus. Hence, the initial emphasis was put on the calibration of CDSS apparatus and on the measurement of frictional forces acting on the apparatus during a cyclic loading test, before running the CDSS tests on undisturbed specimens from Adapazarı.

3.2 Cyclic direct simple shear apparatus

The CDSS test apparatus used in this study is a Geocomp™ ShearTrac II-DSS system [Geocomp, 2007a] located in the Soil Mechanics Laboratory of General Directorate of Highways in Ankara (Figure 3.3).

Figure 3.3 ShearTrac II, the cyclic direct simple shear apparatus used for the tests.

The device allows load-controlled constant-volume CDSS tests with a load frequency up to 1 Hz on a consolidated soil specimen, as well as the conventional displacement-controlled slow monotonic loading (i.e., DSS) tests. The constant-volume shearing of soil is achieved by a closed-loop computer controlling the vertical load on specimen according to the feedback from vertical displacement sensors. A computer controls the micro-stepper motors that apply vertical and horizontal loads on specimen.

Figure 3.4 shows a simplified diagram of the CDSS device: A soil specimen of diameter 63.5 mm is confined by a rubber membrane supported by Teflon covered aluminum rings instead of conventional reinforced membranes. The load capacity of the device is 4.4 kN. The allowed range of velocity for the load pistons is from 0.00003 to 15 mm/min. The peak displacement allowed for load units (i.e., travel length of load pistons) is 24.45 mm in vertical direction and ±12.5 mm in horizontal direction. The resolution (i.e., step-size) in displacements allowed by micro-stepper motors is 0.0013 mm in both directions.

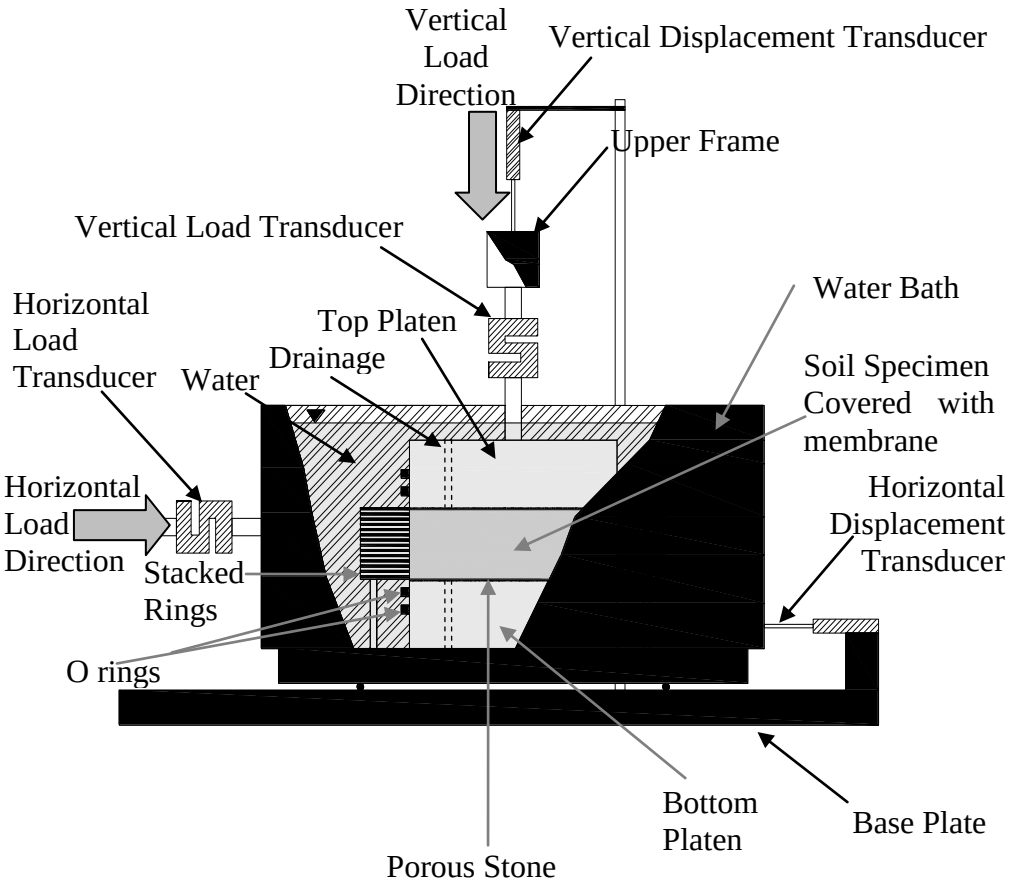

Figure 3.4 Simplified diagram of the CDSS device.

3.2.1 Testing procedure

CDSS test in this study consists of three phases: Specimen preparation and setting up the test apparatus, consolidation, and constant-volume shearing. The phases of CDSS, which are consistent with the standard ASTM D 6528 -07, are explained in the following.

3.2.1.1 Specimen preparation and setting up the test apparatus

A circular plate attached to an electro hydraulic jack is used to drive soil samples out of the Shelby tubes (Figure 3.5.a). The specially manufactured sharp-edged rings with the internal diameter of 63.5 mm and the height of 20 mm (Figure 3.5.b) are located on the openings of tubes successively, such that the soil specimens fill the rings one after another with the least disturbance as they leave the tubes. After trimming the free faces of specimens filling the rings (Figure 3.5.c), the specimens are immediately identified, stored in desiccators and are tested as soon as possible.

For a CDSS test, each trimmed specimen is carefully placed on the porous stone that is mounted on the bottom platen of ShearTrac II-DSS equipment (Figure 3.6.a). Top and bottom faces of specimen are covered with filter papers to avoid contact between those faces and the porous stones. Then, the sides of specimen are covered with a rubber membrane with the help of a suction tube (Figure 3.6.b). The top porous stone and platen are placed on the specimen and the membrane is fixed to the top and bottom platens by O-rings (Figure 3.6.c). The Teflon covered aluminum rings are placed around the membrane (Figure 3.6.d). Then, the bottom platen is fixed inside the water bath (Figure 3.6.e). Finally, the vertical load transducer connected to the upper frame is fixed to the top platen in order to complete the test set-up (Figure 3.6.f).

Figure 3.5 Lab equipment used for specimen recovery: a) Shelby tube installed on an electro-hydraulic jack, b) specially manufactured small rings, c) knife trimming the specimen.

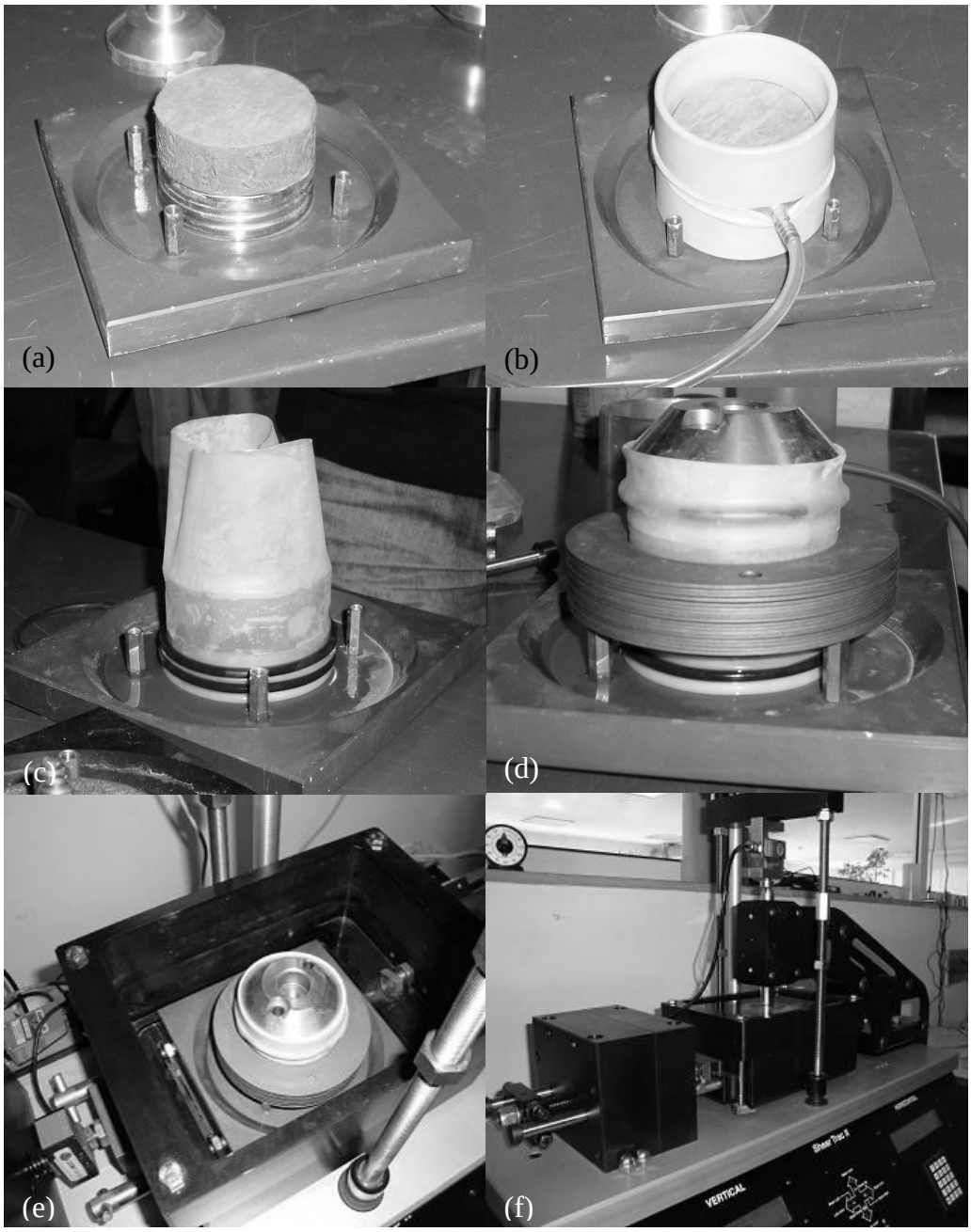

Figure 3.6 Phases of specimen preparation for CDSS tests: a) placing specimen on the bottom plate, b) covering specimen with a membrane, c) fixing membrane to bottom plate by O-rings, d) installing Teflon covered rings around specimen and fixing membrane to top and bottom plates, e) fixing base plate inside water bath, f) connecting transducers to the system.

3.2.1.2 Consolidation

After setting up the test, the consolidation phase of the test is initiated. The normal stress for consolidation (σ_v) is set to a pre-selected value that is larger than the effective consolidation pressure in situ. According to Lambe and Whitman, (1969) the disturbance during sampling irreversibly changes the compressibility of soil, such that the void ratio in situ cannot be replicated by simply applying effective stresses in situ during consolidation phase of an consolidated-undrained triaxial test: "*For uniform, normally consolidated clays, the best procedure is to consolidate samples to effective stresses greater than twice those existing in situ, and then to correct the measured undrained strength by the ratio of the effective stress in situ to the consolidation stress used in the laboratory test*. *This procedure overcomes the errors caused by sampling procedure."* Since the small-strain shear modulus, G_{max}, is sensitive to void ratio (Equation 4.6) a similar procedure is followed for CDSS tests.

Considering the shallowness of ground water table (at 6 m), the specimens are systematically consolidated under the normal stress equal to total overburden pressure in-situ, which is approximately 50% to 100% greater than the effective overburden pressure at depths between 9 m to 33 m. Only two tubes were recovered from very shallow layers above the ground water table. Hence, σ_v is only 20% higher than the effective overburden pressure for specimens recovered from those very shallow layers, because a large reduction in void ratio can result in an inordinate change in response of soils to cyclic loading. The density of each specimen is calculated by measuring the specimen mass before setting up the test, so that a density profile can be developed for calculation of total and effective overburden pressure. The mean and standard deviation of sample for soil density is 1.85 and 0.79 t/m^3. No significant relationship between the density, soil type, depth, and S-wave velocity is observed. Hence, it is concluded that the dispersion in soil density through the profile is random and the mean overburden pressure at depth *z* can be reasonably estimated by the equation $\sigma_v = z \cdot 18.1 (kPa/m)$.

During the consolidation phase of a CDSS test, the normal consolidation pressure is increased to the target value in steps. Then, the specimens are left to consolidate for a day, which is longer than the duration necessary for completion of primary consolidation. The consolidation procedure is consistent with the standards

ASTM D6528 – 07 and ASTM D2435 – 04. In order to increase the number of cyclic loading tests on the same specimen, the staged loading method is employed {Ishihara, 1996]. Following a cyclic loading test the specimens are reconsolidated under the same vertical consolidation pressure, in order to dissipate excess pore-pressures before the next cyclic loading stage. The staged loading procedure is similar to that for cyclic triaxial (CTX) testing, which is explained by ASTM D3999-91. In order to finalize a consolidation phase, the degree of consolidation is continuously monitored by plotting the displacement of vertical load piston versus square root of time, similar to the plot proposed by Taylor, (1948) for estimation of coefficient of consolidation (Figure 3.7). Hence, the end of a (re)consolidation phase is not before the end of primary consolidation, such that there is no significant increase in vertical displacement readings.

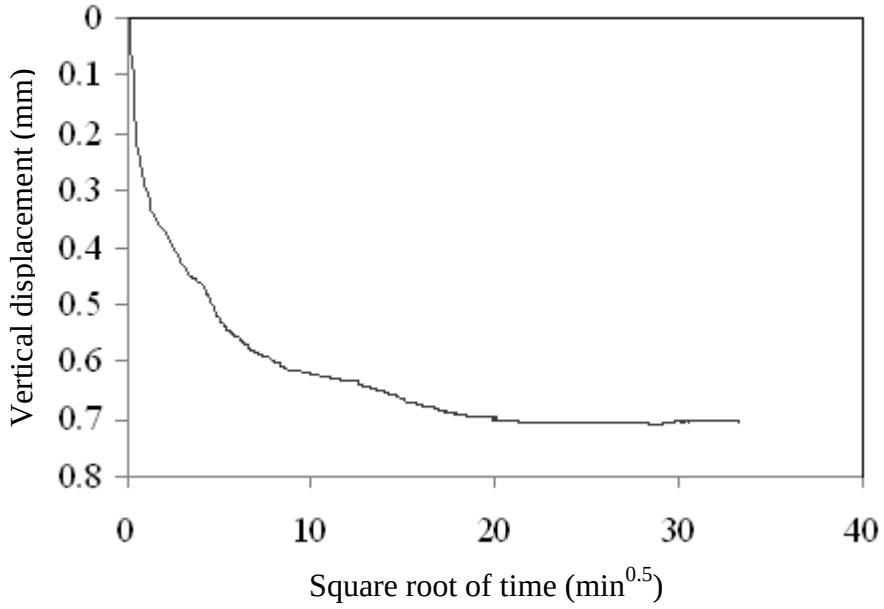

Figure 3.7 The change in vertical displacement with square root of time during a consolidation phase of test.

3.2.1.3 Cyclic shearing

After a (re)consolidation phase, constant-volume cyclic shearing of specimen begins. The horizontal load history acting on specimen is considered as a sinusoidal waveform. The frequency of cyclic load, *f*, is 1.0 Hz. Nonetheless, the form of the load

applied by motors may not follow the ideal sinusoidal waveform due to the quality of load control system. The problem of achieving an ideal waveform is particularly important for cyclic load-controlled tests on soils whose response is excessively nonlinear, whereas the simple manual control of strain (or, displacement) rate in a cyclic displacement-controlled test provides very satisfactory results [Doroudian and Vucetic, 1995]. The criteria of acceptable waveforms used in a load-controlled CTX test can also be considered for a similar CDSS test. Hence, the waveforms are acceptable provided that the difference between the amplitudes and durations of successive half-cycles is less than 10%, the noise (ringing) in the waveform is not significant, and there are not any prominent spikes near the peaks of waveform [Silver, 1977]; see Figure 3.8. The unacceptable waveforms can cause abnormal changes in pore water pressure resulting in significant deviations from the actual soil response to an ideal sinusoidal waveform.

The ShearTrac II apparatus uses a closed-loop load control system in order to provide a load-history consistent with that of an ideal sinusoidal waveform. For the best results, the software controlling the loading unit requires the input of the parameter called "*Update A*", which is dependent on several factors such as the stiffness and the dimensions of soil specimen, frequency of loading (*f*), and calibration factors of the apparatus [Geocomp, 2007a]. The parameter is used for automatic updating of the load increments in a closed-loop loading system during a cyclic loading test due to nonlinear response of the material. A calculation tool for *Update A* is provided by the manufacturer such that the factors necessary for calculation of *Update A* are entered in cells of a spreadsheet file, on which *Update A* is computed by a series of built-in functions. Among those factors, the material stiffness is the most difficult one to be justified before a test. The material stiffness factor (*Gdr*) varies in range from 0.5 for a very stiff material to 10 for a very soft material. Hence, the choice for material stiffness factor requires experience on similar material tested with the ShearTrac II device. After several tests on reconstituted specimens with properties similar to those of Adapazarı deposits and initial tests on the undisturbed specimens, it is concluded that the factor to be used is between 2 and 2.5 for the soil samples recovered from Adapazarı. Figure 3.9shows the waveform generated with a non-appropriate *Gdr* value. Apparently, the waveform of applied load is far from the criteria stated by Silver [1977]. In contrast, Figure 3.10 shows an acceptable waveform that is generated by an appropriate selection of *Gdr*.

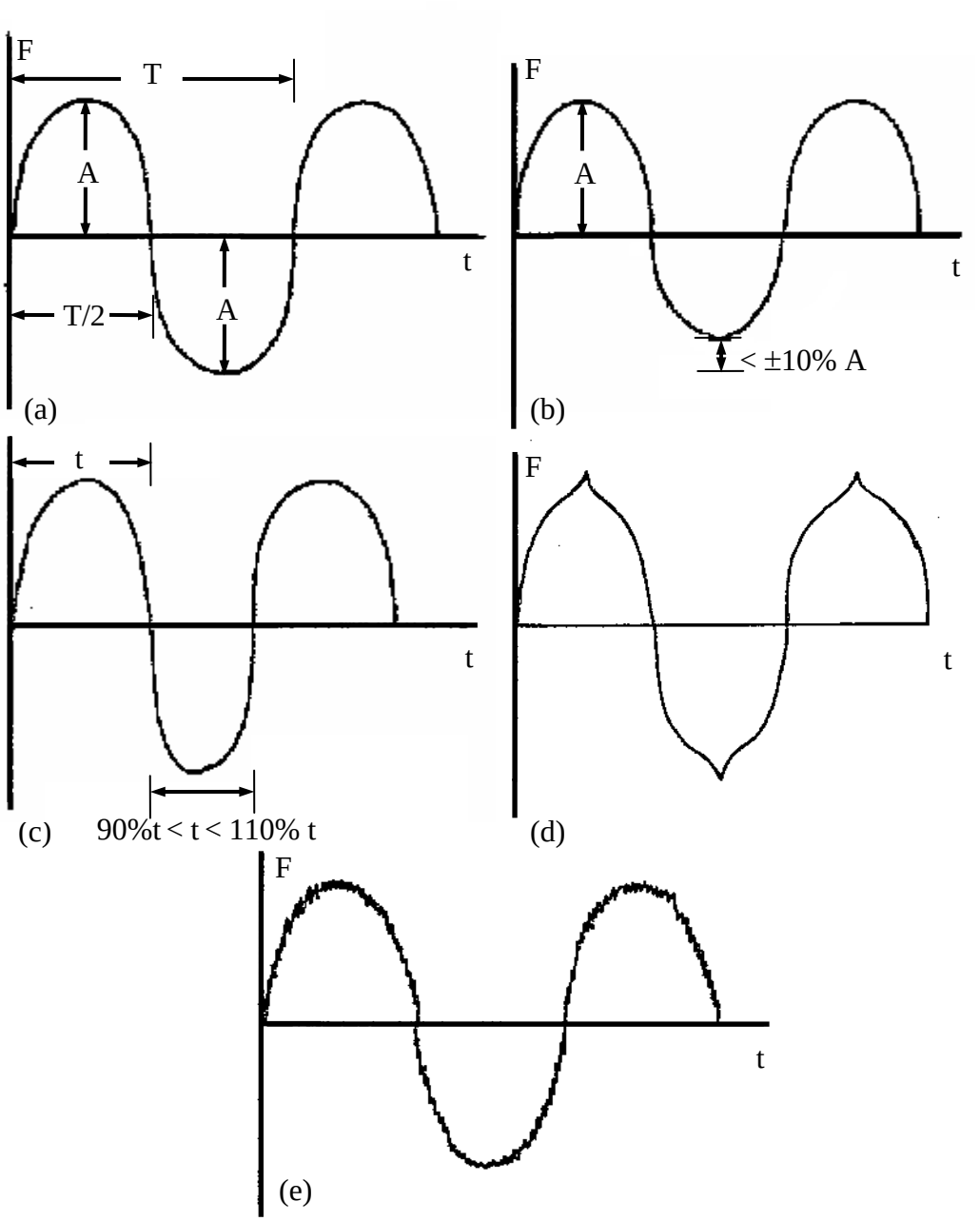

Figure 3.8 Acceptability criteria for cyclic load-histories: a) an ideal waveform, b) the limit for difference in amplitudes of successive half-cycles, c) the limit for difference in duration of successive half-cycles, d) unacceptable waveform due to spikes at peaks, and e) unacceptable ringing on waveform [Silver, 1977].

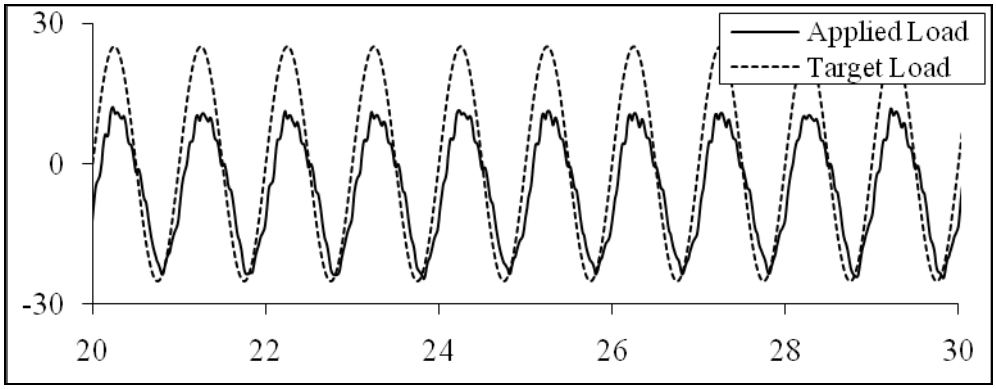

Figure 3.9 Unacceptable waveform generated by an inappropriate selection of *Gdr*.

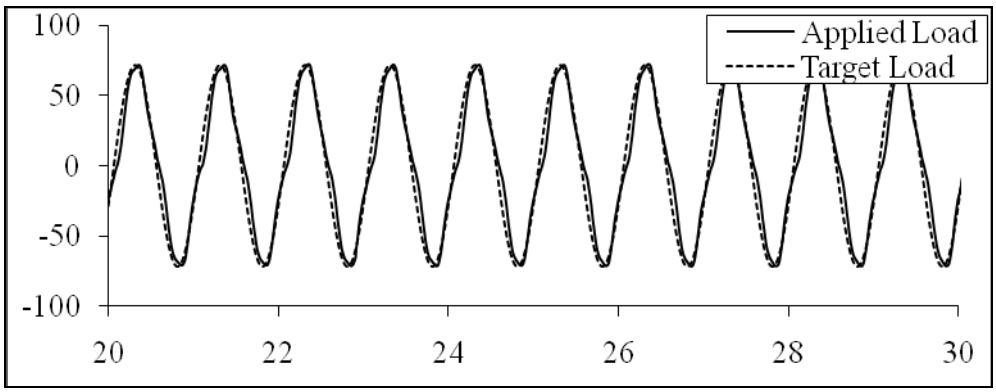

Figure 3.10 Acceptable waveform generated by an appropriate selection of *Gdr*.

The other important parameter in the algorithm of closed-loop control is the *P-Gain* [Geocomp, 2007a], because it is related to the response rate of load control to change in material stiffness. Parameters of the algorithm that instantaneously calculates the load increments for the motors are dependent on the stiffness of the material. On the other hand, the necessary information for determination of optimum parameters is only available after the first cycle of loading. In the case that the initial rate of updating is too slow or too fast, the applied waveform can respectively undershoot or overshoot the target amplitude of sinusoidal waveform during its first cycle. A careful adjustment of the parameter *P-Gain* is particularly important to reduce the testing error due to an inappropriate first load cycle. After several trials with reconstituted specimens, it is concluded that the default value (*P-Gai*n=2.5) stated by the manufacturer is the optimum value for the most satisfactory results. Hence, considering the difficulty in achieving an acceptable form in the first load cycle, the second load cycle is considered as being representative for the ideal first-cycle

response of specimens. The other closed-loop control parameters, *I-Gain* and *D-Gain*, that can be entered in the computer program building the closed-loop algorithm; do not significantly affect the test results. The latter conclusion is verified with tests on reconstituted specimens and through personal communications with the manufacturer.

3.2.2 Estimation of frictional forces on the test apparatus

During a CDSS test with the ShearTrac II apparatus, the horizontal load transducer measures the load exerted on the water bath, which is equal to the shear load on specimen in the ideal case that the components of test apparatus (e.g., connection between water bath and base plate, and the stacked Teflon covered faces of aluminum rings) are frictionless. Besides, the membrane contributes to reaction of the specimen to shearing. Hence, it is necessary to estimate the total resistance of testing apparatus and the membrane to horizontal displacements induced during a cyclic loading test. Then, the net shear force exerted on the specimen should be calculated by eliminating the contribution of friction forces and membrane reaction in total load applied on the water bath, which is recorded by the horizontal load transducer, before any interpretation of test results [ASTM D6528 – 07]. The test results are obviously acceptable only in the case that the frictional forces and the membrane resistance to shearing are very small than the reaction of specimen. In the other case, the test results will be sensitive to the apparatus's compliance with the behavior of soil, and to the parameters assumed for the calculation of net stress acting on specimen.

As a simple rheological model for calculation of the total frictional resistance of the apparatus and the membrane reaction to horizontal displacements, the simple visco-elastic (Voigt) model shown in Figure 3.11 is considered [Fung, 1994].

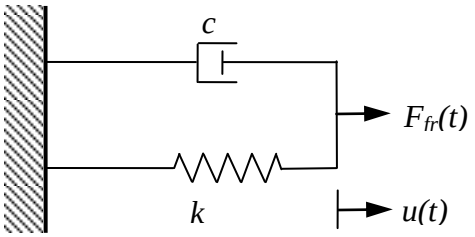

Figure 3.11 Voigt model of linear visco-elasticity, [Fung, 1994].

The total reaction (F_{fr}) on the rigid support of a linearly elastic spring with a viscous damper in parallel is

$$F_{fr}(t) = k \cdot u(t) + c \cdot \frac{\mathrm{d}u(t)}{\mathrm{d}t} \qquad [3.1]$$

where k is the stiffness of spring, c is the viscous damping coefficient, $u(t)$ is the nodal displacement acting on spring and dashpot, and t is time [Chopra, 1995]. In the case the spring behaves nonlinearly, such that the reaction force acting on spring is equal to $k_{sec}(u) \cdot u(t)$, Equation 3.1 can be restated as

$$F_{fr}(t) = k_{\mathrm{sec}} \cdot u(t) + c \cdot \frac{\mathrm{d}u(t)}{\mathrm{d}t} \qquad [3.2]$$

where k_{sec} is the secant stiffness of nonlinear spring. For a sinusoidal displacement-history with amplitude u_0, the variation of displacement with t is defined by

$$u(t) = u_0 \cdot \sin(2\pi \cdot f \cdot t) \qquad [3.3]$$

When $\mathrm{d}u(t)/\mathrm{d}t=0$, $u(t)$ attains its maximum absolute value, u_0, and k_{sec} can be calculated by Equation 3.4. Supposing that maximum absolute value of F_{fr} is approximately equal to its value at $u(t)=u_0$ (i.e., $F_{fr}(u_0) \cong (F_{fr})_{\max}$) when $2\pi fc/k_{sec}$ is small, k_{sec} can be approximately calculated by the formula

$$k_{\mathrm{sec}} = \frac{F_{\max} - F_{\min}}{u_{\max} - u_{\min}} \qquad [3.4]$$

Where F_{max} and F_{min} are respectively the maximum and minimum reaction forces, and u_{max} and u_{min} are the maximum and minimum displacements recorded during a cyclic loading test. For ideal test conditions, $F_{min} = -F_{max}$, and $u_{max} = -u_{min} = u_0$.

The parameter c can be calculated by using the equivalent viscous damping concept [Chopra, 1995]. The dissipated energy, E_D, in a single cycle is

$$E_D = 2 \cdot \pi^2 \cdot f \cdot c \cdot u_0^2 \qquad [3.5]$$

which is equal to the area enclosed by a hysteresis loop on a force-displacement plot. Hence, the best-fit of c to experimental data can be calculated by a least-squares

analysis on the scattering of $E_D/(2\pi^2 f)$ with u_0^2, such that the paired sample (u_0,E_D) is gathered by calculating the area enclosed by a hysteresis loop (E_D) with displacement amplitude u_0 during a cyclic loading test. For acceptability of data, a sinusoidal waveform for load-history should be achieved.

In order to determine the frictional loads acting on the apparatus and the membrane reaction, Thin Latex balloon filled with water is used as the specimen in CDSS tests. The volume of water injected in balloon is 63000 mm^3, so that the volume of balloon is approximately equal to that of a soil specimen prior to consolidation phase in CDSS tests. Hence, the balloon under pressure can completely fill the volume enclosed by aluminum rings and porous stones. Figure 3.12 shows a schematic view of these tests.

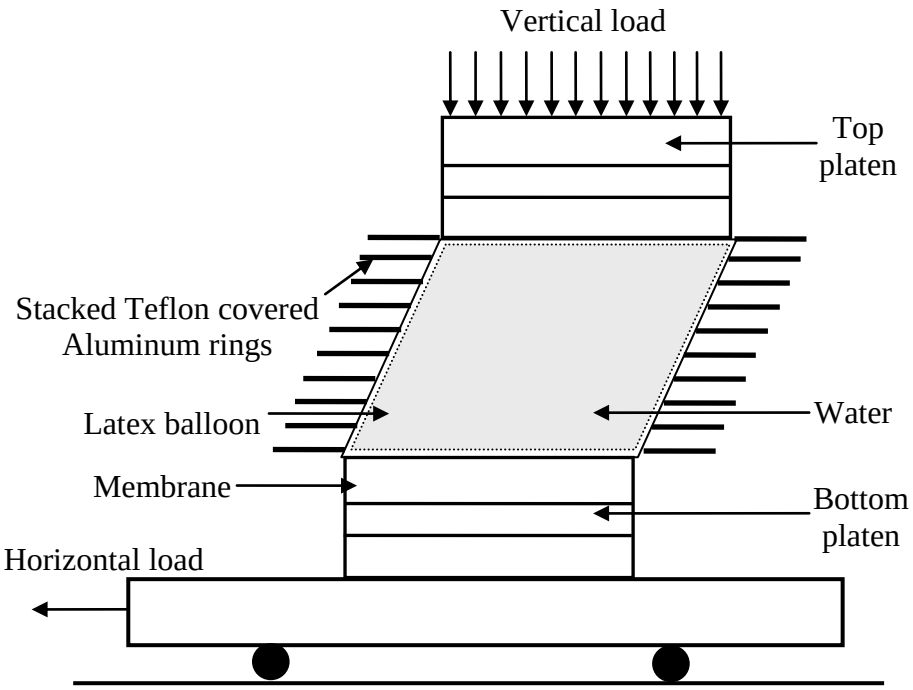

Figure 3.12 Schematic diagram of cyclic simple shear test on a Latex balloon filled with water.

The range of confining pressure applied by vertical load piston is from 50 kPa to 250 kPa, which is reasonably consistent with the range of normal stress considered in testing undisturbed specimens. The lower and upper limits of the pressure range are determined after a set of initial tests, in which the parameter *Gdr* is justified for a range of cyclic shear and vertical stress amplitudes. It is observed that the minimum confining pressure to be considered in the balloon tests is about 50 kPa so that the

closed-loop load-control system can satisfactorily follow a sinusoidal waveform. On the other hand, when the vertical pressure exceeds 250 kPa, a stiffer response to shearing is observed, and any further increase in confining stress resulted in tearing of the balloon before or during cyclic loading phase of the tests. By observation, the behavior at stress levels exceeding 250 kPa is attributed to the penetration of the balloon into the very thin gap between porous stones and aluminum rings. Setting *Gdr* to 2.5 provided satisfactory waveforms for most tests; however, the value is slightly increased for greater ranges of confining pressure and horizontal displacement amplitudes. No change in the default *P-Gain* stated by the manufacturer of ShearTrac II apparatus is deemed necessary.

Figure 3.13.a shows hysteresis loops of a cyclic simple shear test on a Latex balloon filled with water. Figure 3.13.b depicts that the *u(t)* becomes consistent with an ideal sinusoidal waveform following a number of initial cycles. During the tests, it is observed that the relative displacements of adjacent aluminum rings are very uniform, consistent with those of a uniform strain field of a test with soil specimen.

The uniformity is achieved by the interaction between rings and the membrane, such that the tensile force on membrane results in increased horizontal forces acting on rings with larger relative displacements (Figure 3.14), which consequently compel the uniformity in ring displacements. Several tests on water-filled balloons are done. However, some of the results are rejected due to problems related to poor placement of balloon, inconsistent *Gdr*, and tearing of balloon. Those tests resulted in poor and unacceptable waveforms in displacement-histories, and very soft or stiff response to loading compared to tests with reasonably sinusoidal displacement histories.

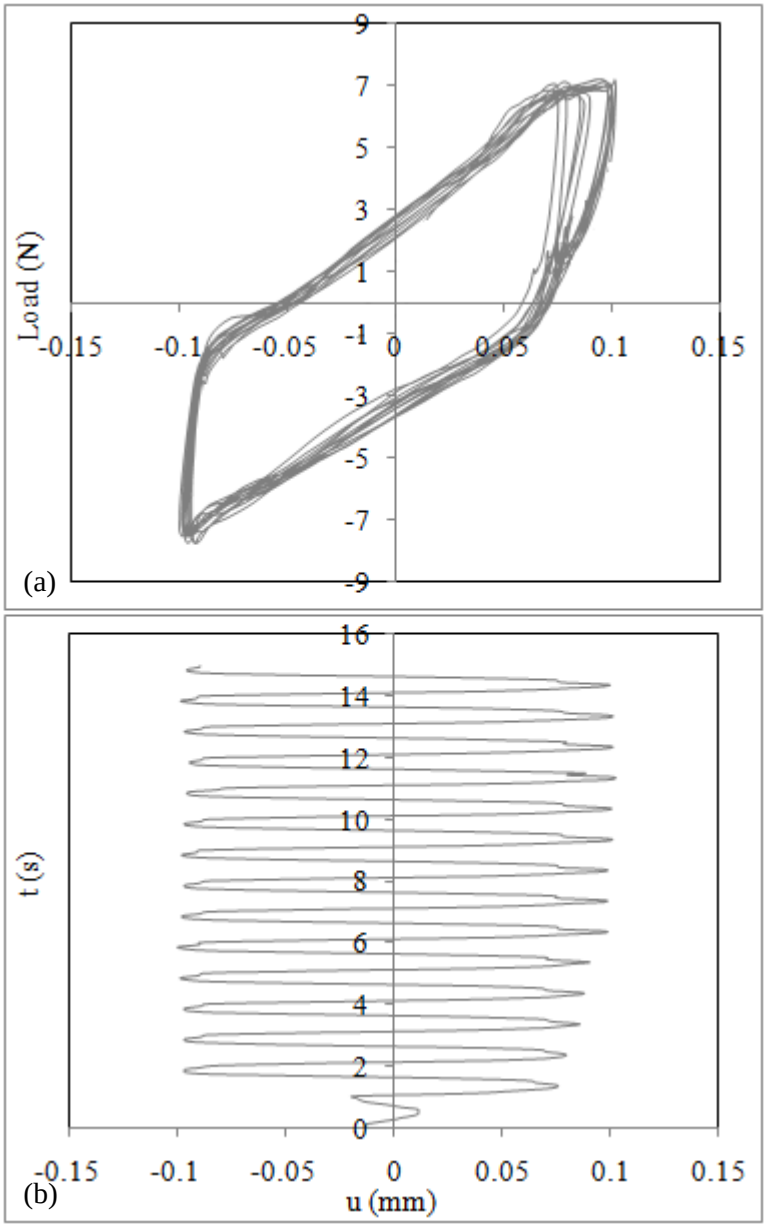

Figure 3.13 a) Hysteresis loops, and b) displacement history during a CDSS test on a water-filled Latex balloon filled under vertical stress of 250 kPa.

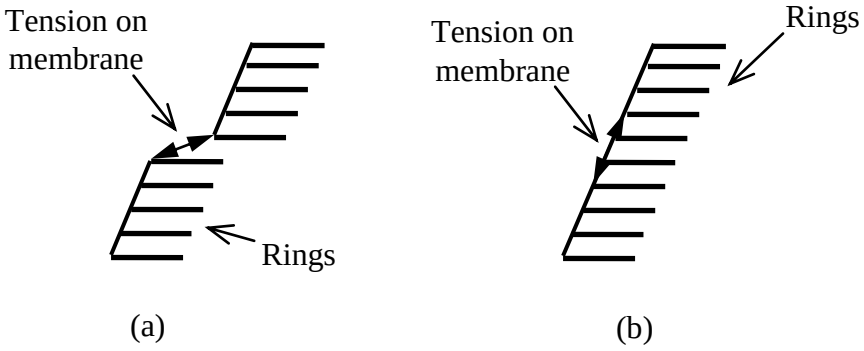

Figure 3.14 a) non-uniform, b) uniform relative displacements of adjacent aluminum rings.

The dissipated energy in each loop, E_D, due to friction in apparatus is plotted against u_0^2 in Figure 3.15 for a range of vertical confining stress (50, 100, 150, 200, and 250 kPa). The increase in E_D with u_0^2 follows a linear trend, which is consistent with Equation 3.5. Through a least-squares analysis, the equivalent viscous damping coefficient, c, for tests with 1.0 Hz of load frequency is computed as 3.99 N·s/mm (r^2=0.95). In contrast, a strong correlation between log(k_{sec}) and log(u_0) is observed in Figure 3.16, which proposes the relationship (r^2=0.93)

$$\log(k_{\text{sec}}) = 1.251 - 0.549\log(u_0) \qquad [3.6]$$

where, the units of k_{sec}, and u_0 are N/mm and mm respectively. Hence, substituting Equation 3.6 and c=3.99 N·s/mm into Equation 3.2, and dropping the superscript in u_0, the approximate nonlinear relationship between F_{fr}(t) and u(t) is formulated as

$$F_{fr}(t) = 17.8 \cdot \left(u(t)\right)^{0.451} + 3.99 \cdot \frac{\mathrm{d}u(t)}{\mathrm{d}t} \qquad [3.7]$$

where, the units of u, F_{fr}, and t are mm, N, and s respectively.

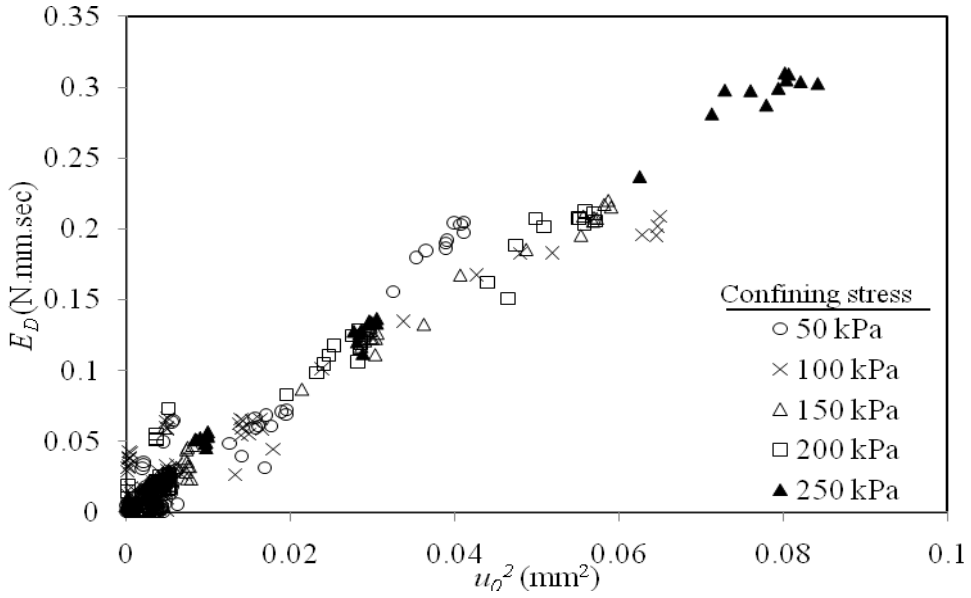

Figure 3.15 The dissipated energy in each loop (E_D) versus squared displacement amplitude (u_0^2) in balloon tests.

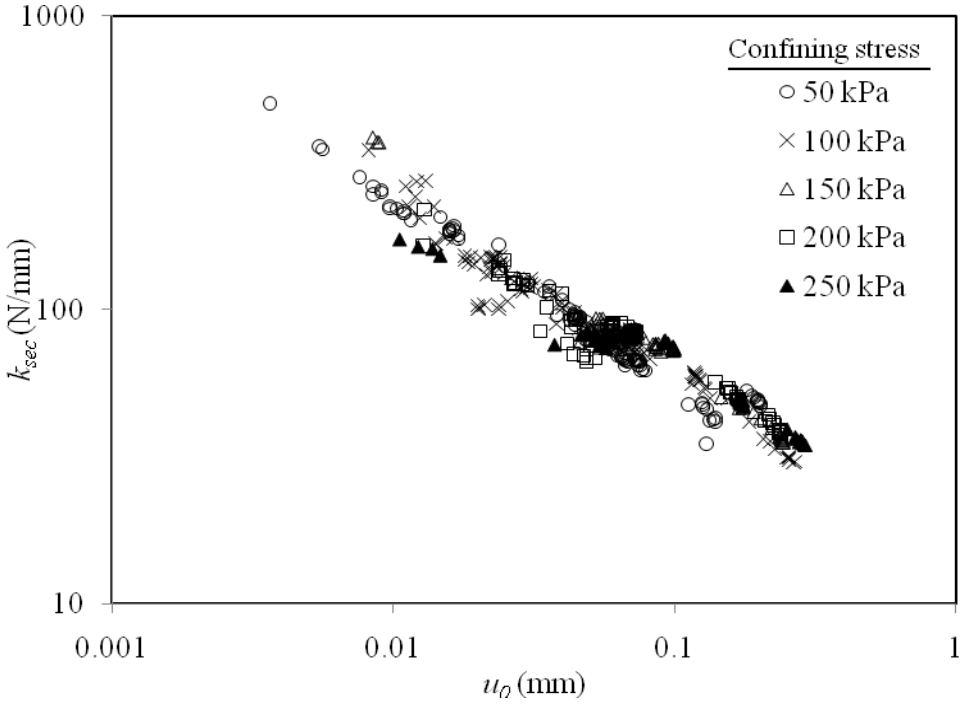

Figure 3.16 The relationship between k_{sec} and u_o.

Figure 3.15 andFigure 3.16 depict that c and k_{sec} are independent of the confining pressure. In order to verify the independency, the mean E_D and the mean k_{sec} for test

groups with different confining pressures (i.e., 50, 100, 150, 200 and 250 kPa) are contrasted by the single-factor analysis of variance (ANOVA) tool in the software Ms-Excel. The null and alternative hypotheses of the statistical test are, [Devore, 2008]:

H_0: $\mu_{50}=\mu_{100}=\mu_{150}=\mu_{200}=\mu_{250}$

H_a: at least two of the μ_ps are not equal.

where μ_p is the (population) mean of the property measured under the confining pressure p. Since it is difficult to achieve a constant u_0 in a load-controlled test, the sample is gathered from the test results with displacement amplitudes in a narrow range of u_0. The test results with 0.033 mm < u_0 <0.056 mm, corresponding to the range of shear strains from 0.21% to 0.35%, are used for ANOVA. The sample is presented in Table 3.1. The sample mean and the sample variance for E_D and k_{sec} are given in Table 3.2 and Table 3.3 respectively. Since the test assumes constant variance for each class, it is important that the magnitudes of individual sample variances for compared classes should be similar [Devore, 2008]. Nonetheless, the sample variance for E_D of the group 200 kPa is very small compared to those of the others, and the strength of statistical conclusions may be somewhat limited. On the other hand, an increase in number of tests may also increase the dispersion for this group.

The computed P-values, the observed significance levels of statistical tests, are equal to 0.17 and 0.10 for E_D and k_{sec} respectively. Therefore, the sample does not strongly support the rejection of H_0 for any reasonable significance level, which is usually less than 0.10. Besides, the variations in individual sample means are apparently random, because the sample mean for each group is not dependent on the vertical confining stress (Tables 3.2 and 3.3). As a conclusion, the proposed relationship between c, k_{sec}, and u_0 are presumed to be independent of the vertical confining stress.

Table 3.1 Randomly selected E_D and k_{sec} values for ANOVA, for u_0 between 0.033 and 0.056 mm under different vertical stresses.

u_0 (mm)	k_{sec} (N/mm)	E_D (N.mm.sec)	Vertical stress (kPa)	u_0 (mm)	k_{sec} (N/mm)	E_D (N.mm.sec)	Vertical stress (kPa)
0.038	113.226	0.038	50	0.053	93.739	0.063	100
0.038	95.944	0.234	50	0.054	74.542	0.235	100
0.039	106.292	0.056	50	0.054	93.328	0.180	100
0.040	108.045	0.027	50	0.055	82.112	0.319	100
0.040	101.275	0.107	50	0.055	88.780	0.026	100
0.043	92.673	0.284	50	0.056	75.661	0.369	100
0.043	100.034	0.130	50	0.056	78.144	0.015	100
0.044	94.183	0.228	50	0.056	78.026	0.023	100
0.044	96.230	0.185	50	0.056	79.262	0.057	100
0.044	92.898	0.303	50	0.033	84.432	0.100	150
0.044	97.946	0.238	50	0.035	102.110	0.070	150
0.044	95.927	0.170	50	0.044	70.645	0.004	150
0.046	93.412	0.191	50	0.056	93.452	0.127	150
0.046	95.043	0.304	50	0.056	89.985	0.097	150
0.048	79.315	0.003	50	0.056	86.536	0.200	150
0.049	91.220	0.312	50	0.037	75.913	0.084	200
0.049	78.265	0.303	50	0.045	92.734	0.116	200
0.051	75.466	0.017	50	0.046	82.224	0.180	200
0.055	81.003	0.235	50	0.048	69.487	0.012	200
0.040	101.634	0.080	100	0.048	82.825	0.186	200
0.044	98.092	0.207	100	0.049	92.014	0.234	200
0.046	86.204	0.324	100	0.049	87.514	0.245	200
0.049	90.123	0.244	100	0.052	76.683	0.003	200
0.049	87.729	0.074	100	0.049	84.596	0.335	250
0.051	87.752	0.312	100	0.052	82.091	0.247	250
0.053	79.048	0.048	100	0.052	83.663	0.318	250
0.055	81.674	0.133	100	0.053	80.615	0.022	250
				0.054	76.199	0.306	250

Table 3.2 Anova analyses results for E_D values under different vertical stresses.

Source of Variation	SS	df	MS	F	P-value	F crit
Between Groups	0.078404	4	0.019601	1.660153	0.174003	2.557179
Within Groups	0.590335	50	0.011807			
Total	0.668738	54				

Table 3.3 Anova analyses results for k_{sec} values under different vertical stresses.

Source of Variation	SS	df	MS	F	P-value	F crit
Between Groups	736.3468	4	184.0867	2.072128	0.098437	2.557179
Within Groups	4441.972	50	88.83943			
Total	5178.318	54				

Figure 3.17 compares the hysteresis of F_{fr} recorded during three water-balloon tests with the hysteresis of F_{fr} calculated by equation 3.6. The displacement rate ($du(t)/dt$) is computed by a backward difference scheme, which allows instantaneous correction of shear stress on specimen during a test. On the other hand, the substitution of equation 3.3 in equation 3.7 for consideration of an ideal sinusoidal variation in $u(t)$ results in a function smoother than the erratic $F_{fr}(t)$ in Figure 3.17.

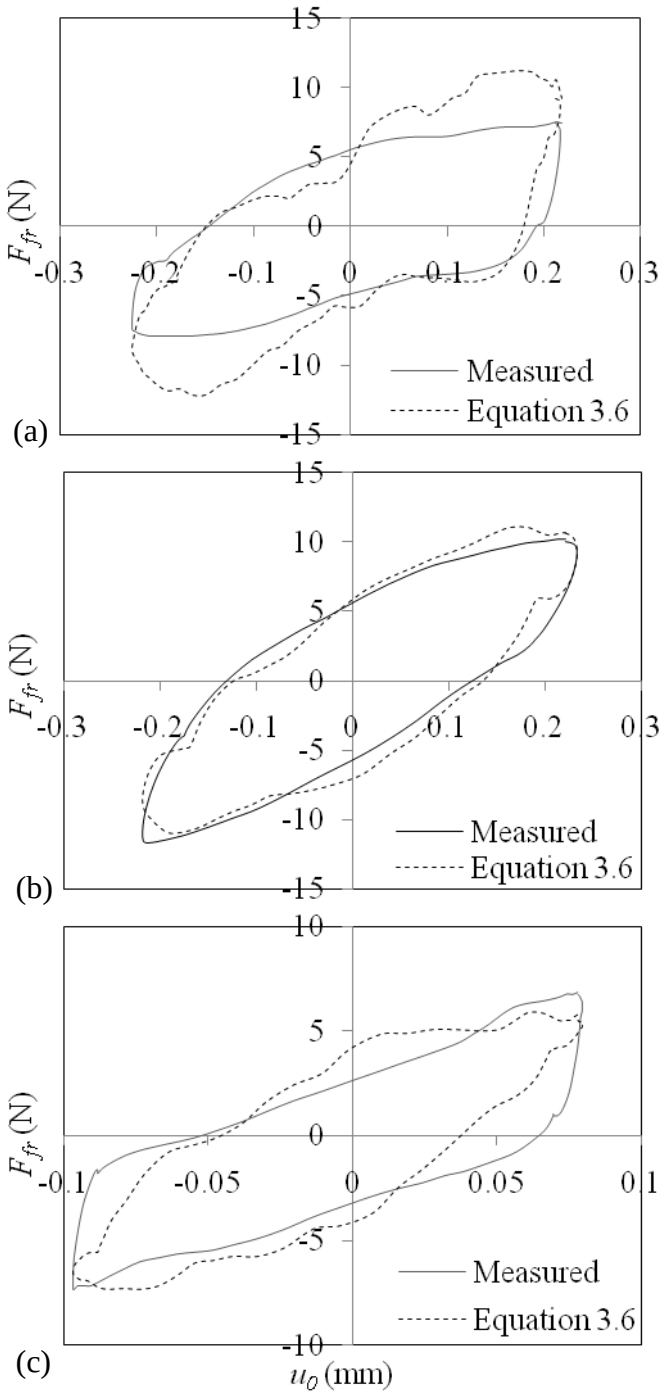

Figure 3.17 Measured and estimated reaction of test apparatus to cyclic loading under several vertical stresses: a) 100 kPa, b) 150 kPa, and c) 250 kPa.

Finally, in order to investigate the significance of frictional forces in test results, the records of horizontal load transducers are corrected by subtracting F_{fr} calculated by equation 3.7. Figure 3.18 compares the ranges of G_{sec} and λ according to corrected data with those according to raw data obtained by doing CDSS test on one of the soft soil specimens recovered from Adapazarı. The Figure 3.18 depicts that the reaction of test apparatus to cyclic displacements is not very significant, and do not significantly affect the dispersion in test results presented in the following chapter. A statistical study on the differences between all corrected and uncorrected test results showed that the mean relative percent error in calculated G_{sec} and λ is 2.3% and 3.2% respectively when raw data is used. Hence, the results of CDSS tests presented in Chapter 5 are simply based on raw data.

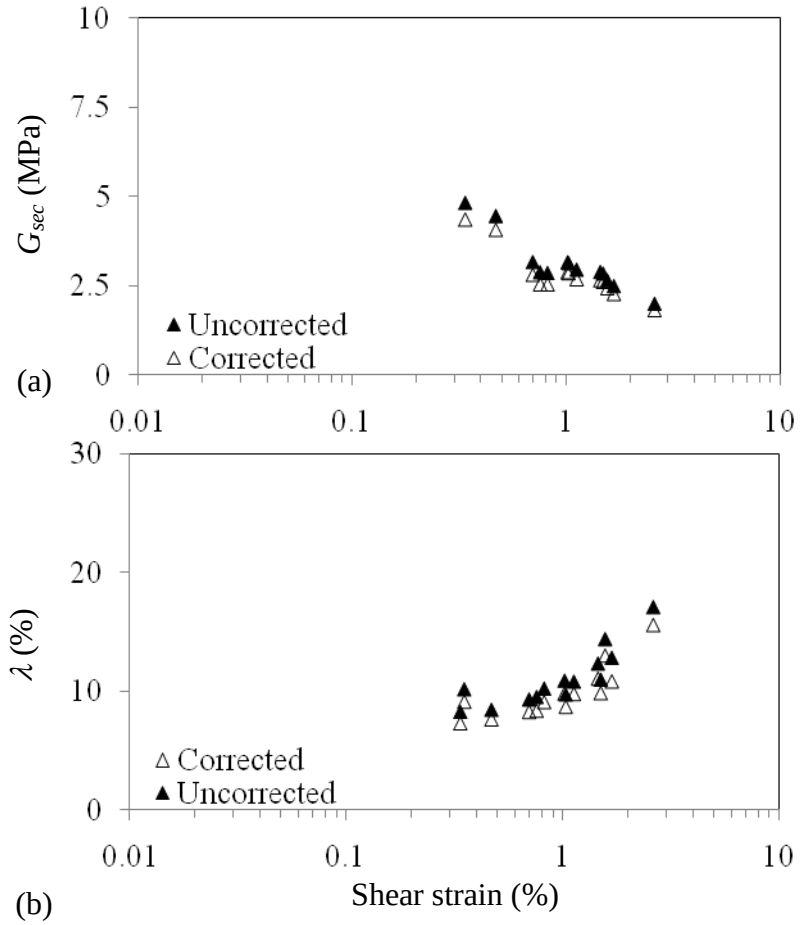

Figure 3.18 The effect of friction correction on a) secant shear modulus, b) damping ratio of a soft specimen recovered from Adapazarı.

CHAPTER 4

INTERPRETATION OF THE TEST RESULTS

4.1 Introduction

In order to investigate cyclic behavior and dynamic properties of Adapazarı deposits, 223 CDSS tests and 7 DSS tests were done on 76 undisturbed specimens that were recovered from 18 Thin-Walled sample tubes. Most CDSS tests followed a multi-staged loading procedure, which is useful for increasing the number of cyclic loading tests. Besides, several single-stage cyclic loading tests were done in order to contrast the results of multi-staged and single-staged tests.

Table 4.1 The distribution of CDSS and DSS tests between several soil classes.

Soil Class	Type of test	
	CDSS	DSS
CH-Clay	32	4
Cl- Clay and Silty Clay	10	-
ML-Clayey Silt	5	1
ML-Silt	17	2
ML-Sandy Silt	7	-
SM-Silty Sand	5	-
Total No.	76	7

Table 4.1 presents the distribution of CDSS and DSS tests between several soil classes. Most of the tested material is cohesive, whereas the number of CDSS tests performed with cohesionless silts and sands is sufficiently large. The DSS tests on 5

cohesive specimens (clays and clayey silts) provided information on strength of cohesive deposits under monotonic loading. In contrast, only 2 silt specimens were tested monotonically in order to investigate the shear strength of cohesionless soils. The number of CDSS tests is much larger than that of DSS tests, because the emphasis was put on the response of soils to cyclic loading. All tests along with the calibration studies on apparatuses were started on 22.01.2010 and finished on 17.04.2010. Hence, 85 working days were spent in order to test 83 specimens. Ability to recover a large number of specimens from a limited number of tubes and the relatively low time-cost of a test were the main reasons of preferring a simple shear apparatus to a cyclic triaxial apparatus. If a triaxial apparatus had been used for cyclic loading tests, the number of tests in 85 days would have been substantially lower, mostly because of the duration necessary for saturation of fine materials. Preparation of a cohesionless specimen for a CDSS test is also easier than that prepared for a cyclic triaxial test.

Examples of CDSS test results are presented in the following. The cyclic responses of several specimens are also compared with the monotonic responses of similar materials recorded during 7 DSS tests. In the light of information provided by monotonic and cyclic tests, general conclusions on the cyclic behavior of Adapazarı deposits are given. Finally, the properties of nonlinear cyclic response of specimens are compared with the predictions of widely-used empirical relationships.

4.2 Characteristics of soils tested

The index properties of soil samples recovered from thin-walled tubes are summarized in Tables 4.2. Table 4.3 separately presents the index properties of specimens used for DSS tests. Both tables provide the following information on soil samples:

1) The identification number of sample tube
2) The depth of sample recovery.
3) The number of test specimens successively recovered from the tube.
4) The class of soil in the tube, according to the Unified Soil Classification System (USCS) [ASTM D-2487-98].

5) The fines content, FC, of soil (i.e., percentage of soil particles passing #200 - 0.075mm- sieve by weight).

6) The clay content, CC, of soil (i.e., percentage of soil particles <0.002mm by weight).

7) Atterberg limits of soils: water content (w_c), liquid limit (LL), plastic limit (PL), and plasticity index (PI) of soils.

8) Specific gravity (G_S) of soil particles.

9) Wet unit weight of soils.

10) The sample means for initial (e_0) and final void ratio (e_{ps}) at the end of consolidation phase of tests.

11) Normal stress on specimens during consolidation (σ_v).

The Atterberg limits and particle size distribution were determined by following the procedures consistent with the standards ASTM D 4318-10, ASTM D 422-63 and TS ENV 1997-2 in Soil Mechanics Laboratory of General Directorate of Highways in Ankara. The wet unit weights and void ratios of specimens are calculated by measuring weights and heights of constant-diameter specimens used in CDSS tests. The cyclic loading tests are identified according to the format "Tube No _ Specimen No _ Stage No". For instance, the test *t12_s04_sn03* is recognized as the 3rd stage of cyclic loading test (3rd lowest cyclic stress amplitude) on 4th specimen recovered from Tube 12.

Figure 4.1 shows a histogram of specimens grouped according to the sampling depth. At depths exceeding 35 m, no undisturbed sample was recovered because of encountering stiff and gravelly soils. Besides, the sample recovery was limited at depths less than 10 m, due to lack of adequate cohesion within those soils. The sample size between the depths of 10 and 30 m were almost uniform. Hence, most of the samples tested in this study are recovered from the depths between 10 and 30 m.

Table 4.2 Index properties of samples and applied consolidation stress before CDSS tests.

Tube No.	Depth (m)	No of samples	Soil Class	Description	FC	CC	w_C	LL	PL	PI	G_S	Wet unit weight (kg/m^3)	e_0	e_{ps}	σ_v (kPa)
3	9.0	4	CH	Clay	100	14	45	68	25	43	2.63	1680	1.26	0.61	190
4	10.5	6	CH	Clay	94	25	52	60	25	35	2.66	1766	1.46	0.55	220
8	16.5	4	CH	Clay	75	27	45	56	24	32	2.56	1767	1.09	0.53	310
12	22.5	6	CH	Clay	98	48	36	56	20	36	2.57	1809	0.96	0.47	410
13	24.0	4	CH	Clay	99	62	34	71	28	43	2.57	1876	0.83	0.49	440
18	33.0	3	CH	Clay	93	39	41	73	32	41	2.49	1789	0.85	0.43	610
14-01	25.5	3	CH	Clay	100	47	35	60	23	37	2.58	1768	1.09	0.58	470
6	13.5	2	CH	Fat Clay	99	65	55	86	31	55	2.65	1639	1.23	0.87	265
7	15.0	6	CL	Silty Clay	60	24	38	29	17	12	2.61	1859	1.01	0.37	290
16	28.5	3	CL	Silty Clay	93	24	31	44	27	18	2.56	1885	0.86	0.44	530
14-00	25.7	1	CL	Silty Clay	100	32	35	47	26	21	2.61	1768	0.98	0.47	470
9	18.0	5	ML	Clayey Silt	100	36	35	43	26	17	2.6	1808	1.00	0.61	350
1	3.0	5	ML	Sandy Silt	65	8	35	-	NP	-	2.63	1869	0.90	0.35	70
5	12.0	1	ML	Sandy Silt	55	20	34	-	NP	-	2.61	1890	0.78	0.39	240
17	30.0	1	ML	Sandy Silt	76	12	35	-	NP	-	2.65	1818	1.02	0.58	560
10	19.5	5	ML	Silt	100	23	39	40	27	13	2.61	1843	0.91	0.50	380
11	21.0	5	ML	Silt	99	24	37	42	28	13	2.61	1819	0.99	0.53	390
15	27.0	4	ML	Silt	87	13	37	-	NP	-	2.59	1877	0.92	0.51	500

Table 4.2 continued.

Tube No.	Depth (m)	No of samples	Soil Class	Description	FC	CC	w_C	LL	PL	PI	G_S	Wet unit weight (kg/m^3)	e_0	e_{ps}	σ_v (kPa)
14-02	25.8	3	ML	Silt	95	17	35	33	28	5	2.64	1862.66	0.94	0.48	470
2	2.0	5	SM	Silty sand	32	11	31	-	NP	-	2.66	1828.76	0.84	0.52	55

Table 4.3 Index properties of samples and applied consolidation stress before DSS tests.

Tube No.	Depth (m)	No of samples	Soil Class	Description	FC	CC	w_C	LL	PL	PI	G_S	Wet unit weight (kg/m^3)	e_0	e_{ps}	σ_v (kPa)
18	33.0	1	CH	Clay	93	39	41	73	32	41	2.5	1789	0.85	0.43	610
8	16.5	1	CH	Clay	75	27	45	56	24	32	2.6	1767	1.09	0.53	310
12	22.5	1	CH	Clay	98	48	36	56	20	36	2.6	1809	0.96	0.47	410
13	24.0	1	CH	Clay	99	62	34	71	28	43	2.6	1876	0.83	0.49	440
9	18.0	1	ML	Clayey Silt	100	36	35	43	26	17	2.6	1808	1.00	0.61	350
10	19.5	1	ML	Silt	100	23	39	40	27	13	2.6	1843	0.91	0.50	380
11	21.0	1	ML	Silt	99	24	37	42	28	13	2.6	1819	0.99	0.53	390

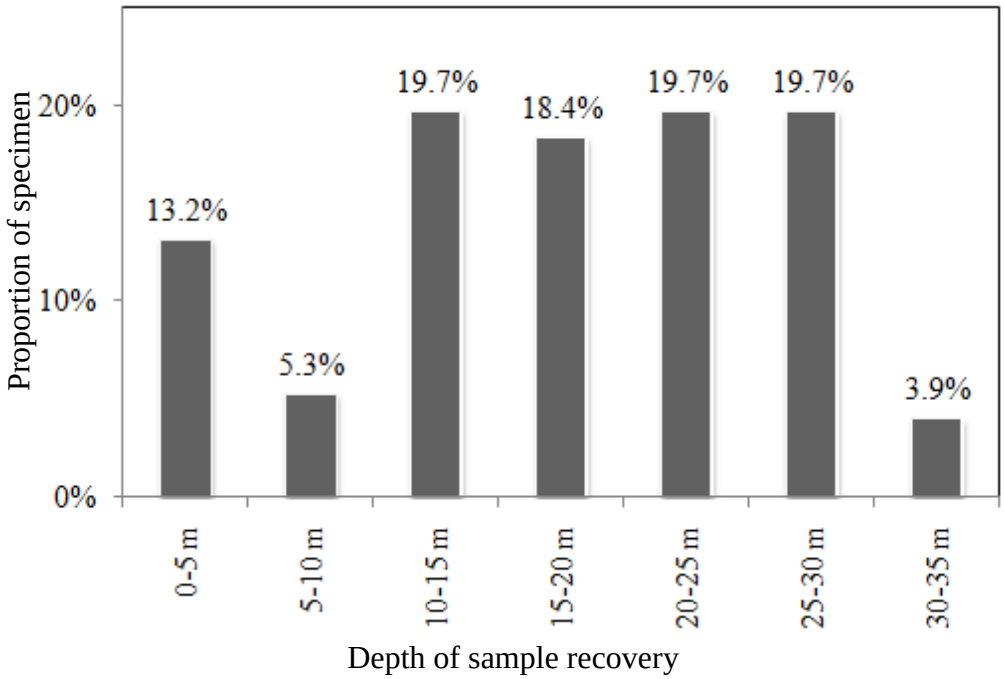

Figure 4.1 The distribution of specimens between bins of sampling depth.

Figure 4.2 shows the histogram of specimens grouped according to PI. CDSS tests were performed on soils with a relatively wide range of PI. 24% of samples used in CDSS tests were either non-plastic materials or low-plasticity materials. On the other hand, most of the samples had PI greater than 30. The maximum PI was determined as 55.

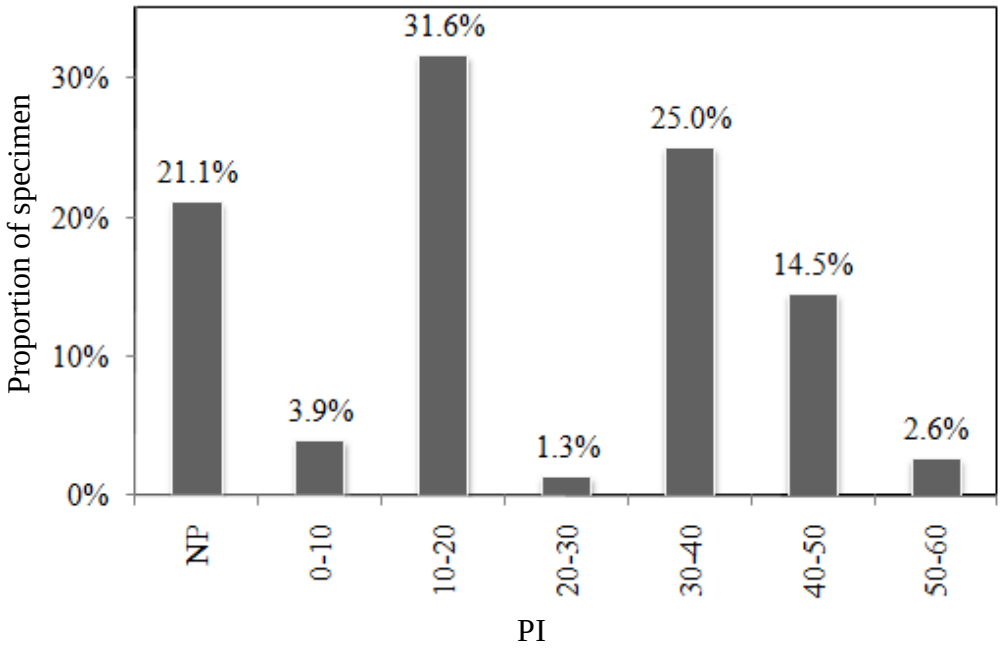

Figure 4.2 The distribution of specimens between bins of PI.

4.3 Hysteresis of soil behavior observed in CDSS tests

A practical range of cyclic shear stress amplitudes was considered for performing the CDSS tests, such that the test range covers the possible ranges of severe stress amplitudes exerted on those soils during the 1999 Kocaeli Earthquake. Conventionally, the cyclic shear stress should be normalized with the normal stress acting on specimen for comparisons of different cyclic loading test results. Hence, the cyclic-stress ratio, CSR, is defined as

$$CSR = \frac{\tau_{cyc}}{\sigma_v} \qquad [4.1]$$

where, τ_{cyc} is the amplitude of cyclic stress, and σ_v is the normal consolidation stress. The range of *CSR* employed by Bray et al., 2004 for cyclic loading tests on shallow Adapazarı soils was from 0.3 to 0.5, whereas the range from 0.15 to 0.53 was considered by Yilmaz et al., 2004 for testing anisotropically consolidated specimens recovered from shallow layers of Adapazarı.

Figure 4.3 shows the ranges of *CSR* applied in CDSS tests on samples recovered from different depths. The minimum *CSR* is 0.005 and the maximum is 0.5. The *CSR* is usually between 0.01 and 0.4. Representative tests results for different soil classes are presented in the following.

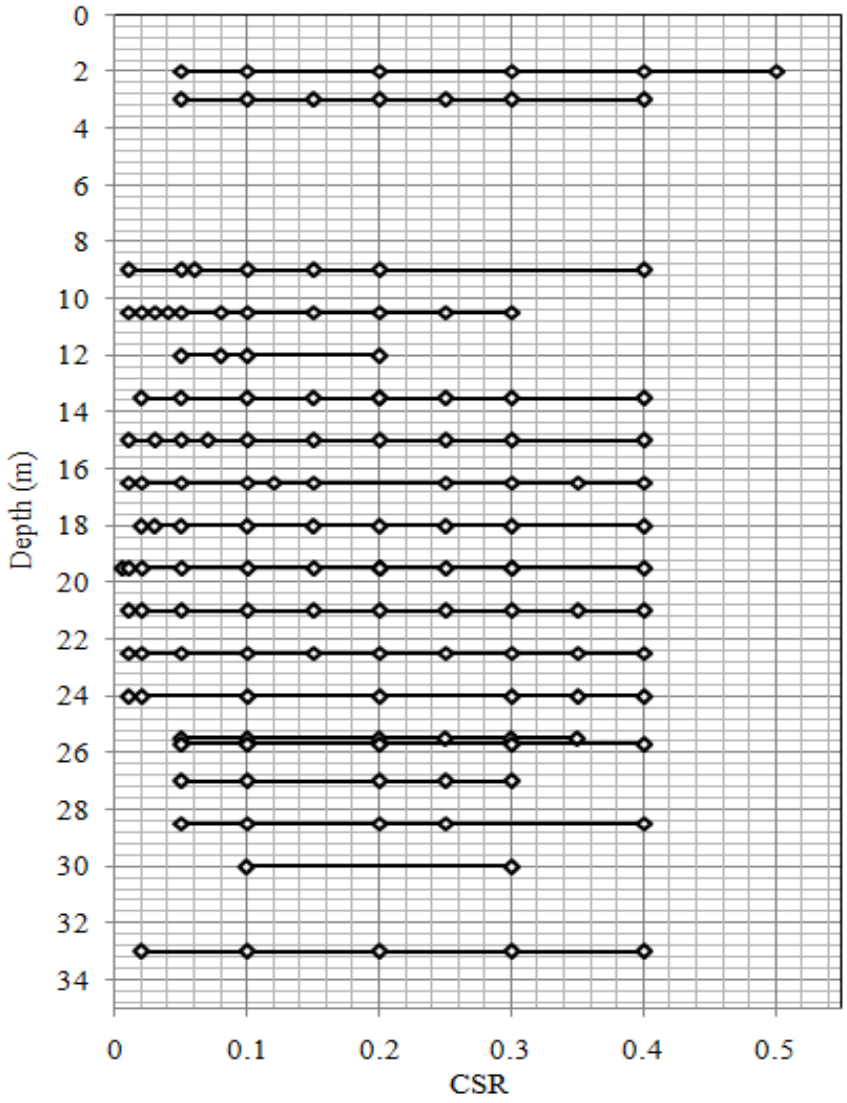

Figure 4.3 The variation of ranges of *CSR* applied during CDSS tests with depth of sample recovery.

4.3.1 CH-class clays

Clay samples from the tubes 3, 4, 6, 8, 12, 13, 14_01, and 18, which have the highest PI among the undisturbed samples, are classified as CH. Only the results of six tests,

which are representative for all CH-class soils tested, are presented in this section. Those representative specimens were recovered from the depths of 16.5 m (t08_s03_sn02, and t08_s01_sn05), 22.5 m (t12_s04_sn03, t12_s02_sn03), and 24.0 m (t13_s05_sn02, t13_s02_sn03). PI of the specimens is between 30 and 40.

The variation of shear stress (kPa) with shear strain (%) recorded during CDSS and DSS tests are plotted in Figure 4.4 for specimens recovered from the tubes 12, 13 and 18. The range of CSR considered in those tests is from 0.02 to 0.3. The hysteresis loops of specimens from two different tubes are similar for both lower and higher amplitudes of shear strain. The similarity resulted in calculation of virtually the same damping ratio for both specimens. One important observation is that the positive peaks of the hysteresis loops converge to the monotonic loading curve during successive load cycles, although the response of soil to the first load cycle is stiffer than its response to the (slow) monotonic loading. In other words, degradation in G_{sec} becomes more pronounced with increasing number of cycles, but G_{sec} ultimately converges to the value given by a slow monotonic loading test. Hence the observed rate-dependent response of CH-class soils is consistent with the observed viscous behavior of silt and clay mixtures observed during consolidated-undrained cyclic triaxial tests (Yılmaz et al., 2004). Apparently, the rate-dependent response of fine materials tested by a cyclic triaxial equipment may not solely be attributed to the lack of uniformity of pore pressure distribution in a saturated clay specimen, since the unsaturated CDSS specimens show a similar rate-dependent response.

Figure 4.5 depicts the gradual increase in the ratio of excess pore pressure to σ_v, namely the excess pore-pressure ratio (r_u), and the decrease in effective normal stress (σ_v) induced by successive load cycles applied on the two specimens. Although significant increases in pore-pressures were observed in similar tests on CH-class specimens, none of those specimens could achieve the condition $r_u \cong 100\%$, when amplitudes of cyclic shear stresses were significantly less than the monotonic shear strength.

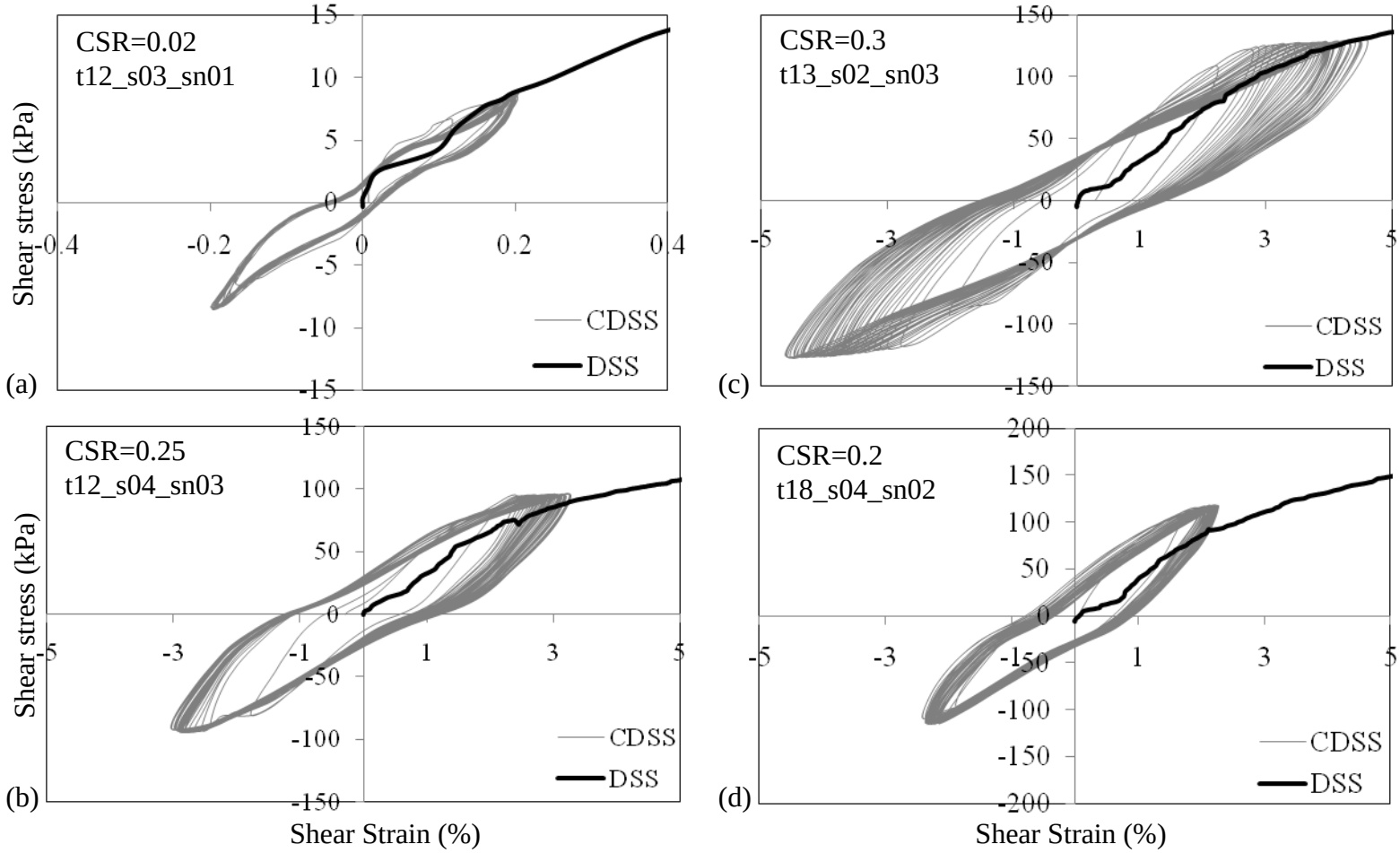

Figure 4.4 CDSS and DSS test results for CH-class specimens: a) t12_s03_sn01, b) t12_s04_sn03, c) t13_s02_sn03, and d) t18_s04_sn02.

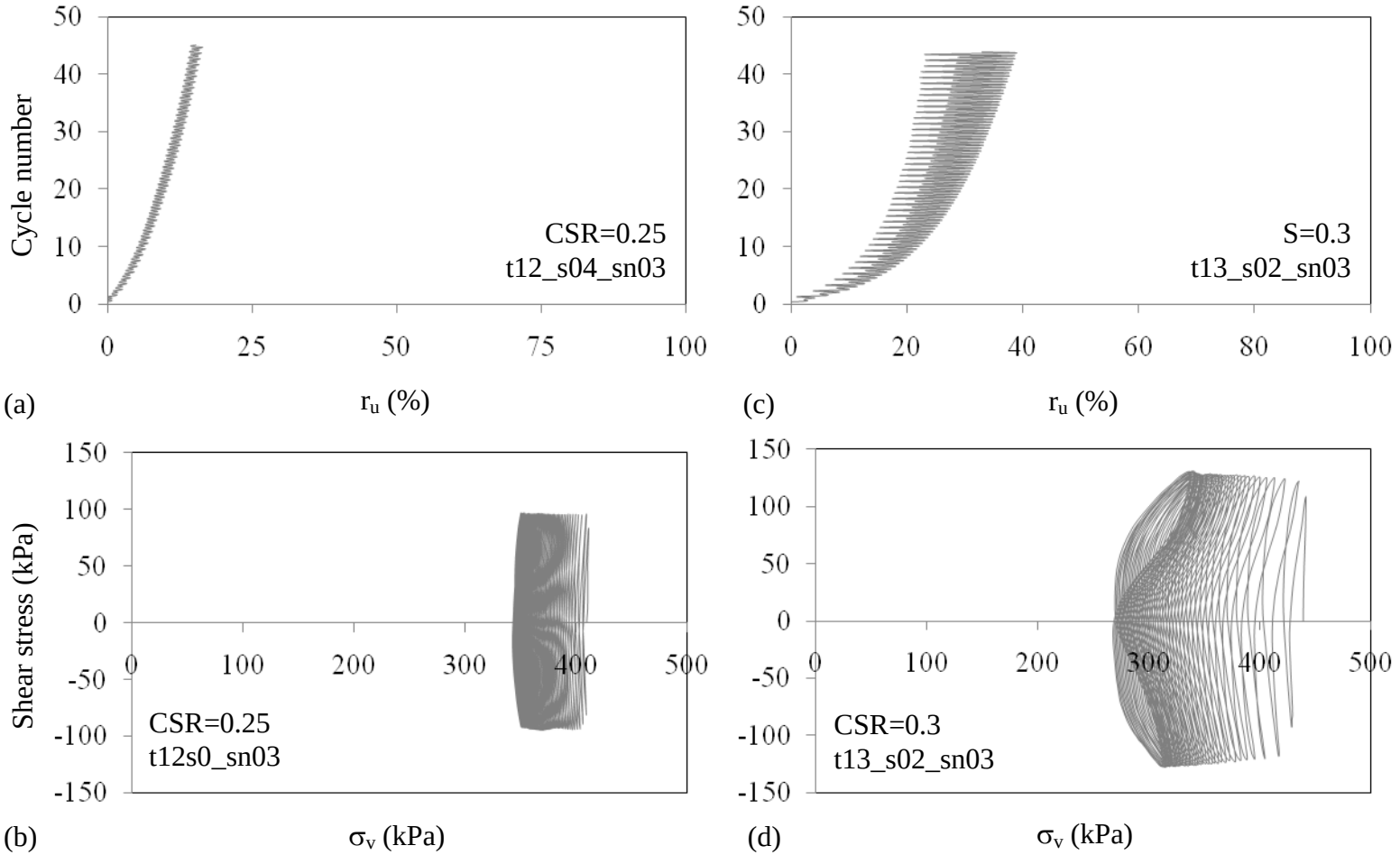

Figure 4.5 a)Excess pore pressure ratio, and b) effective stress path during the test t12_s04_sn03; and c)excess pore pressure ratio, and d) effective stress path during the test t12_s02_sn03.

4.3.2 CL-class silty clays

Specimens recovered from tubes 7, 14_00 and 16 are CL-class silty clays that have PI of 12, 26 and 27 respectively. The range PI of CL-class specimens is lower than that of CH-class specimens, but clay-contents of the former are comparable with those of the latter. No DSS test was done on CL-class specimens. Figure 4.6 shows the hysteresis loops of specimens recovered from the tubes 7, 14_00, and 16 during CDSS tests. Tests t07_s02_sn02, t07_s01_sn03, and t16_s03_sn01 show significant "reversed-S" shape of loops, such that the tangential shear modulus about zero strain is smaller than that about peak strain. The reversed-S shaped loops were typical of most silty clay specimens. Test t07_s02_sn02 showed cyclic failure, such that the rate of cyclic increase in peak strain is boosted when the cycle number exceeded 35.

Figure 4.7 compares the pore-pressure accumulation and effective stress paths of two similar specimens tested with the same *CSR*. The rate of pore pressure accumulation in test t07_s02_sn02 is higher than that of test t16_s03_sn01. The former specimen eventually liquefies with $r_u \cong 80\%$, such that the increase in pore-pressure results in significant increase in accumulation of cyclic strains. Since no DSS test result is available for comparison, no further comments can be given. However, a similar response is observed for silty specimens, as explained in the following.

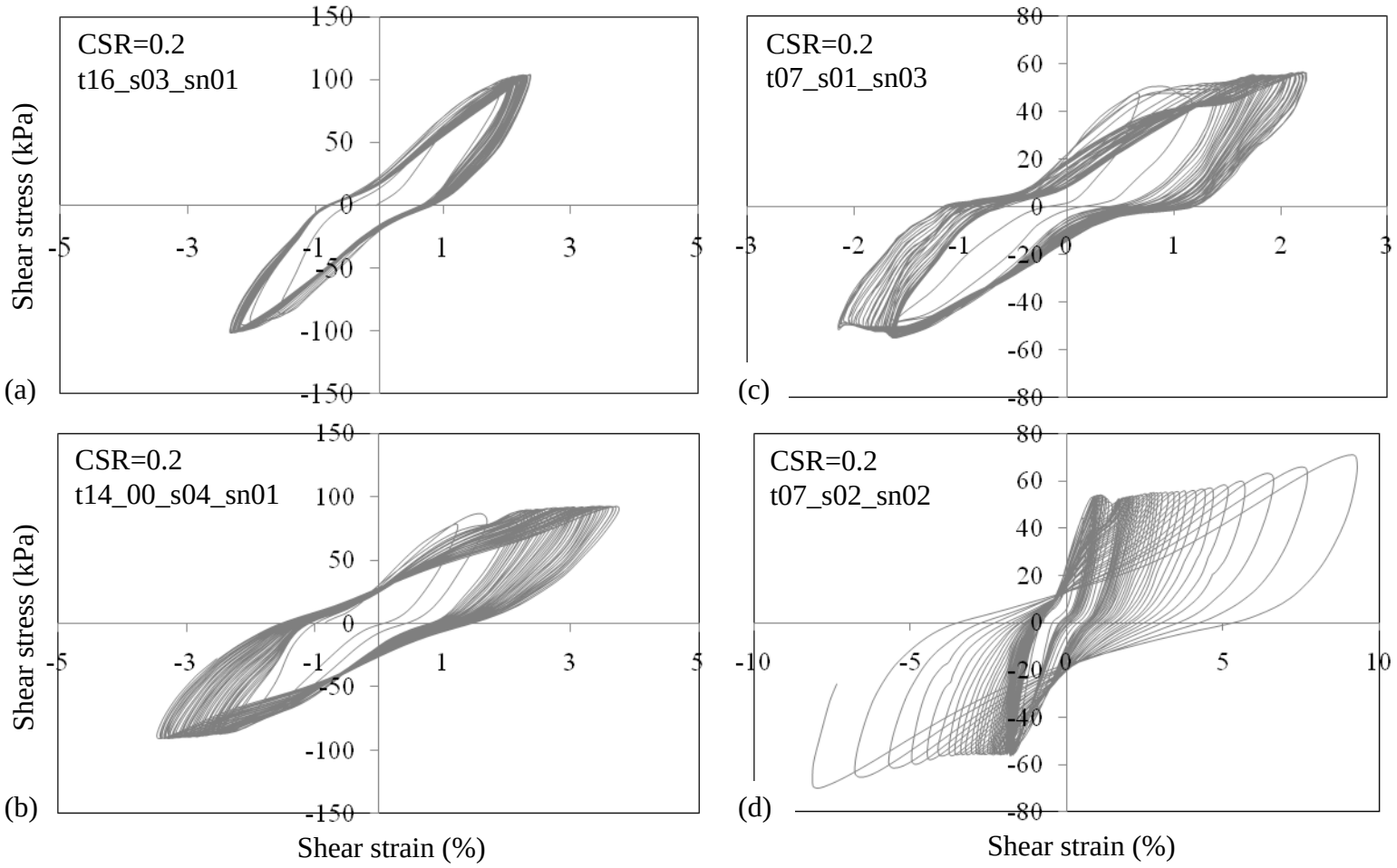

Figure 4.6 CDSS and DSS test results for CL-class specimens: a) t16_s03_sn01, b) t14_00_s04_sn01, c) t07_s01_sn03, and d) t07_s02_sn02.

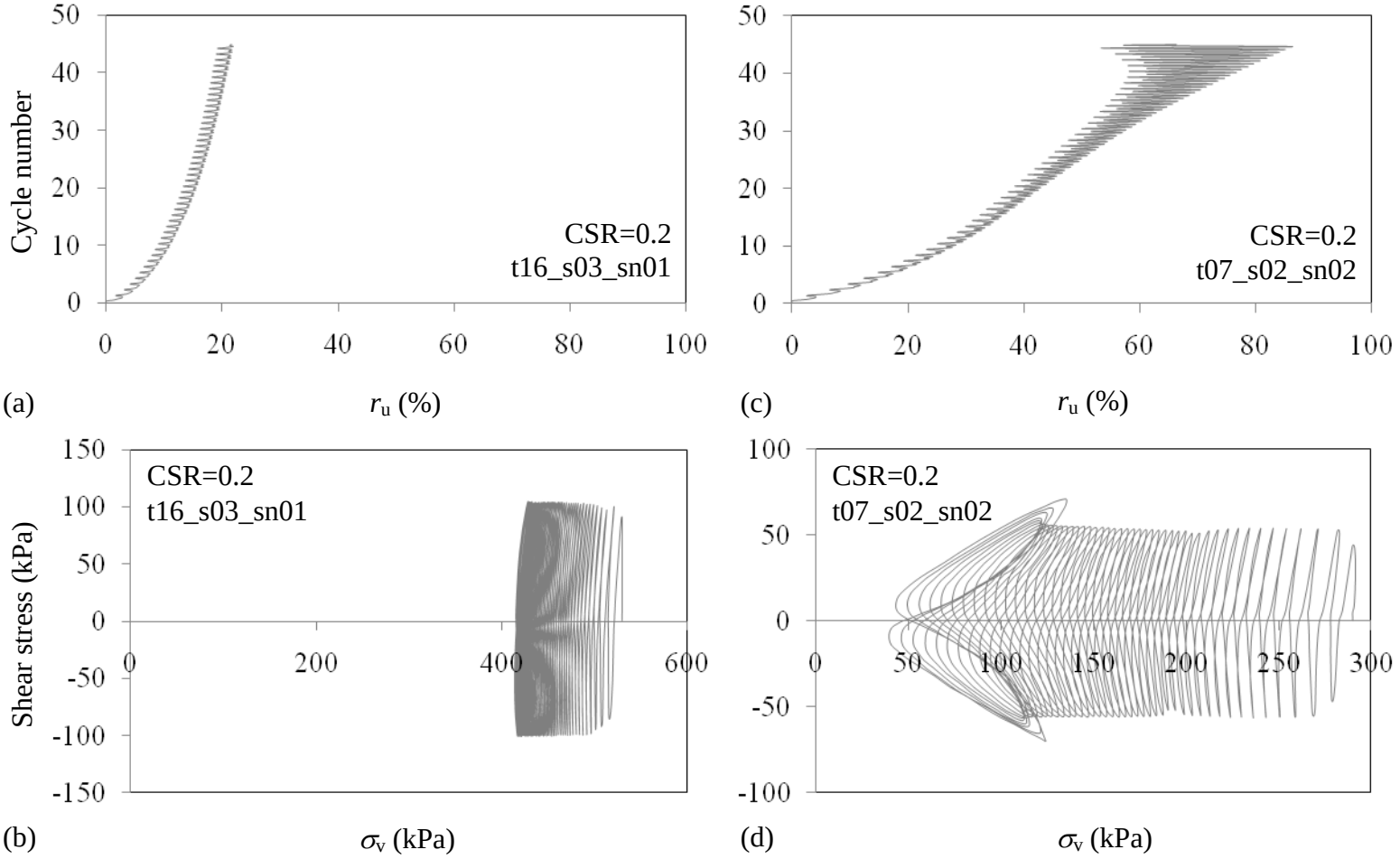

Figure 4.7 a)Excess pore pressure ratio, and b) effective stress path during the test t16_s03_sn01; and c)excess pore pressure ratio, and d) effective stress path during the test t07_s02_sn02.

4.3.3 ML-class silts and clayey silts

The specimens recovered from the tubes 10, 11, 15, and 14_02 are ML-class silts, those recovered from the tubes 1, 5, and 17 are ML-class sandy silts, and those recovered from the tube 9 are clayey silts. Excluding the specimens from the tube 9, the clay contents of those non-plastic or low-plasticity materials are less than 25%. Typical CDSS and DSS test results are presented in Figure 4.8. In some of the test, hysteresis loops with significant reversed-S shapes were observed. Most of the hysteresis loops were similar to those of CL-class soils. Similar to the case of CH-class soils, a good agreement between the secant shear moduli of cyclic and monotonic loading tests was observed. The accumulation of pore pressures and effective stress path followed during CDSS tests are shown for two of the tests in Figure 4.9.

The response of specimen in test t10_s04_sn03 (Figure 4.9.d) show important similarities to that observed in test t07_s02_sn02 (Figure 4.7.d). However, a DSS test result is available for an assessment of the cyclic response of specimen in test t10_s04_sn03. It is observed that, although a significant increase in r_u and rate of cyclic strain accumulation occurs when the cycle number exceeds 30, the peak of hysteresis loops follow the stress-strain curve determined by monotonic loading tests.

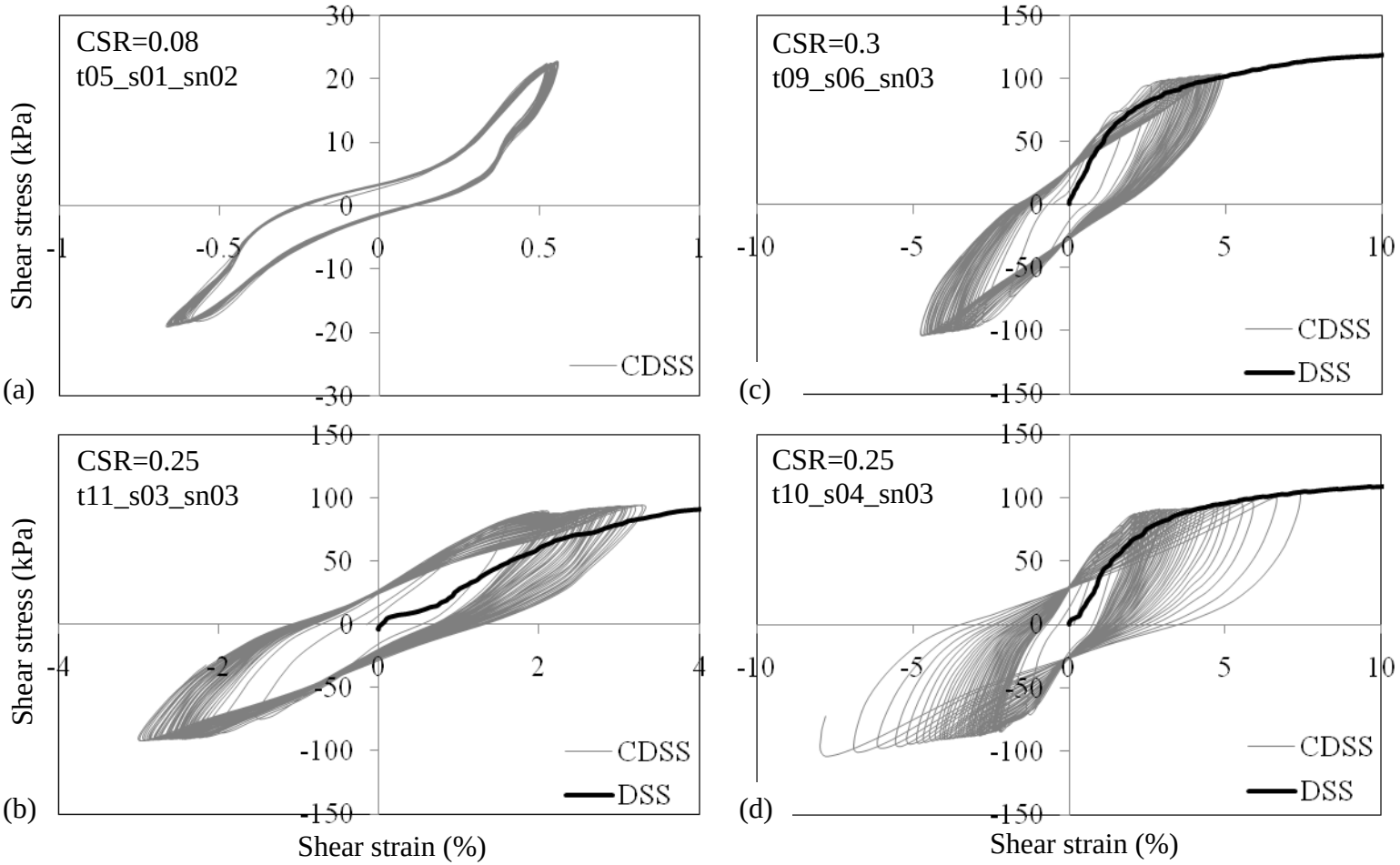

Figure 4.8 CDSS and DSS test results for ML-class specimens: a) t05_s01_sn02, b) t11_03_s03, c) t09_s06_sn03, and d) t10_s04_sn03.

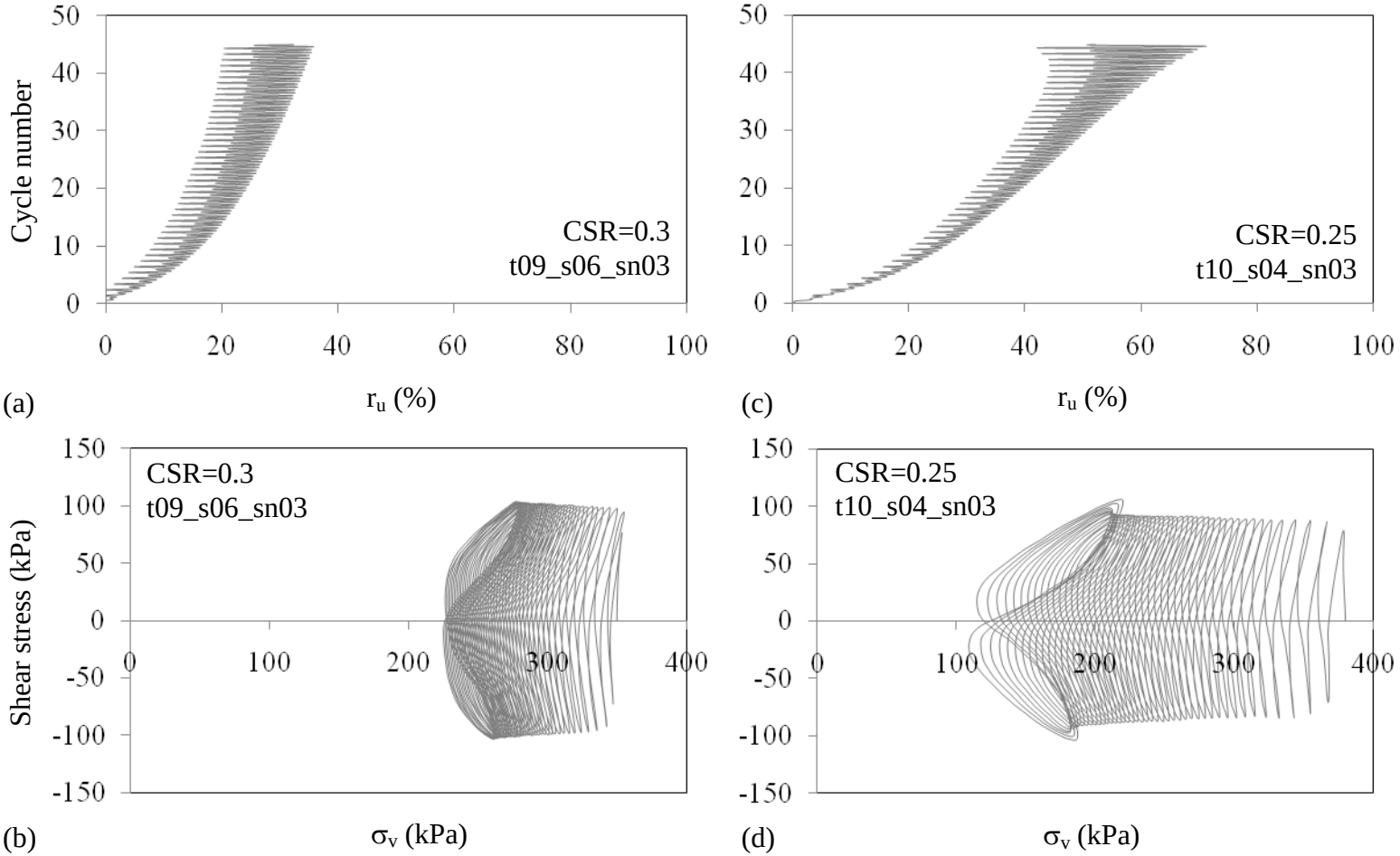

Figure 4.9 a) Excess pore pressure ratio, and b) effective stress path during the test t09_s06_sn03; and c)excess pore pressure ratio, and d) effective stress path during the test t10_s04_sn03.

4.3.4 SM-Class silty sands

Only the tube 2 provided the non-plastic SM-class silty sand specimens. The tube contained the shallowest sample recovered from the depth of 2 m. Figure 4.10 presents the hysteresis loops, the increase in pore-pressure and in amplitude of strains, and the effective stress path recorded during the test t02_s03_sn04. Although the CSR was as high as 0.3, the specimen of the test did not liquefy, but showed significant cyclic degradation in G_{sec}. Consequently, the behavior of the specimen in test t02_s03_sn04 was typical for non-liquefying SM-class materials in cyclic loading tests.

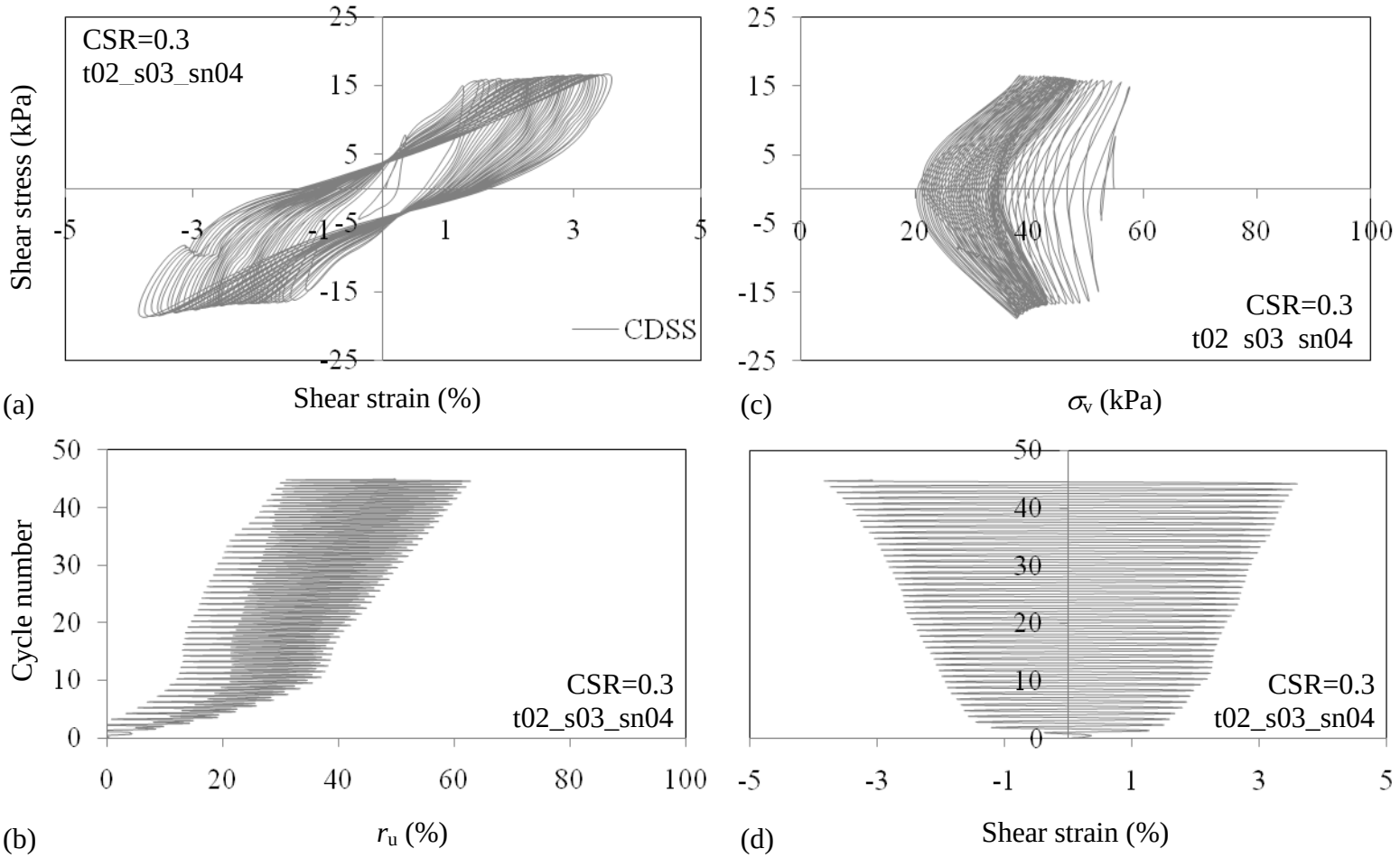

Figure 4.10 a) Hysteresis loops, b) excess pore-pressure ratio, c) effective stress path, d) cyclic shear strains during the test t02_s03_sn04.

4.4 General cyclic-response characteristics of soils tested

The result of each CDSS test is summarized as a pair of secant shear modulus (G_{sec}) and damping ratio (λ) corresponding to the amplitude of cyclic shear strains measured in test (Section 1.2.2, Equation 1.3). Since significant cyclic degradation of soil stiffness can occur especially during the tests with higher ranges of CSR, the response of specimen to the 2nd load cycle is considered as being representative for each test. The computed stiffness and damping characteristics of specimens are summarized and compared with the empirical relationships given in literature. The cyclic degradation of material stiffness is also investigated for each specimen by comparing its response to 40th load cycle with its response to 2nd load cycle

4.4.1 Damping ratio (λ)

Figure 4.11 shows the scatter plot of λ according to the results of CDSS tests. The maximum of λ is 18.92% and the minimum is 6.73%. λ is lower for specimens with larger PI and normal consolidation stress, σ_v. In order to investigate the effect of σ_v on λ further, the test results are divided into 4 groups according to the PI of specimens, so that the effect of PI on λ can be roughly eliminated. The ranges of PI are chosen as 0-10, 10-30, 30-40, and 40-60 (Figure 4.12).

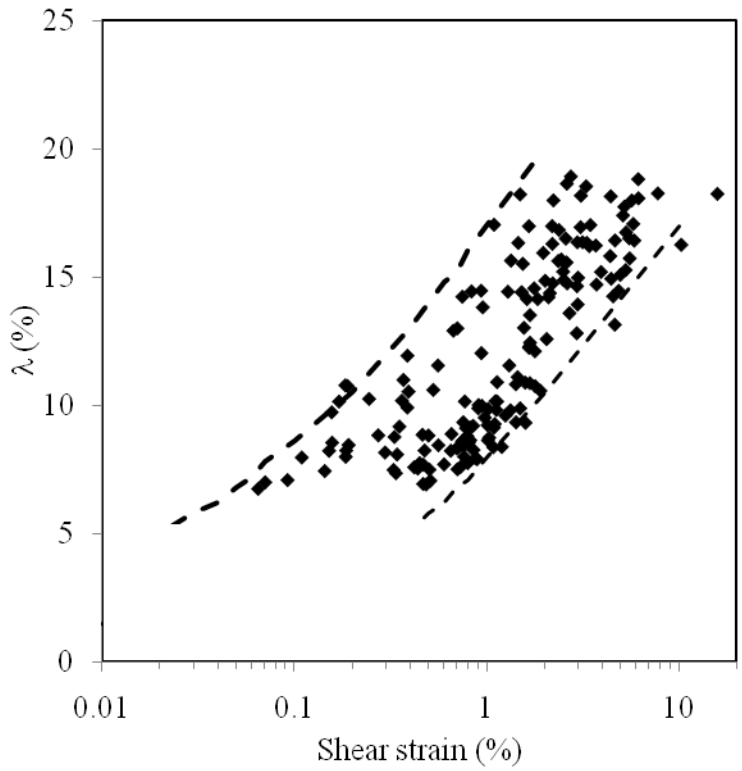

Figure 4.11 The scatter plot of damping ratio against shear strain.

Apparently, the effect of σ_v on λ is more pronounced for lower ranges of PI, as stated by several researchers [Seed et al., 1986; Ishibashi, 1991; Ishibashi and Zhang, 1993; and Darendeli, 2001]. The range of σ_v for the group PI=10-30 is very limited for any inference. However, Figure 4.12.c and Figure 4.12.d depict that σ_v has no significant effect on λ when PI is greater than 30, and the scatter plot for the range PI=10-30 (Figure 4.12.b) weakly suggests that the upper bound for PI is 10 for consideration of a pronounced effect of σ_v on λ.

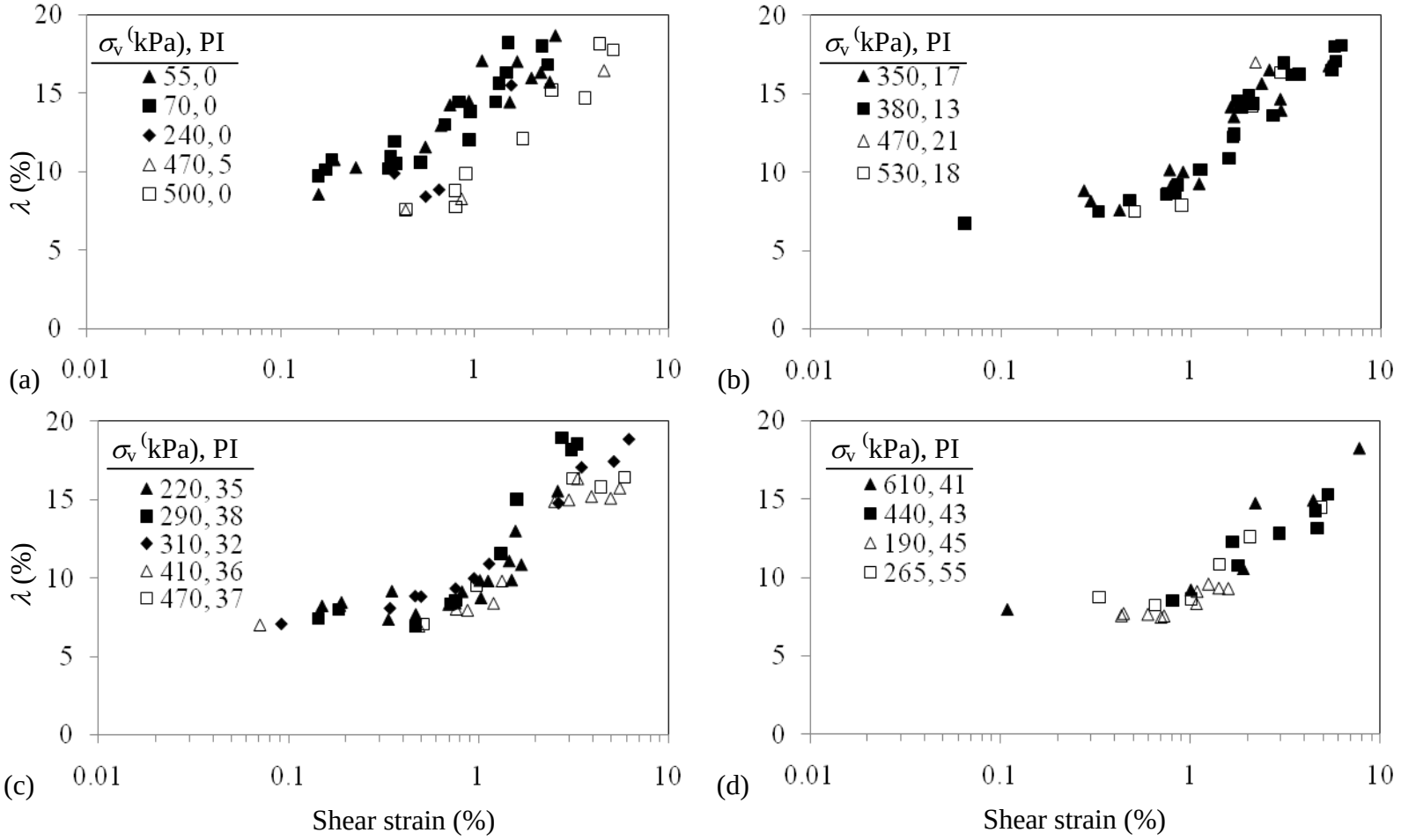

Figure 4.12λ versus shear strain for specimens with PI in the range a) 0-10, b) 10-30, c) 30-40, and d) 40-60.

The ranges of λ determined by CDSS tests are compared with the widely-known empirical relationships proposed by Vucetic and Dobry (1991), Ishibashi and Zhang (1993), and Darendeli (2001). The modulus reduction and damping relationships that are graphically presented by Vucetic and Dobry (1991) omit the effect of effective confining stress on λ, even for low PI values. Nevertheless, the curves suggested by Vucetic and Dobry (1991) are compared with the test results for a first evaluation of damping ratios determined in this study. Figure 4.13 compares the scatter of λ with the curves suggested by Vucetic and Dobry (1991). The trend of λ with increasing shear strain is generally consistent with that of empirical curves. Although the range of PI is from 0 to 55 for the specimens tested by CDSS equipment, all of the data for λ fall in the range bounded by the curves given for PI=30 and PI=200 (Figure 4.13).

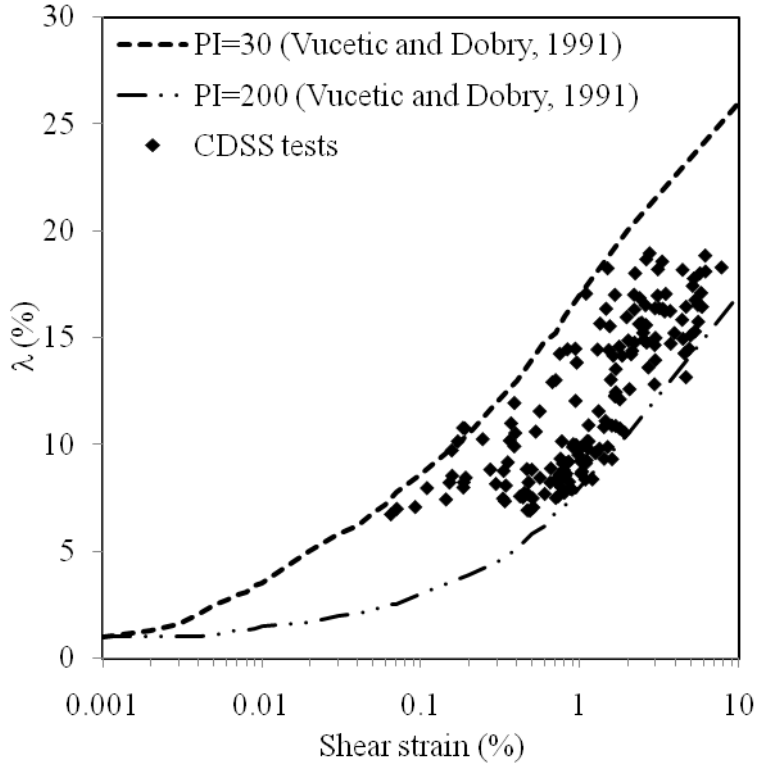

Figure 4.13 The comparison of λ with the curves recommended by Vucetic and Dobry (1991).

Hence, λ for a given value of PI and shear strain is lower than that is suggested by Vucetic and Dobry. For a detailed comparison, the data for λ is divided into four groups according to the PI of specimens.

In Figure 4.14, each group is compared with the empirical curves given by Vucetic and Dobry (1991). The test data for PI=10-30, and PI=40-60 are located between the empirical curves given for PI=50-100, and PI=100-200 respectively (Figure 4.14.b and 4.14.d). The scatter of λ for the range of PI from 30 to 40 is usually around the curve given for PI=100 (Figure 4.14.c). In contrast, the data of the group PI=0-10 is more scattered than the data of other PI groups due to the effect of σ_v on λ. Nevertheless, the data points usually fall on the area bounded by the curves given for PI=30 and PI=100 (Figure 4.14.a).

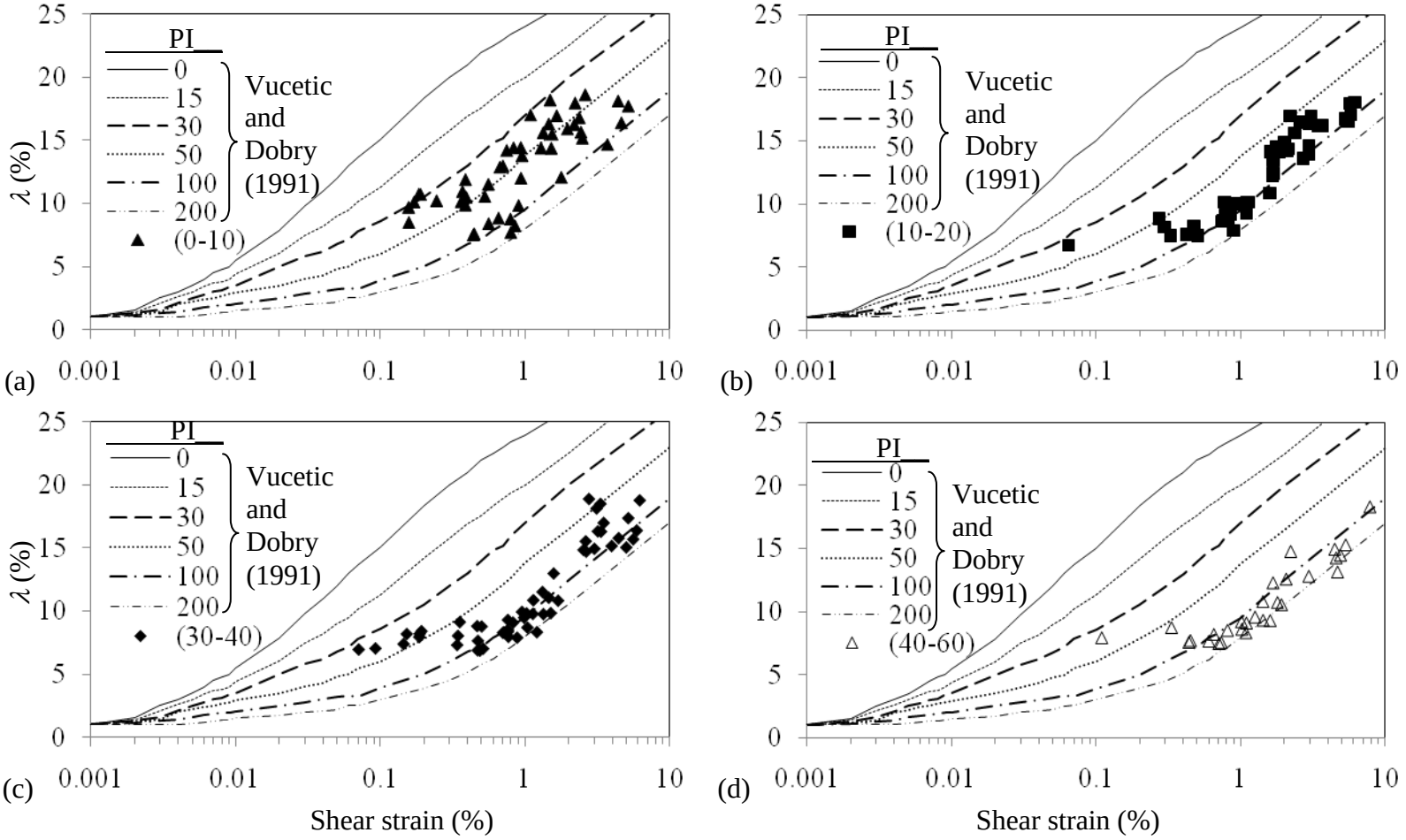

Figure 4.14 The comparison of λ with the curves recommended by Vucetic and Dobry (1991) for different ranges of PI: a) PI=0-10, b) PI=10-30, c) PI=30-40, and d) PI=40-60.

The test data on damping ratio is also compared with the empirical relationship proposed by Ishibashi and Zhang (1993) in Figure 4.15. The empirical relationship employs PI, shear strain and mean effective stress σ_m' acting on specimen, as parameters necessary for estimation of λ. Since the radial stress acting on a CDSS specimen is unknown, the mean effective stress σ_m' at the beginning of a CDSS tests is estimated by

$$\sigma'_m = \frac{2\sigma_v}{3} \qquad [4.2]$$

assuming that the radial stress is approximately equal to $\sigma_v/2$ during consolidation.

The empirical relationship proposed by Ishibashi and Zhang overestimate the test results for any given amplitude of cyclic strain. The difference between the data and the empirical relationship is more pronounced for lower ranges of PI.

The test data is also compared the curves defined by Darendeli (2001), the most recent one among the three comprehensive studies on the relationship between soil damping and cyclic-strain amplitude, in Figure 4.16. It is observed that the difference between the test results and empirical curves are highest when the curves of Darendeli are considered. Besides, the disagreement is stronger for larger ranges of PI, because the ranges of damping ratio estimated by using the curves of Darendeli are higher than those according to the other two studies.

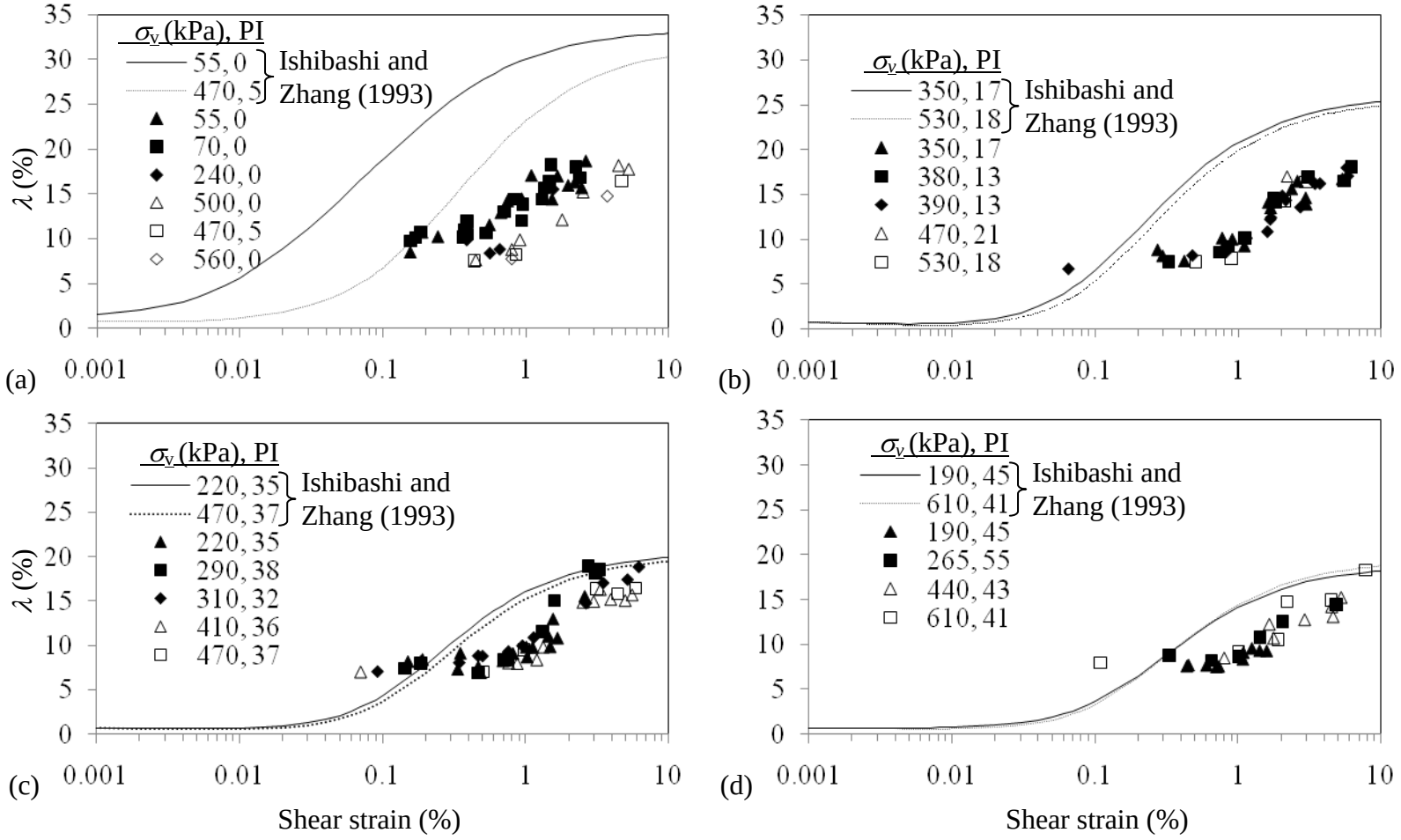

Figure 4.15 The comparison of λ with the empirical relationship recommended by Ishibashi and Zhang (1993) for different ranges of PI: a) PI=0-10, b) PI=10-20, c) PI=30-40, and d) PI=40-60.

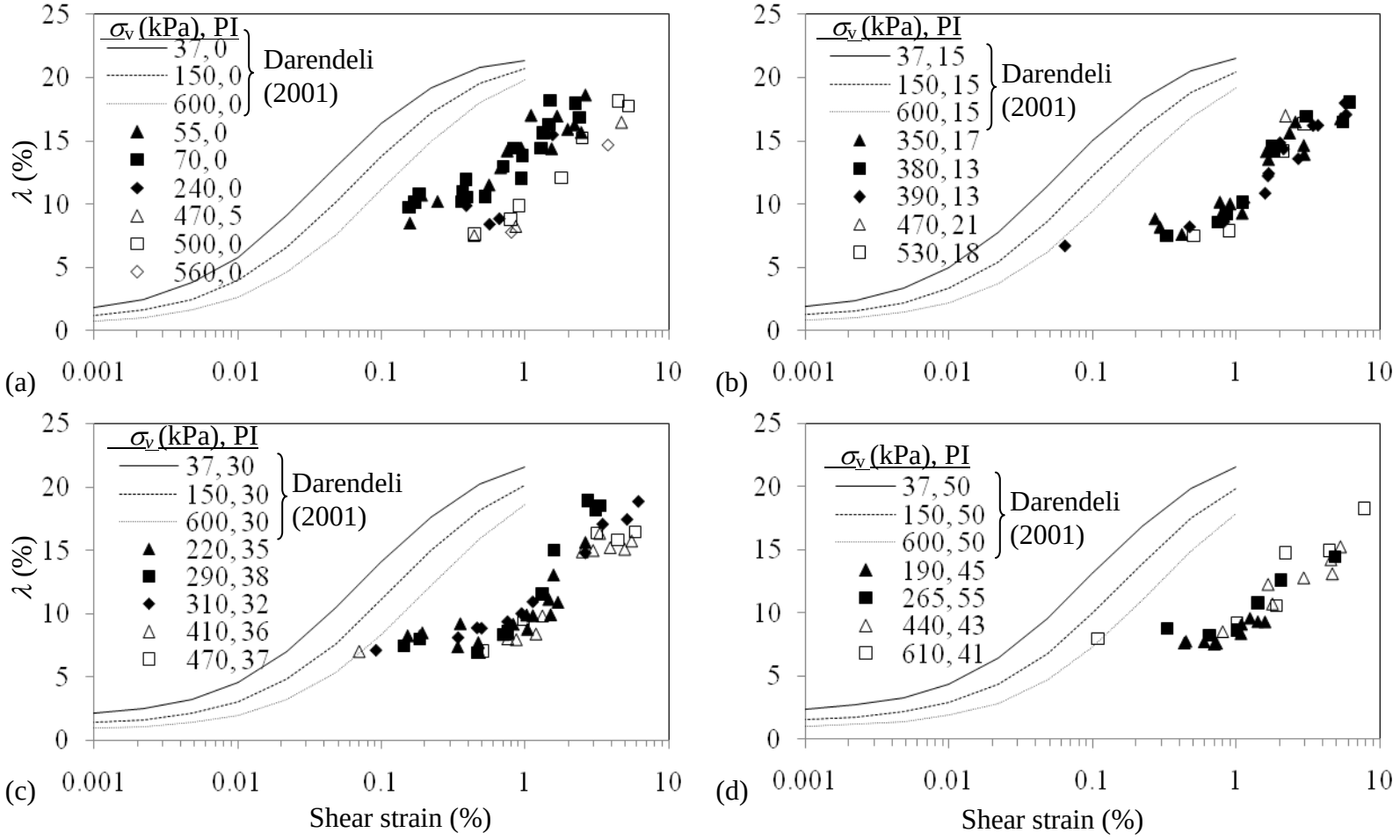

Figure 4.16 The comparison of λ with the empirical relationship recommended by Darendeli (2001) for different ranges of PI: a) PI=0-10, b) PI=10-30, c) PI=30-40, and d) PI=40-60.

It is concluded that the soil specimens recovered from Adapazarı dissipate less energy during cyclic loading when compared with the typical ranges reported in literature. Nonetheless, the conclusion is valid for cyclic shear-strain amplitudes around 1%, which are presumably achieved by the levels of CSR induced on Adapazarı deposits during the 1999 Kocaeli earthquake. Lower energy dissipation capacity of Adapazarı soils can be a consequence of reversed-S shape of hysteresis loops, which may be a characteristic of normally consolidated or lightly over-consolidated Adapazari deposits. The reversed-S shape is also reported by Yilmaz et al. (2003) and Sancio et al. (2003) after cyclic triaxial tests with specimens recovered from Adapazarı (Figure 4.17.a-b). Besides, the similar response of Fraser Silt in CDSS tests is reported by Sanin and Wijewickreme (2005), (Figure 4.17.c), and that of normally-consolidated reconstituted Keuper Marl silt in cyclic triaxial tests is reported by Yasuhara et al. (2003), (Figure 4.17.d-e).

Figure 4.18 shows a schematic view of typical hysteresis loops reported after the cyclic loading tests run by several researchers (e.g., Hardin and Drnevich, 1972; Puzrin et al., 1995; Vucetic et al., 1998; Lanzo and Vucetic, 1999; Darendeli, 2001), and a typical reversed-S shaped loop recorded in this study. Both loops follow a similar stress-strain path between A and B, and between D and E in Figure 4.18.

On the other hand, the tangent shear modulus of Adapazarı specimen decreases sharply at point B and E, and is roughly constant thereafter. In contrast, the typical hysteresis loops reported in literature show a gradual reduction in tangent modulus after point B and E. Consequently, the area enclosed by a reversed-S shaped hysteresis loop (i.e., energy dissipated during a load cycle) is less than that enclosed by a typical hysteresis loop with gradual change in tangent stiffness.

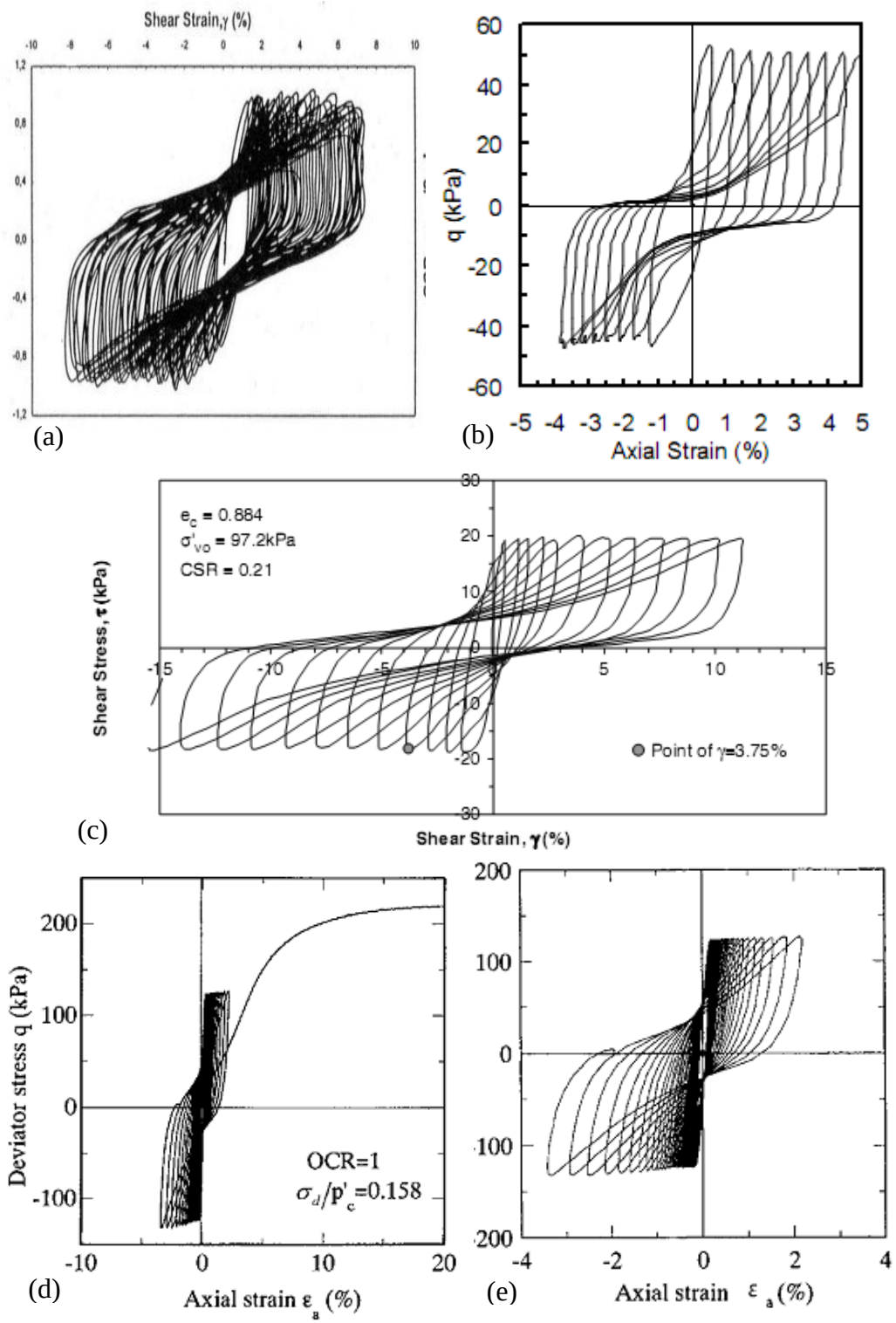

Figure 4.17 Test results with reversed-S shape: a) Pekcan (2001) b) Sancio et. al. (2003), c) Sanin and Wijewickreme (2005), d) and e) Yasuhara et al., 2003.

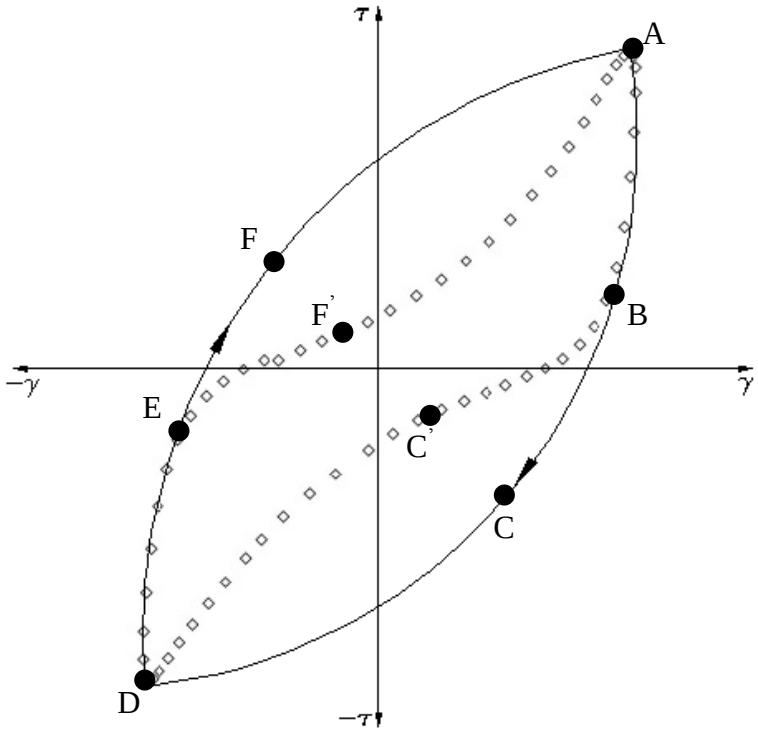

Figure 4.18 Comparison of an ideal hysteresis loop with a "Reversed S" shaped loop.

4.4.2 Shear modulus (G_{sec})

Figure 4.19 shows the scattering of G_{sec} according to the results of CDSS tests. G_{sec} decreases by shear strain with a similar trend for all ranges of PI. For further details, the test results are divided into the four groups of PI in Figure 4.20. It is observed that G_{sec} increases with increasing σ_v for all ranges of PI.

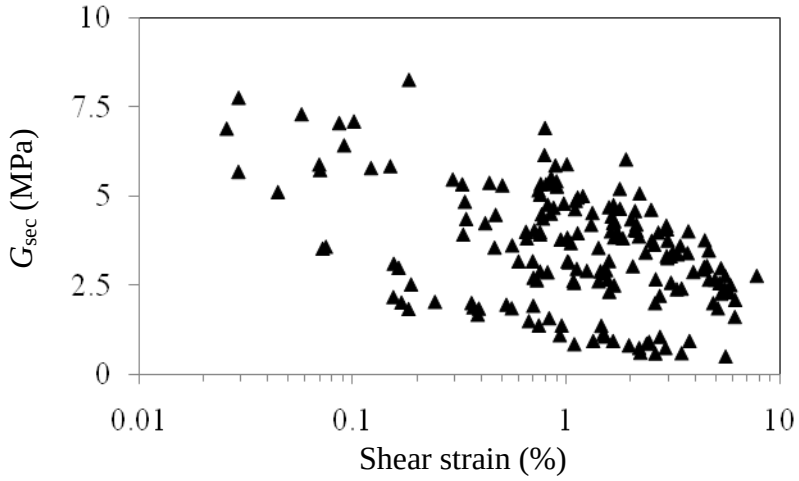

Figure 4.19 Scatter of G_{sec} versus shear strain for CDSS tests.

The relationship between PI and G_{sec} is assessed in Figure 4.21. In order to eliminate the effect of confining pressure on G_{sec}, the data is divided into 4 groups according to σ_v. Apparently there is no significant relationship between G_{sec} and PI. Most differences between test results with different PI can be attributed to the more prominent effect of σ_v. As a conclusion, G_{sec} of Adapazarı soils for shear strain amplitudes about 1% is dependent on effective overburden pressure, whereas PI has no or negligible effect on G_{sec} of those soils.

The rate of loading during a CDSS test may have a pronounced effect on the soil behavior. Therefore, the ranges of G_{sec} calculated by using the results of CDSS tests are compared with those obtained by DSS tests in order to validate the previous conclusions about G_{sec}. Instantaneous shear stress is divided by the instantaneous shear strain in order to calculate the history of G_{sec} during a DSS test. The agreement between G_{sec} obtained by both types of tests is shown in Figure 4.22 for the results of seven DSS tests. Consequently, the relationship between G_{sec} and shear-strain for Adapazarı deposits can also be estimated by employing monotonic loading tests, provided that the soil response to shearing does not show strong dependency on the loading rate and does not exhibit excessive stiffness degradation (e.g., liquefaction) during cyclic loading.

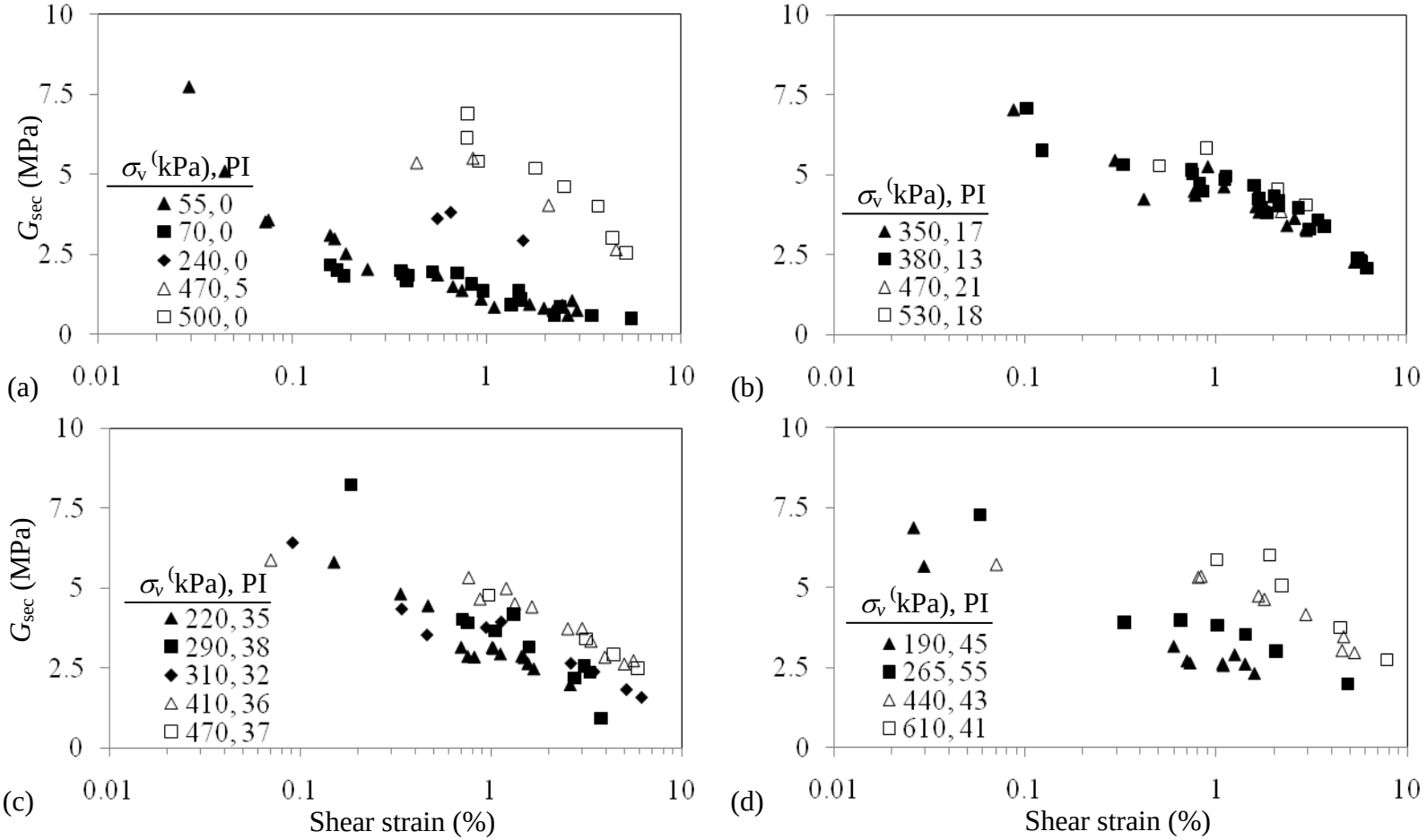

Figure 4.20 G_{sec} versus shear strain for specimens with PI in the range a) 0-10, b) 10-30, c) 30-40, and d) 40-60.

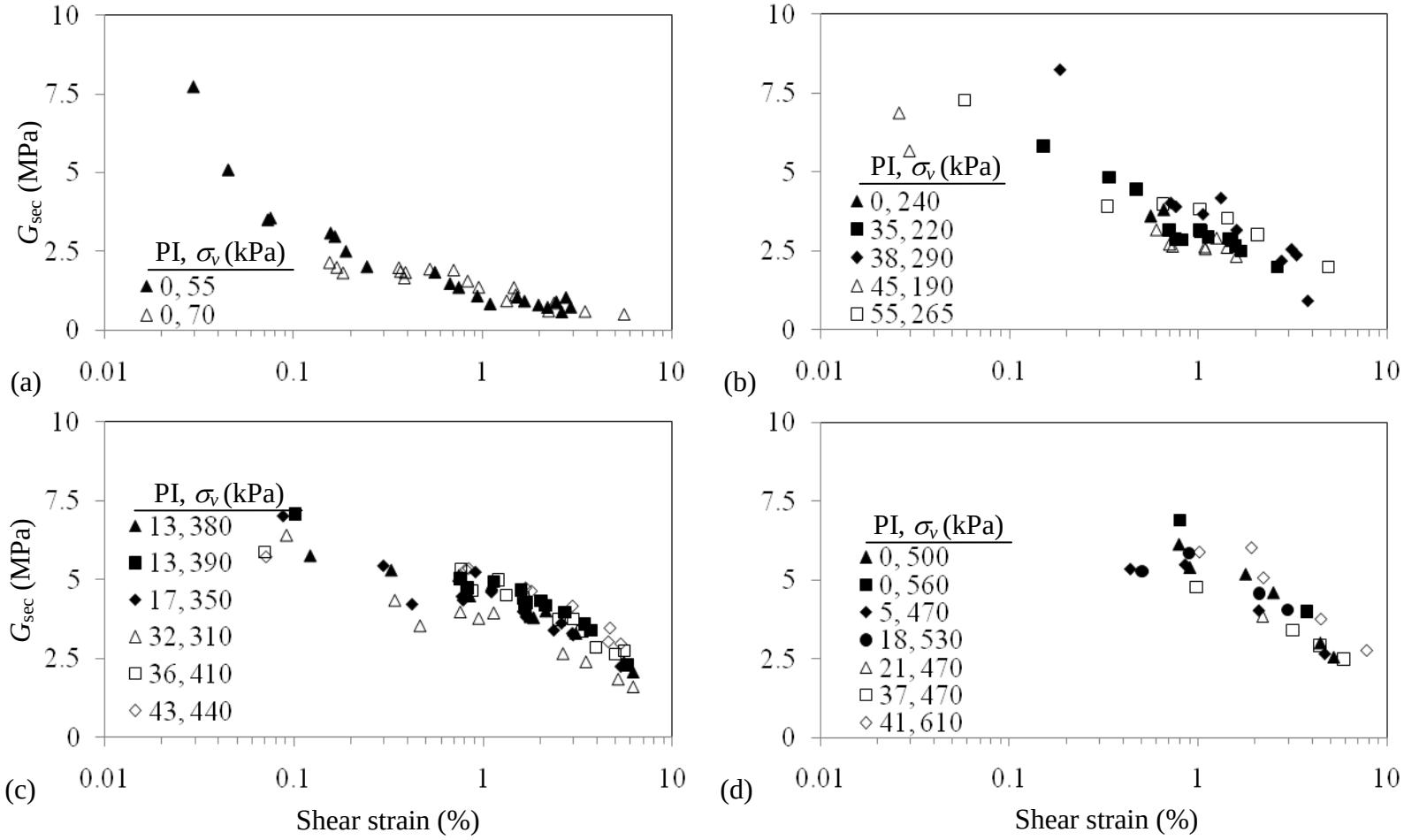

Figure 4.21 G_{sec} versus shear strain for specimens tested with σ_v (kPa) in the range a) 0-150, b) 150-300, c) 300-450, and d) 450-600.

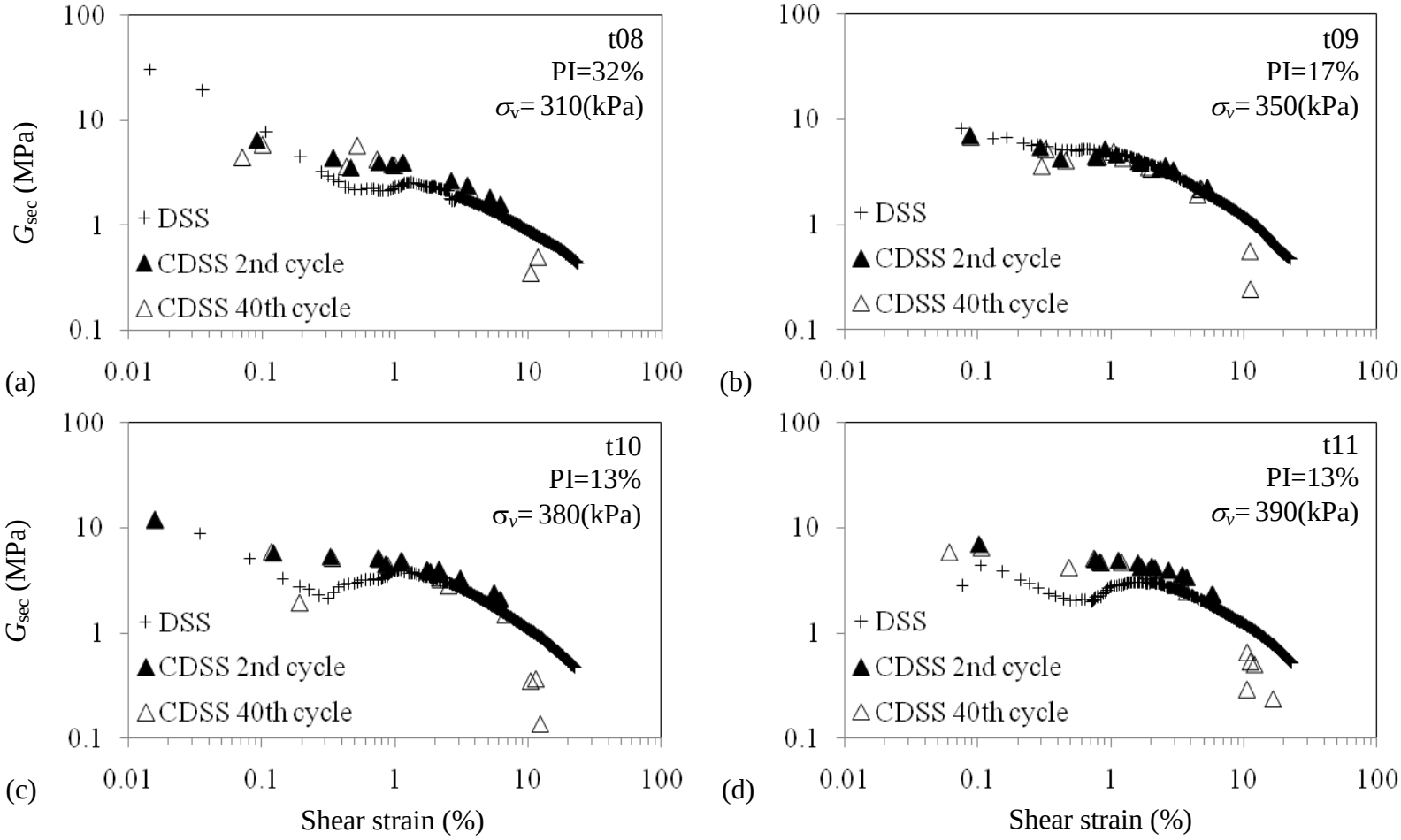

Figure 4.22 Comparison of G_{sec} calculated by DSS tests and CDSS tests results for samples from the tubes a) 8, b) 09, c) 10, d) 11, e) 12, f) 13, and g) 18.

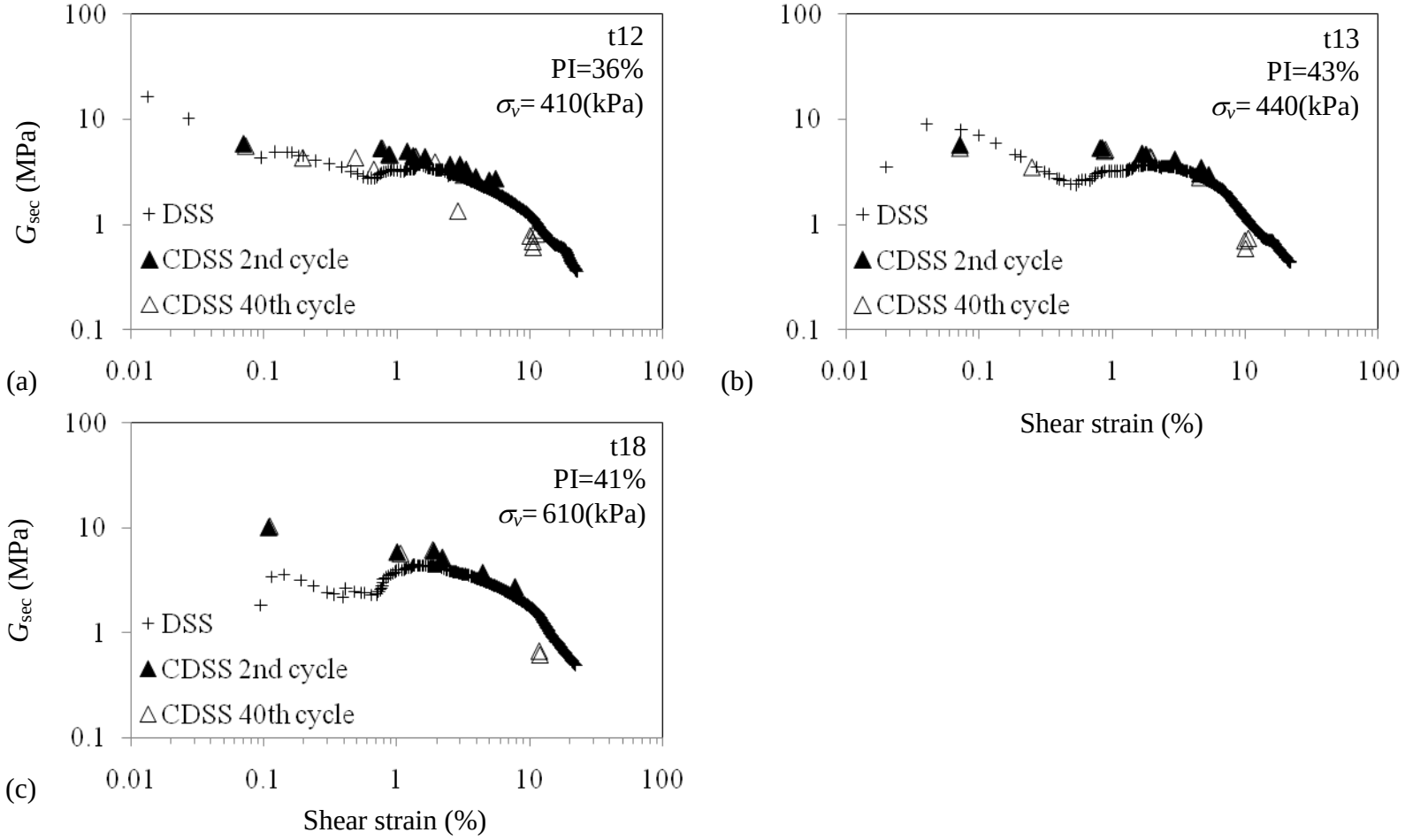

Figure 4.22 Continued.

4.4.2.1 Estimation of (G_{max})

In order to extend the relationships between shear modulus and shear strain to lower amplitudes of loading, it is necessary to estimate G_{max}, the maximum shear modulus of soil that occur at extremely small ranges of shear strain. G_{max} is not a unique characteristic of soil, since its relation with void ratio (e) and mean effective confining stress (σ_m') is denoted by several researchers (e.g. Hardin and Black, 1969; Hardin 1978; Jamiolkowski et al. 1991; Kawaguchi and Tanaka, 2008). Besides, at the end of each stage of cyclic loading, the specimens are reconsolidated before the next stage with larger amplitudes of load cycle. A reconsolidation phase results in a limited decrease in void ratio (e) of specimen, which may result in a limited increase in G_{max}. Therefore, considering a single value of G_{max} for normalization of G_{sec} obtained after a staged cyclic loading test may result in biased comparisons with other normalized test results. Therefore, several empirical relationships to estimate G_{max} (e.g. Hardin and Black, 1969; Hardin 1978; Shibata and Soelarno, 1978; Zen et al. 1987; Jamiolkowski et al. 1991; Shibuya and Tanaka, 1996; Kawaguchi and Tanaka, 2008) are compared with the range of G_{max} calculated by using the results of PS-suspension logging (Equation 1.3). The relationship suggested by Hardin (1978) yields the best agreement between the empirical ranges of G_{max} based on geotechnical properties of soils, and V_s. The empirical relationship of Hardin is given as

$$G_{max} = 625 \cdot F_e(e)(\mathrm{OCR})^K P_a^{1-n} (\sigma'_m)^n \qquad [4.3]$$

where P_a is the atmospheric pressure, OCR is the overconsolidation ratio, σ'_m is the mean effective stress on soil, K and n are characteristic coefficients for different soil classes, and $F_e(e)$ is a dimensionless function of void ratio which is suggested as

$$F_e(e) = \left(0.3 + 0.7e^2\right)^{-1} \qquad [4.4]$$

The suggested values of K are 0.00, 0.18, 0.30, and 0.41 when PI of soil is 0, 20, 40, and 60 respectively [Hardin, 1978]. Hence, the term OCR in equation 4.3 can be omitted for normally or lightly overconsolidated soils with low PI. With the intention of adopting functional form of Equation 4.2 to predict G_{max} for specimens recovered

from Adapazarı, the term σ'_m is substituted by σ_v, the effective overburden pressure in situ, which is equivalent to normal consolidation stress on a specimen:

$$G_{max} = \frac{C}{Ae^B + D} P_a^{1-n} (\sigma_v)^n \quad [4.5]$$

In order to determine the coefficients *n*, *A*, *B*, *C*, and *D* that minimize the total sum of squared difference between G_{max} empirically predicted and that based on in-situ V_s, the optimization tool of Microsoft Excel, namely *Solver*, is used. Hence, the parameters that are best in the least-squares sense are given in the following empirical relationship:

$$G_{max} = \frac{502}{2.95e^{0.175} - 2.30} P_a \quad [4.6]$$

Hence, there is no significant relationship between σ_v and V_s. The conclusion is meaningful since *e* and σ_v. Hence *e* can be practically considered as the sole parameter related to G_{max} (or, V_s when unit weight of soil is given) of soils recovered from Adapazarı. The in-situ void ratios ($e_{in\text{-}situ}$) are determined by backward extrapolation of the virgin compression lines determined in the consolidation phases of CDSS tests to the logarithm of in-situ effective overburden stress ($\sigma'_{v,in\text{-}situ}$) on the *e-log*($\sigma_v$) plots as shown in Figure 4.23.

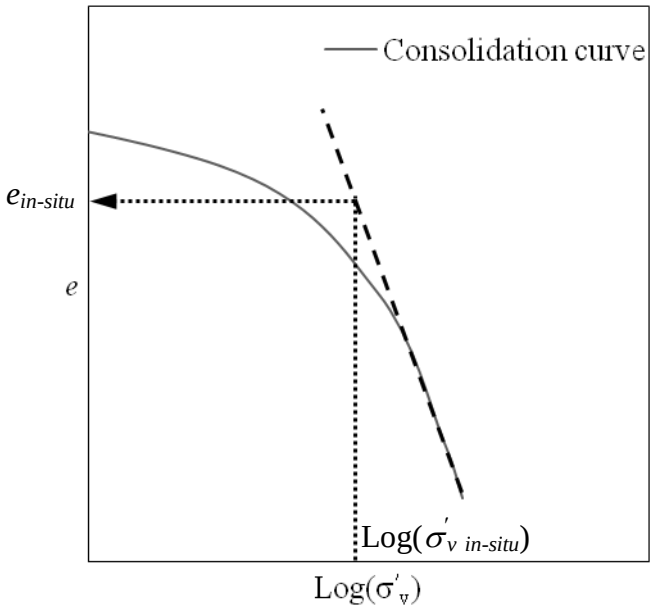

Figure 4.23 Determination of $e_{in\text{-}situ}$ according to consolidation of specimen.

Figure 4.24 compares V_S according to PS-suspension logging with V_S estimated by using equation 4.3 and 4.6 and 1.3.

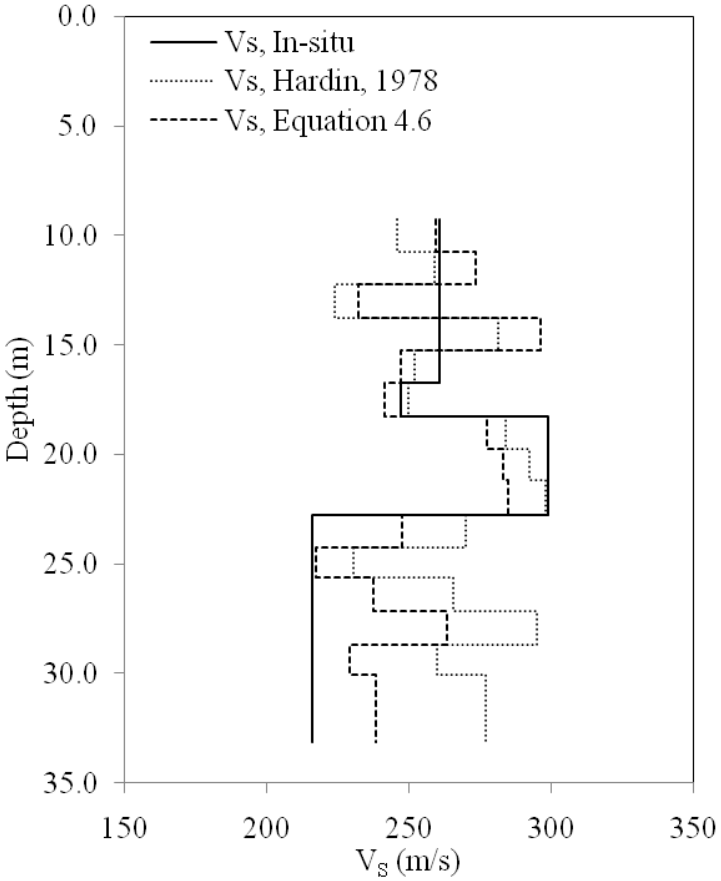

Figure 4.24 Comparison of in-situ V_s with the estimated V_S according to Hardin (1978) empirical relationship and with V_s according to equation 4.6.

Figure 4.25 shows a similar comparison for G_{max}. The reasonable agreement between G_{max} obtained by two approaches points out that Equation 4.6 can be used for normalizing G_{sec}, which is also useful in interpretation of bias in test results due to void-ratio decrease in staged CDSS tests. By using equation 4.6 and void ratios determined at the beginning of each shearing stage, the increase in G_{max} through successive shearing stages can be estimated.

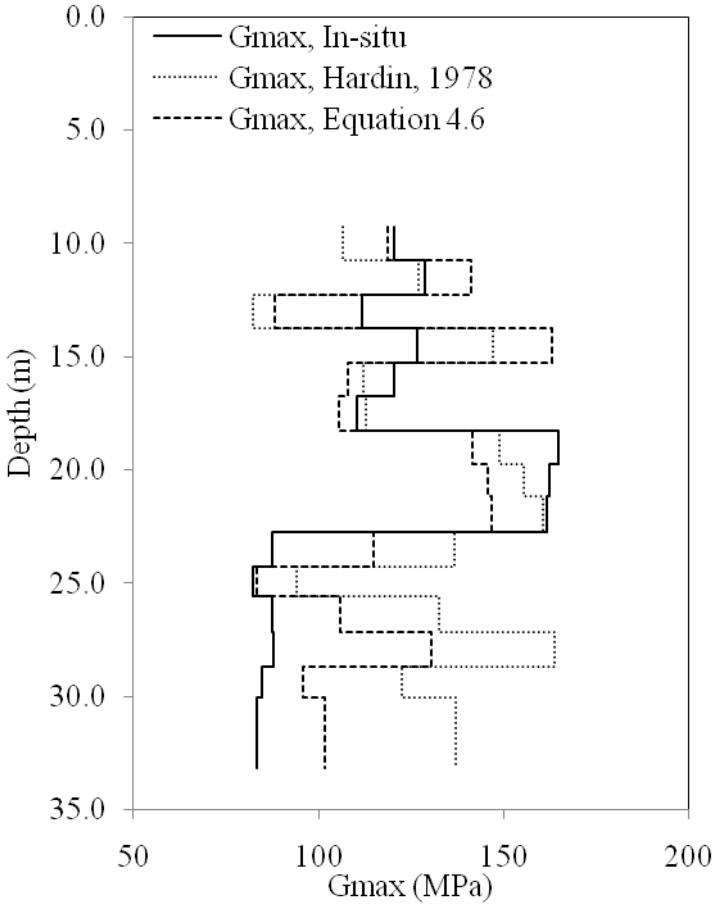

Figure 4.25 Comparison of in-situ G_{max} with the estimated G_{max} according to Hardin (1978) empirical relationship and with G_{max} according to equation 4.6.

Figure 4.26 compares the estimated G_{max} with that of first stage. It is concluded that the difference is usually less than 20%. Hence, the magnitudes of change in G_{sec} among stages of shearing do not explain the difference between empirical relationships on modulus reduction and the results of CDSS tests.

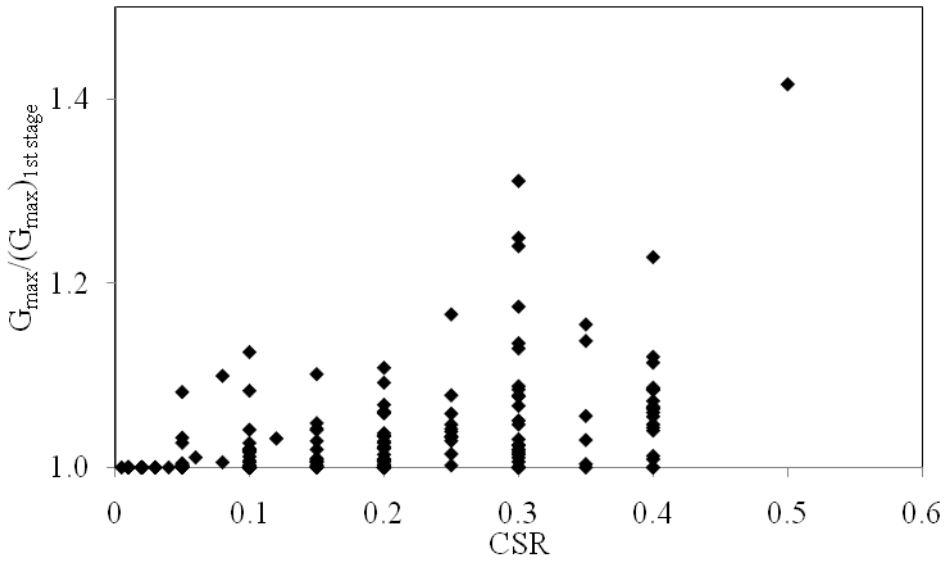

Figure 4.26 The estimated increase in G_{max} in staged CDSS tests.

4.4.2.2 Normalization of G_{sec} by G_{max}

G_{sec} is normalized by G_{max} so that the results can be compared with the strain-dependent modulus reduction curves for soils reported in literature. Equation 4.6 is used for calculation of G_{max}. The test results are divided into four groups according to PI of specimens (Figure 4.27).

A comparison of Figure 4.20 and Figure 4.27 reveals that G_{sec}/G_{max} shows less dispersion than G_{sec} for a given range of shear strain. On the other hand, the range of G_{sec}/G_{max} for some of the specimens with large σ_v is distinctly above from the others with similar PI. Normalized results for a ML-class specimen (PI = 0) tested under normal stress of 500 kPa (Figure 4.27.a) is such an example. Hence, the test results support that G_{sec}/G_{max} is also dependent on σ_v especially for the low PI range, as stated by Ishibashi and Zhang (1993), and Yamada et al. (2008). Some of the results can be inconsistent with that conclusion; however they can be explained by the uncertainty in estimation of G_{max}.

It can be stated that the use of equation 4.6, instead of V_s measured in-situ, may result in loss of precision in estimation of G_{max}. Therefore, the in-situ G_{max} shown inFigure

4.25 is also used for normalization of G_{sec}. However, in that case the dispersion of G_{sec}/G_{max}, shown in Figure 4.28, is larger than the dispersion shown in Figure 4.27. Hence, the use of equation 4.6, which proposes a relationship between G_{sec} and e, provides more precise estimations for G_{sec}.

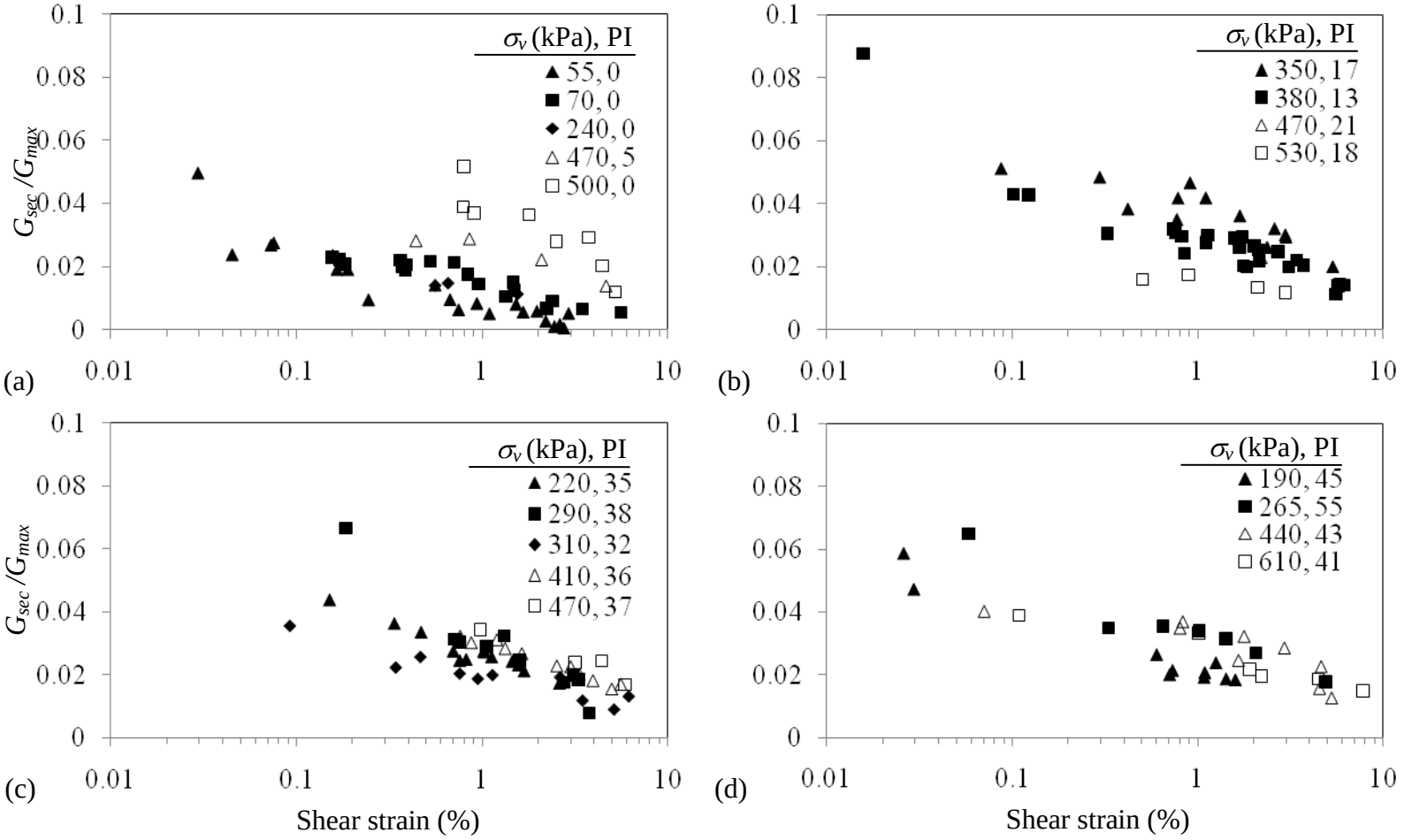

Figure 4.27 The relationship between in G_{sec}/G_{max} and shear strain for specimens with a) PI=0-10, b) PI=10-30, c) PI=30-40, and d) PI=40-60.

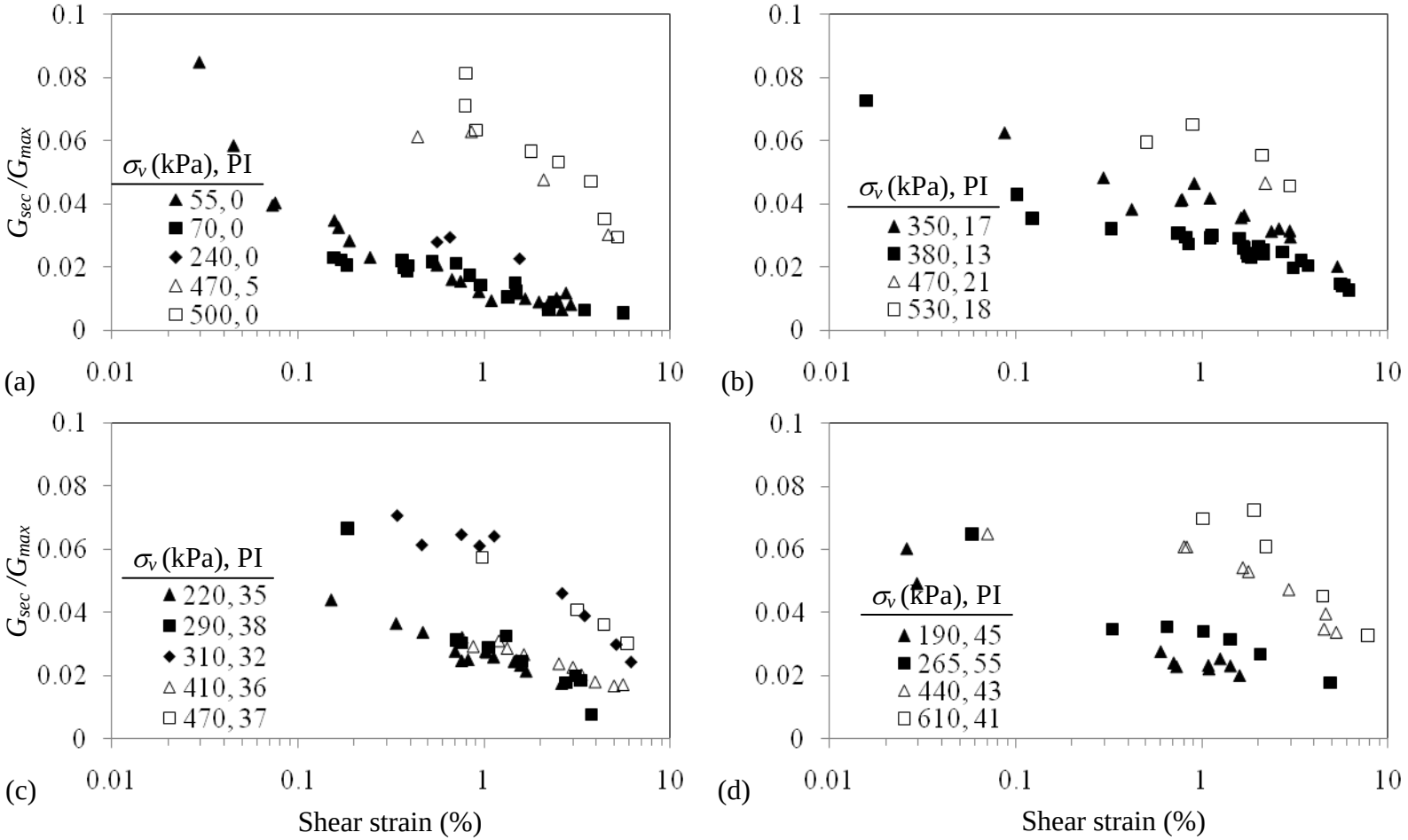

Figure 4.28 The relationship between in G_{sec}/G_{max} and shear strain for specimens with a) PI=0-10, b) PI=10-30, c) PI=30-40, and d) PI=40-60, in case V_S is used for estimation of G_{max}.

The relationship between normalized shear modulus (G_{sec}/G_{max}) and amplitude of cyclic shear strains that is observed by CDSS tests is compared with the empirical relationships proposed by Vucetic and Dobry (1991), Ishibashi and Zhang (1993), and Darendeli (2001). Equation 4.6 is used for calculation of G_{max}. Figure 4.29 depicts that the ranges of G_{sec}/G_{max} due to the results of CDSS tests are always considerably smaller than those suggested by Vucetic and Dobry (1991).

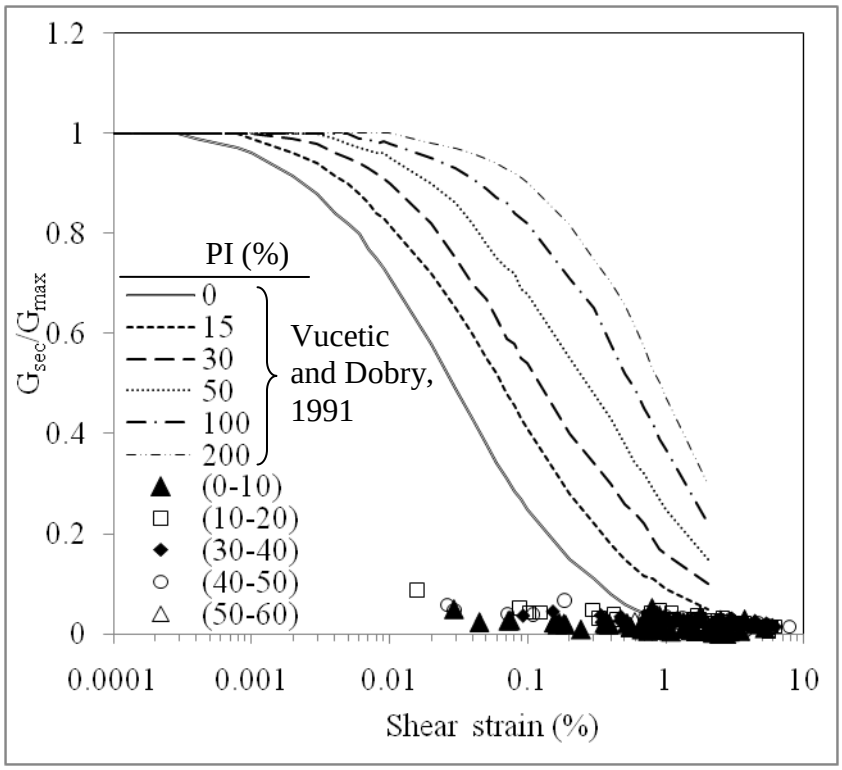

Figure 4.29 Comparison of the ranges of G_{sec}/G_{max} with the empirical modulus degradation curves suggested by Vucetic and Dobry (1991) curves.

The same conclusion on the difference between test results and empirical relationships is obtained when the empirical relationships of Ishibashi and Zhang, and Darendeli are considered. The severe difference between the test results and the empirical relationships can be explained by a possible substantial error in estimation of G_{max}, which is based on PS-suspension logging performed in Adapazarı. However, the similarity between empirical equation of Hardin (1978) for estimation of G_{max} and in-situ V_s (Figure 4.24 and Figure 4.25) impairs the potential of a substantial error in the

velocity log. Another explanation is that the rate of modulus degradation of Adapazarı soils by increasing amplitudes of shear strain is substantially higher than most fine soils that are tested for similar studies.

For a final discussion on the relationship between G_{sec}/G_{max} and shear strain, an alternative procedure for estimation of G_{max} is followed. It is assumed that the relationship between G_{sec}/G_{max} and shear strain is grossly consistent with the empirical relationships given in literature. The coefficient n in Equation 4.3 is assumed to be 0.5, which is acceptable for most soils, and the term $(OCR)^K$ is substituted by 1.0 considering lightly over-consolidated low-plasticity soils. (Yasuhara et al., 2003). Then, substitution of Equation 4.4 in 4.3 results in the following equation:

$$G_{max} = A \cdot \left(0.3 + 0.7e^2\right)^{-1} \cdot P_a^{0.5} \cdot \left(\sigma'_{\mathrm{m}}\right)^{0.5} \qquad [4.7]$$

The coefficient A in Equation 4.7 should be empirically determined by employing G_{max} determined in laboratory tests (Yasuhara et al., 2003). Here, the value of A that minimizes the sum of squared difference (i.e., the least squares) between test data on G_{sec}/G_{max} and the empirical relationship proposed by Ishibashi and Zhang (1993) is computed. σ_m' is calculated by Equation 4.2. Consequently, A=70, which is significantly less than the value of 625 suggested by Hardin (1978), provides the least squared difference (Figure 4.30). Then, the range of G_{max} calculated by using Equation 4.7 is converted to V_s. The back-calculated values of V_s, which range from 75 m/s to 100 m/s, are compared with the in-situ measurements in Figure 4.31. It is concluded that although such low ranges of V_s are possible for shallow loose soils of Adapazarı basin, (Figure 1.9) the shear-wave velocity in stiffer and deeper deposits showing considerably high penetration resistance (SPT-N) should be larger.

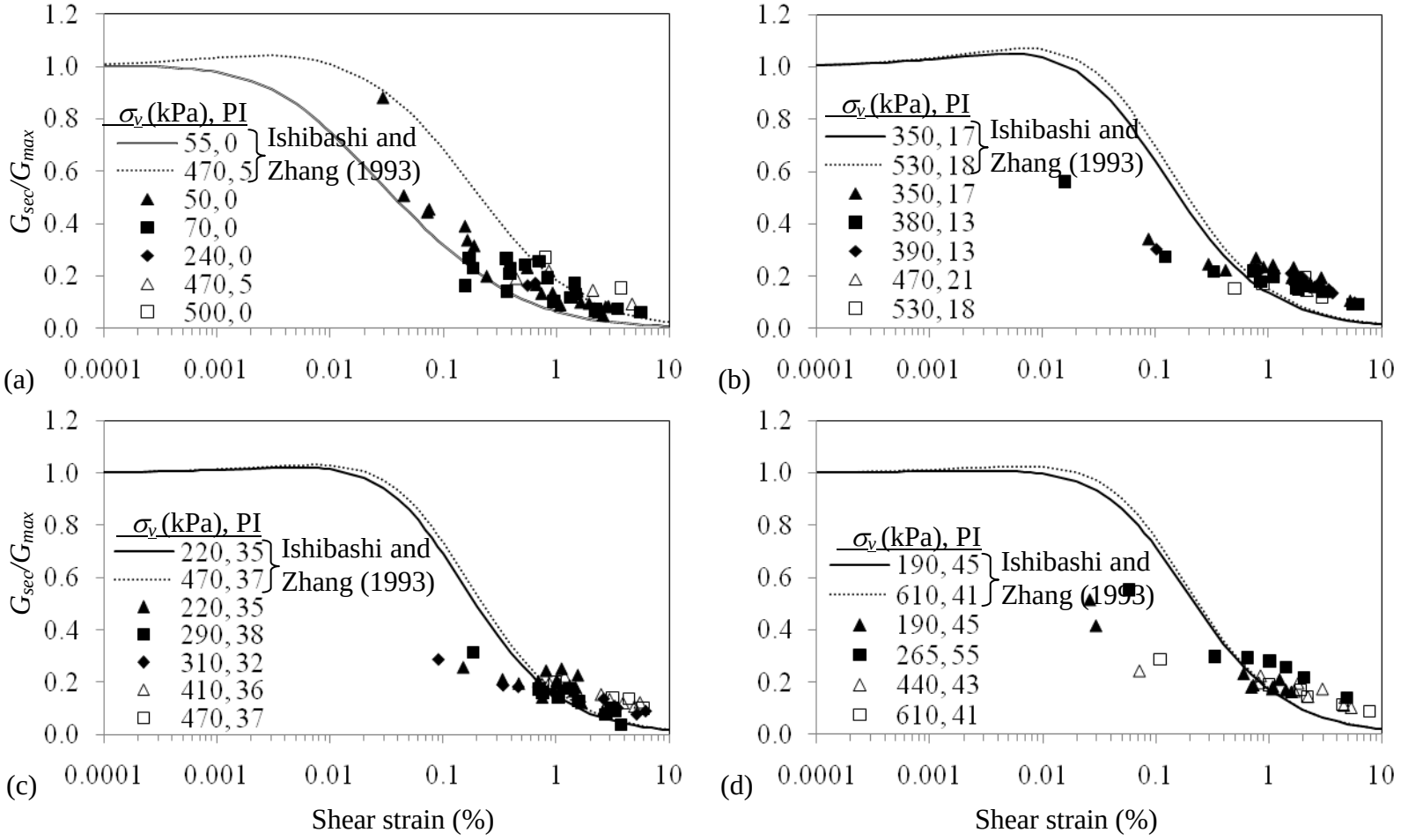

Figure 4.30 G_{sec}/G_{max} versus shear strain for PI between: a) 0-10; b) 10-30; c) 30-40; d) 40-60 using back calculated G_{max}.

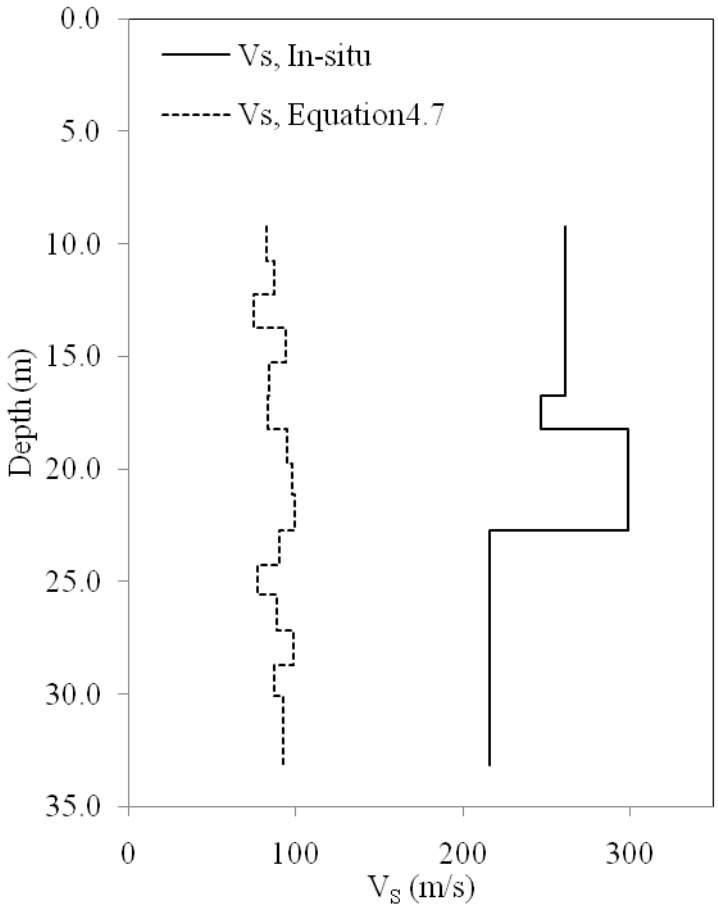

Figure 4.31 Comparison of back-calculated V_S with in-situ V_S.

Hence, supposing that the stiffness and strength characteristics of specimens that are observed in DSS tests reflect the actual response of Adapazarı deposits to severe shearing, the conventional empirical models for estimation of modulus degradation (G_{sec}/G_{max}) with increasing strain may not be used for geotechnical site response analysis of Adapazarı deposits. Otherwise, estimated G_{sec} for any soil layer can be considerably larger than its actual in-situ value, when an accelerograph that is comparable to those recorded in 1999 Kocaeli Earthquake is considered in analyses. A practical approach for equivalent-linear site-response analyses is to use equation 4.7 with A=70 in order to estimate $G_{max,}$ and then to use a modulus reduction curve that is consistent with the scattered data of all test results shown in Figure 4.32, wherever the shear strain exceeds the threshold of 0.1%.

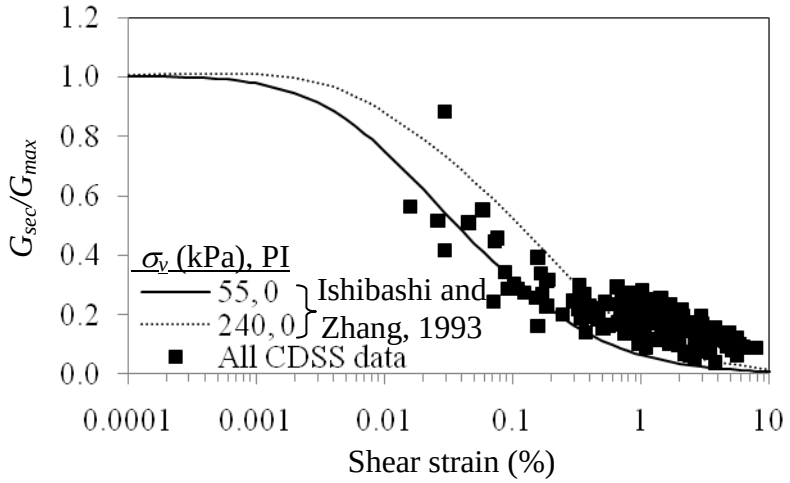

Figure 4.32. The scattering of normalized G_{sec}, in case that G_{max} is calculated by equation 4.5.

4.4.2.3 Cyclic degradation of G_{sec}.

In order to investigate the cyclic stiffness degradation of specimens, the G_{sec} at the last load cycle ($G_{sec\text{-}ultimate}$) is compared with that at the second cycle ($G_{sec\text{-}2nd\ cycle}$) for all test stages in Figure 4.33. The ultimate cycle number is usually 40, but some of the tests were stopped at a lower cycle number because of extreme cyclic degradation of G_{sec}. It is observed that the cyclic degradation of G_{sec} is more pronounced for specimens with lower PI. On the other hand, significant cyclic degradation of all specimens occur when CSR is greater than 0.3. It is concluded that, cyclic degradation in G_{sec} of soils should be taken into consideration in site-response analyses for Adapazarı, when CSR is greater than 0.3. The practical minimum limit can be reduced to 0.2 for non-plastic or low-plasticity soils.

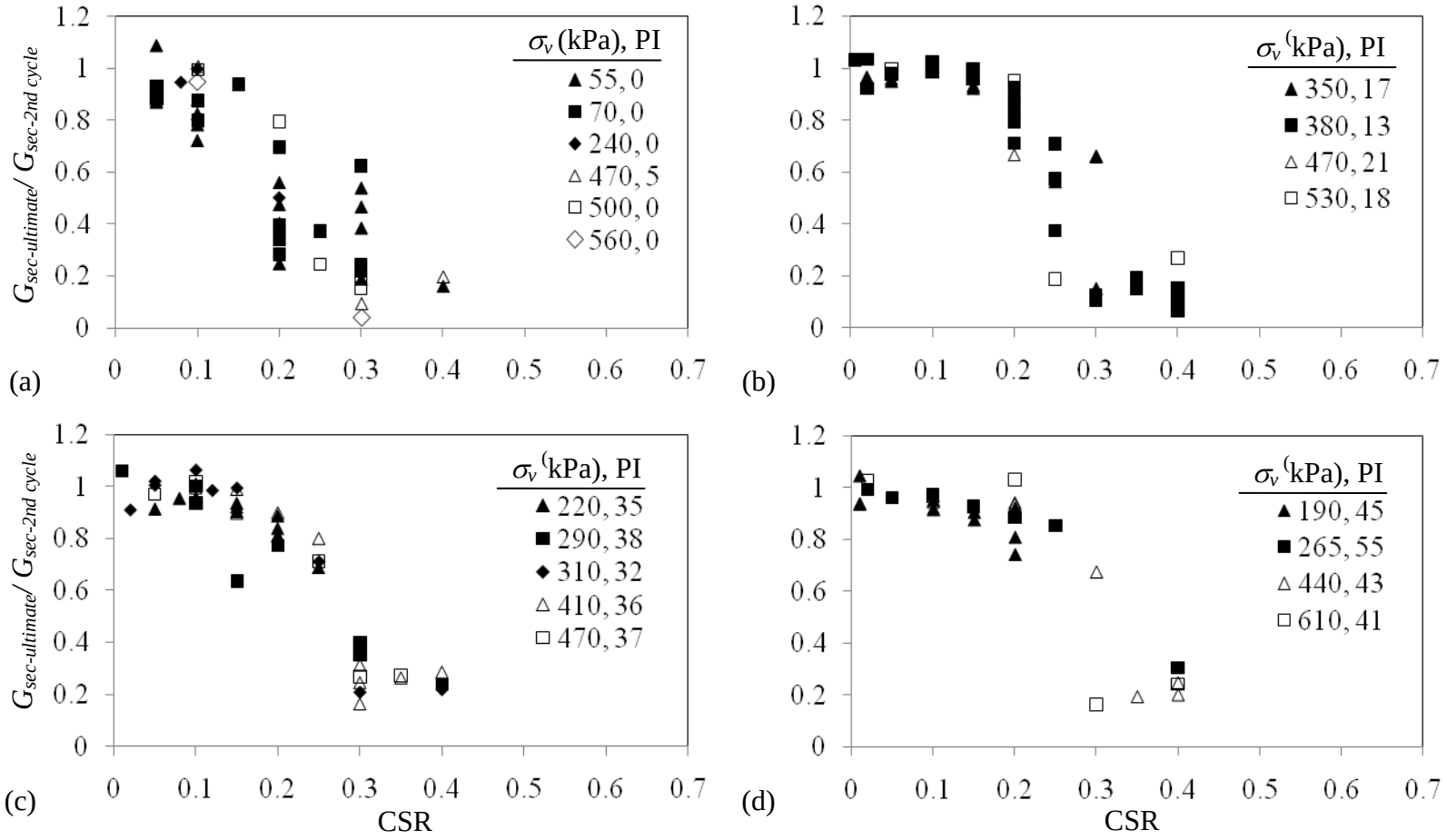

Figure 4.33 Degradation of G_{sec} after 40 cycles for specimens with PI in the range a) 0-10, b) 10-30, c) 30-40, and d) 40-60.

4.4 Discussion

Several CDSS tests were conducted by considering the range of cyclic stress ratio (CSR) imposed on Adapazarı deposits during 1999 Kocaeli Earthquake. The frequency of cyclic loads was chosen as 1 Hz, which is supposed to be reasonably consistent with the frequency content of vertically incident S-waves that propagated in the alluvium basin. All of the tests resulted in cyclic shear-strain amplitudes that are greater than 0.1%, whereas most of the empirical models presented in literature for estimation of strain-dependent modulus reduction and damping are generally based on test results for strain levels lower than 0.1%. The energy dissipation capacities of specimens recovered from Adapazarı were observed to be significantly lower than those predicted by empirical relationships. The difference can be explained by the reversed-S shaped hysteresis loops observed during CDSS tests. On the other hand, regarding the relationship between G_{sec}/G_{max} and the cyclic shear-strain amplitude, the difference between the results of this study and several empirical relationships proposed in literature is substantial. G_{sec} determined by a CDSS test is reasonably consistent with that determined by a monotonic DSS test. The reasonable consistency between the results of monotonic loading tests and cyclic loading tests points out that the relatively low range of G_{sec} experienced during cyclic loading tests can be attributed to low-stiffness response of specimens to monotonic loading, but not to a severe problem in cyclic loading test procedure. The strain-dependent variation in G_{sec}/G_{max} could be consistent with the empirical relationships proposed in literature if the shear-wave velocity measured in the borehole was around 90 m/s at depths of sample recovery.

One possibility that explains the discrepancy between the test results and empirical relationships proposed in literature is that the P-S suspension logging technique leaded to artificially high velocity measurements due to improper quality of borehole, or due to misinterpretation of records. Unfortunately, no

other seismic measurements in the close vicinity of site are available for comparisons. Nevertheless, the range of *SPT-N* is in good agreement with the range of VS (Figure 2.15) according to NEHRP (2003), such that both data confirms that the site is composed of stiff (NEHRP Class D) soils. However, the down-hole soundings reaching to the depth of 25 m on PEER sites J, G (very close to J), and F (very close to D) with the seismic cone method (see Figure 1.1 for locations and Figure 1.9 for velocity ranges) reveal that shear-wave velocity measurements around 90 m/s are possible at the depths experienced in this study (Sancio et al., 2002). One important observation is that the SASW technique applied on site J resulted in greater velocity ranges of V_s than those measured by seismic cone (see Figure 2.17 for the results of SASW on site J). At depths between 11 m and 26 m, the ratio between the two sets of V_S is roughly between 2 and 3. No explanation for the discrepancy between the two velocity logs is found in literature.

Another explanation could be the effect of sample disturbance on G_{max}, since advancing borehole in drilling operation, penetration of sampling tube and sample retrieval to ground surface, water content redistribution in the tube, transportation of tube from site to lab, extrusion of the sample from the tube, drying and/or changes in water pressure, trimming and other sample preparation procedures in laboratory, and saturation and consolidation phases prior to undrained shearing provide opportunities for sample disturbance [Lambe and Whitman, 1969; Baligh et al., 1987; Hight et al., 1992; Cho et al., 2007]. The sample disturbance is particularly important for sensitive and structured soils, since the routine sampling methods and lab preparation for testing can destroy the cementation bonds and consequently the soil fabric [Lambe and Whitman, 1969, Raymond et al., 1971; Hight and Georgiannou, 1995; Lunne et al., 2006; Prasad et al., 2007]. The disturbance can result in severe loss in undrained small-strain stiffness of sensitive soils, especially in G_{max}, even for high-quality samples. The reduction in G_{max} due to disturbance tends to be more significant with increasing V_S in-situ [Baligh et al., 1987; Ishihara, 1996; Hight et al., 1997; Santagata and Germaine, 2002; Tan et al.,

2002; Chiara and Stokoe II, 2006; Landon et al., 2007; Long and Menkit, 2007; Long et al., 2010; Hosseini et al., 2010]. Hence, the sampling and particularly specimen preparation procedures followed in this study may be a reason for explaining the severe difference between the G_{max} determined in-situ and that estimated by using lab tests. No special very low-strain tests could be performed in lab to determine G_{max} in order to investigate the level of sample disturbance, because of the lack of necessary equipment (e.g., bender elements) for testing.

It is possible to estimate a reasonable value of G_{max} considering a Hyperbolic stress-strain relationship by using the test results on strain-dependent variation in G_{sec} (e.g., Yasuhara et al., 2003, Song et al., 2004), or by using empirical relationships that employ the index properties of specimens and confining pressure on specimens (Section 1.2.2), so that empirical relationships between G_{sec}/G_{max} and the shear strain can be obtained (see Figure 4.32). Then, in-situ G_{Sec} for a given shear strain can be calculated by multiplying the G_{max} in-situ (i.e., by seismic tests) by normalized shear modulus (G_{sec}/G_{max}) that is based on laboratory tests, as usual practice. However, the assumption that relationships between G_{sec}/G_{max} and shear strain amplitude determined in lab tests are consistent with those in-situ is not verified [Kurtulus and Stokoe II, 2008]. The following findings in literature provide evidence for the invalidity of the assumption.

The severe effect of destructuring of soil on its undrained stiffness diminishes with increasing shear strain amplitudes, and can be negligible at large shear strain levels (i.e, exceeding 0.1%) [Hight et al., 1997; Santagata and Germaine, 2002]. Besides, Hight and Georgiannou (1995) provided test results showing that the increase in undrained stiffness due to aging is partially removed at small strains by sampling and reconsolidation, and that the effect of damage on soil structure is compensated at larger strains by the reduction in void ratio during the reconsolidation of specimen in lab. Hence it is possible that the undrained in-situ brittleness of soils may not be observed in lab tests. Similarly,

Yamada et al. (2008) reported test results supporting that the effect of soil plasticity and fines content on soil structure and consequently on undrained secant modulus vanishes at larger strains such that the undrained secant modulus of remoulded and undisturbed specimens with different index properties are approximately equal at shear strain levels exceeding 0.5%. The stiffness degradation is also strongly dependent on the rate and the form of loading in lab tests, such that different test devices and stress paths can result in different relationships between G_{sec}/G_{max} and induced strain [Hight et al., 1997]. Although all those test results reported in literature may only be valid for particular soil types and test procedures, they point out the likelihood of a significant inconsistency between the G_{sec}/G_{max} in-situ and that observed in lab for a given cyclic shear-strain amplitude.

Considering the data gathered by testing samples recovered from the parking lot in Adapazarı, it is concluded that the lab-based relationships between G_{sec}/G_{max} and shear strain should be cautiously used for the geotechnical site response analyses, since G_{max} determined (or, estimated) by lab tests can be substantially lower than the value in-situ. Hence, the degree of soil nonlinearity can be underestimated if empirical relationships based on laboratory tests are used. On the other hand, the way the specimens are assembled in a DSS apparatus causes sample disturbance to some extents, because small clearances along the sample perimeter existing before consolidation phase unavoidably leads to accumulation of radial strains during consolidation, before the constant-volume shearing phase [Lunne et al., 2006]. No consideration to initial radial strains before shearing is given by ASTM D 6528-07. The issue is apparently important for the specimens recovered from Adapazarı, since Bray et al., (2001) reported sensitivity ratios (i.e., the ratio of peak to residual shear strength) between 3 and 4 due to the vane shear tests in very shallow fine soils experienced through a single borehole in Adapazarı.

The discussion above and the comments given are limited to the interpretation of results provided by the CDSS tests and to samples recovered in this study.

Hence, further studies are necessary to explain why the strain-dependent modulus reduction determined in this study is more pronounced than those given by empirical relationships presented in literature. For stronger conclusions, particular emphasis should be put on the effects of sample disturbance and on the sensitivity of Adapazarı soils.

CHAPTER 5

SUMMARY AND CONCLUSION

5.1 Summery

In order to investigate dynamic properties of Adapazarı soil deposits, disturbed and undisturbed samples were recovered from a single borehole located in central Adapazarı. The penetration resistance and shear-wave velocity of soils in-situ are measured by standard penetration tests and P-S suspension logging. The disturbed samples were used for determination of index properties of soils. The Thin-Walled tubes were used to recover undisturbed samples. 223 cyclic direct simple shear tests and 7 (monotonic) direct simple shear tests were done on 76 undisturbed specimens in 85 days. Before the cyclic direct simple shear tests, several calibration studies were carried out in order to optimize the parameters that control the cyclic load unit. A simple method was developed in order to estimate mechanical friction in the Geocomp model cyclic direct simple shear (CDSS) apparatus.

The load amplitudes applied in CDSS tests were consistent with the range of cyclic stress ratio (CSR) imposed on Adapazarı deposits during 1999 Kocaeli Earthquake. The frequency of cyclic loads was set to 1 Hz, which is supposed to be consistent with the frequency content of vertically incident S-waves that propagated in the alluvium basin during the event. The secant shear modulus and damping ratio of soil response were calculated for each CDSS test. The results were compared with the empirical relationships given in literature. The response to cyclic loading was compared with the response to slow monotonic loading. Finally, cyclic stiffness degradation characteristics of specimens were investigated by comparing the secant shear modulus in ultimate load cycle with that in second cycle.

5.2 Conclusion

The following conclusions, limited to the specimens recovered from a single borehole opened in central Adapazarı, are drawn following a series of laboratory and field tests:

- The shear strain amplitudes measured during cyclic loading tests range from 0.02% to 10% under cyclic stresses consistent with that of 1999 Kocaeli Earthquake.
- The hysteresis loops of most tests showed a reversed-S shape, such that the tangential shear modulus near zero strain is smaller than that near peak strain.
- The range of G_{sec}, the secant shear modulus, determined by cyclic loading tests was reasonably consistent with that determined by monotonic loading tests.
- The cyclic degradation of G_{sec} is more pronounced for specimens with lower PI. On the other hand, significant cyclic degradation of all specimens occur when CSR is greater than 0.3.
- Excess pore-pressure ratio of specimens did not reach to 100%, in the cases that the amplitude of cyclic shear stress was less than the monotonic shear strength.
- Considering the tests that shear strain amplitudes are in the order of 1%, G_{sec} is significantly dependent on effective overburden pressure, whereas the plasticity index has no pronounced effect on the stiffness of material.
- Efficiency of multi-staged cyclic tests was shown by the observation that the change in maximum shear modulus, which is a function of void ratio, is less than 20% for all specimens when CSR of test is below 0.3.
- The range of damping ratio calculated for specimens recovered from Adapazarı is significantly lower than those predicted by empirical relationships presented in literature. The difference can be explained by the reversed-S shaped hysteresis loops observed during CDSS tests.
- The normal stress on specimen has a more pronounced effect on damping ratio for soils of low plasticity. Nonetheless, the effect diminishes when plasticity index is greater than 30.

- The relationship between G_{sec}/G_{max} and the cyclic shear-strain amplitude (i.e., modulus reduction curve) was substantially different from several empirical relationships proposed in literature. However, a reasonably good agreement is obtained in case a lower range of G_{max} is used for normalization.

- The best agreement between the test results and well-known empirical relationships on modulus reduction is obtained when the shear-wave velocity of soils sampled from Adapazarı is between 75 and 100 m/s, approximately one third of the velocity measured in-situ.

5.3 Future studies

The results of this study points out the necessity for research on the following issues:

- The conditions under which reversed-S shaped hysteresis loops are observed in cyclic loading tests should be investigated.

- A constitutive model for cyclic response of Adapazarı soils in the wide-strain range should be developed for more accurate computations of the nonlinear site response.

- Laboratory tests for completion of the modulus reduction curves of Adapazarı deposits on the small-strain range are useful for an investigation of the discrepancy between the test results presented in this study and empirical relationships proposed in literature.

- Effects of sample disturbance on dynamic soil properties on have to be investigated particularly for Adapazarı deposits in order to prevent potential under/over estimation of in-situ G_{Sec} in geotechnical site-response analyses.

- Cyclic tests with alternative apparatuses are necessary for understanding the relationship between the dynamic properties measured in lab and the type of test.

REFERENCES

[1] Anderson, J.G., Sucuoğlu, H., Erberik, A., Yılmaz, T., Inan, E., Durukal, E., Erdik, M., Anooshehpoor, R., Brune, J.N and Ni, S.D. (2000). "*Inplications for seismic hazard analysis,*" Earthquake Spectra, 16, 1, 113-137.

[2] Anderson, D. G., Phukunhaphan, A., Douglas, B.J. and Martin, G.R.. (1983) "*Cyclic behavior of six marine clays,*" Proc. Evaluation of Seafloor Soil Properties under Cyclic Loads, ASCE, 1-27.

[3] ASTM D422 - 63. (2007). "*Standard Test Method for Particle-Size Analysis of Soils,*" ASTM International, West Conshohocken, PA 2008, DOI: 10.1520/D0422-63R07.

[4] ASTM D1586 - 08a. (2008). "*Standard Test Method for Standard Penetration Test (SPT) and Split-Barrel Sampling of Soils,*" ASTM International, West Conshohocken, PA 2008, DOI: 10.1520/D1586-08.

[5] ASTM D1587-08. (2008). "*Standard Practice for Thin-Walled Tube Sampling of Soils for Geotechnical Purposes,*" ASTM International, West Conshohocken, PA, 2008, DOI: 10.1520/D1587-00R07E01.

[6] ASTM D2113-08, (2008). "*Standard Practice for Rock Core Drilling and Sampling of Rock for Site Investigation*," ASTM International, West Conshohocken, PA, 2008, DOI: 10.1520/D2113-06.

[7] ASTM D2435 – 04, (2004). "*Standard Test Methods for One-Dimensional Consolidation Properties of Soils Using Incremental Loading,*" ASTM International, West Conshohocken, PA, 2004, DOI: 10.1520/D2435-04.

[8] ASTM D2487 – 10, (2010). "*Standard Practice for Classification of Soils for Engineering Purposes (Unified Soil Classification System),*" ASTM International, West Conshohocken, PA, 2010, DOI: 10.1520/D2487-10.

[9] ASTM D3999 – 91, (2003). "*Standard Test Methods for the Determination of the Modulus and Damping Properties of Soils Using the Cyclic Triaxial Apparatus,*" ASTM International, West Conshohocken, PA, 2003, DOI: 10.1520/D3999-91R03.

[10] ASTM D4318 – 10, (2010). "*Standard Test Methods for Liquid Limit, Plastic Limit, and Plasticity Index of Soils*," ASTM International, West Conshohocken, PA, 2010, DOI: 10.1520/D4318-10.

[11] ASTM D4767 – 04, (2004). "*Standard Test Method for Consololidated Undrained Triaxial Test for Cohesive Soils*" ASTM International, West Conshohocken, PA, DOI: 10.1520/D4767-04.

[12] ASTM D6528 – 07, (2007). "*Standard Test Method for Consolidated Undrained Direct Simple Shear Testing of Cohesive Soils,*" ASTM International, West Conshohocken, PA, 2007, DOI: 10.1520/D6528-07.

[13] Baligh, M.M., Azzouz, A.S. and Chin, C.T. (1987). "*Disturbances due to 'Ideal' tube sampling,*" Journal of Geotechnical Engineering, ASCE, 113, 7, 739-757.

[14] Bakır, B.S., Sucuoğlu, H. and Yilmaz, M.T. (2002). "*An overview of local site effects and the associated building damage in Adapazarı during the 17 August 1999 İzmit earthquake,*" Bulletin of Seismological Society of America, 92, 509-526.

[15] Bakır, B.S., Yılmaz, M.T., Yakut, A. And Gülkan, P. (2005). "*Re-examination of damage distribution in Adapazarı,*" Engineering Structures, 27, 1002-1013.

[16] Baturay, M.B. and Stewart, J.P. (2003). "*Uncertainty and bias in ground-motion estimates from ground response analyses,*" Bulletin of Seismological Society of America, 93, 2025–2042.

[17] Baxter, C.D.P., Bradshaw, A.S., Ochoa-Lavergne, M., Rodrigues, I. and Hankour, R. (2002). "*Comparison of DSS results using wire-reinforced membranes and stacked rings,*" Technical report, Journal of Testing and Evaluation, 20, 10.

[18] Baxter, C.D.P., Bradshaw, A.S., Ochoa-Lavergne, M., Rodrigues, I. and Hankour, R. (2010). "*DSS results using wire-reinforced membranes and stacked rings,*" Proceedings of the GeoFlorida 2010 Conference, Advances in Analysis, Modeling, & Design.

[19] Beyen, K. and Erdik, M. (2004). "*Two-dimensional nonlinear site response analysis of Adapazarı plain and predictions inferred from aftershocks of the Kocaeli earthquake of 17 August 1999,*" Soil Dynamics and Earthquake Engineering, 24, 261-279.

[20] Boore, D.M, (2004) "*Can site response be predicted?*" Journal of Earthquake Engineering, Imperial college press, 8, 1, 1-41.

[21] Bjerrum, L. and Landva, A. (1966). "*Direct-Simple Shear Tests on a Norwegian Quick Clay,*" Geotechnique, 16, 1, 1-20.

[22] Bray, J.D., Sancio, R.B., Durgunoglu, H.T., Onalp, A., Seed, R.B., Stewart, J.P., Youd, T. L., Baturay, M.B., Cetin, K.O., Christensen, C., Karadayilar, T. and Emrem, C. (2001). "*Ground Failure in Adapazarı*", XVth International Conference on Soil Mechanics & Geotechnical Engineering, Istanbul, August 2001.

[23] Bray, J.D., Sancio, R.B., Riemer, M.F., Durgunoglu, T. (2004). "*Liquefaction susceptibility of fine-grained soils,*" In Proceedings of the 11th international conference on soil dynamics and earthquake engineering and third international conference on earthquake geotechnical engineering, Berkeley, CA, 655–62.

[24] Chen, M.H., Wu, B.R. (2000). "*The Engineering Geological Database for Strong Motion Stations in Taiwan,*" National Center for Research on Earthquake Engineering, Taipai, Taiwan.

[25] Cho, W., Holman, T.P., Jung, Y.H. and Finno, R.R. (2007). "*Effects of Swelling During Saturation in Triaxial Tests in Clays,*" Geotechnical testing Journal, ASTM, 30, 5, 10 p.

[26] Chopra, A.K. (1995). "*Dynamics of structures: theory and application to earthquake engineering,*" Prentice-Hall, Inc. USA.

[27] Chiara, N. and Stokoe II, K.H. (2006). "*Sample disturbance in resonant column test measurement of small-strain shear-wave velocity,*" Soil stress-strain behavior: Measurment, Modeling and Analyses, Geotechnical symposium in Roma.

[28] Cook, D., Malkus, D.S. and Plesha, M.E. (1989). "*Concepts and applications of Finite Element Analysis,*" 3rd Edition, Wiley & Sons, Inc.

[29] DAPHNE. (2009). "*Strong ground motion database of Turkey,*" http://daphne.deprem.gov.tr:89/2K/daphne_v4.php, last visited at: July 2010.

[30] Darendeli, M.B. (2001). "*Development of new family of normalized modulus reduction and material damping curves,*" Ph.D. thesis, University of Texas at Austin, Austin, Tex.

[31] DeGroot, D.J., Germaine, J.T. and Ladd, C.C. (1994). "*Effect of Nonuniform stress on measured DSS stress-strain behavior,*" Journal of Geotechnical engineering, 120, 5, 892-912.

[32] Devore, L.J. (2008). "*Probability and statistics for engineering and the sciences,*" 7th Edition, Cengage Learning, 720 p.

[33] Doroudian, M. and Vucetic, M. (1995). "*A direct simple shear device for measuring small-strain behavior,*" Geotechnical Testing J., ASTM. 18, 1, 69–85.

[34] Doroudian, M. and Vucetic, M. (1998). "*Small-strain testing in an NGI-type direct simple shear device,*" Proc. The 11th Danube-European Conference on soil mechanics and geotechnical engineering. Porec, Croatia, Publisher A.A. Balkema, 687-693.

[35] DSİ. (2001). "*Boring Log, Teverler Binası Adapazarı/ Sakarya,*" 21 p.

[36] Dyvik, R. and Madshus, C. (1985). "*Laboratory measurements of Gmax using bender elements,*" Advances in Art of Testing Soils under Cyclic conditions, ASCE, NY, 186-196.

[37] Dyvik, R., Berre, T., Lacasse, S. and Raadim, B. (1988). "*Comparison of Truly Undrained and Constant Volume Direct Shear Shear Tests,*" Norwegian Geotechnical Institute Publication No. 170, Oslo.

[38] EPRI, (1993). "*Guidelines for determinşng design basis ground motions, Volume 1: Method and guidelines for estimating earthquake ground motion in eastern North America,*" Electrical Power Research Institute TR-102293s-V1-V5 Technical report.

[39] FHWA, (2008). "*Geophysical Methods To Determine Physical Properties - Borehole Logging,*" Federal Highway Administration, Federal Lands Highway Program, US Department of Transportation. (Last visited: 20/05/2010), (*http://www.cflhd.gov/agm/engApplications/SubsurfaceChartacter/622BoreholeLogging.htm*).

[40] Finn, W.D.L., Bransby, P.L. and Pickering, D.J. (1971). "*Sand liquefaction in triaxial and simple shear tests,*" ASCE Journal of Soil mechanics, Found Div. 97, 4, 639–659.

[41] Gazetas, G. and Stokoe II, K.H. (1991). "Free *vibration of embedded foundations: theory versus experiment,*" Journal of Geotechnical Engineering, 117, 9, 1382-1401.

[42] GGDA, General Directorate of Disaster Affairs. (2007). "*Turkish seismic design code: Specification for structures to be built in disaster areas,*" General Directorate of Disaster Affairs, Ankara.

[43] Fähve, D., Christen, A., Greifenhagen, C. (2004). "*Tek istasyon yöntemi ile Adapazarı ve Gölcük şehirlerinde yapılan çevresel titreşim (mikrotremor) ölçümleri ve değerlendirmesi,*" Belediyeler için Sismik Mikrobölgeleme – Örnek Uygulamalar, World Institute for Disaster Risk Management.

[44] Geocomp, 2007 "*Cyclic direct simple shear user's manual: Control and report software for fully automated cyclic direct simple shear tests on ShearTrac II systems using MS-Windows 2000 or XP software version 5.0*" www.geocomp.com, Boxborough, MA- USA.

[45] Geocomp, 2007 "*Cyclic stress path user's manual: Control and report software for fully automated cyclic stress path vertical, horizontal, and combined tests on LoadTrac II/ FlowTrac II systems using MS-Windows 2000 or XP softwares*" www.geocomp.com, Boxborough, MA- USA.

[46] Geocomp, 2007 "*Cyclic triaxial user's manual: Control and report software for fully automated cyclic triaxial tests on LoadTrac II/ FlowTrac II systems using MS-Windows 2000 or XP softwares*" www.geocomp.com, Boxborough, MA-USA.

[47] Hardin, B.O. (1978). "*The nature of stress-strain behavior for soils,*" Proc. ASCE Geotech. Engrg. Div. Specialty Conf. on Earthquake Engineering and Soil Dynamics, 1, 3-90.

[48] Hardin, B. O., and Black, W. L. (1969). "*Closure to vibration modulus of normally consolidated clay,*" J. Soil Mech. and Found. Div., 95, 6, 1531–1537.

[49] Hardin, B.O. and Drnevich, V.P. (1972). "*Shear modulus and damping in soils: Design equations and curves,*" Journal of Soil Mechanics, Foundation Div., Proc. Of ASCE, Vol. 98, No. SM7, 113-119.

[50] Hashash, Y. and Park, D. (2001). "*Non-linear one-dimensional seismic ground motion propagation in the Mississippi embayment,*" Engineering Geology, 185-206.

[51] Hight, D.W., Bennell, J.D., Davis, P.D., Jardine, R.J, and Porovic, E. (1997). "*Wave velocity and stiffness measurements of the Crag and Lower London territories at Sizewell,*" Geotechnique, 47, 3, 451-474.

[52] Hight, D.W. and Georgiannou, V.N. (2005). "*Effects of sampling on the undrained behaviour of clayey sands,*" Geotechnique, 45, 2, 237-247.

[53] Hosseini, S.M.M.M, Hajimohammadi, A.A. and Hajimohammadi, A.R. (2010). "*The validity assessment of laboratory shear modulus using in-situ seismic piezocone test results,*" International Journal of Civil Engineering, 8, 2, 134-142.

[54] Hryciw, R.D., Rollins, K.M., Homolka, M., Shewbridge, S.E., McHood, M. (1991). "*Soil amplification at Treasure Island during the Loma Prieta earthquake*," Second International Conference on Recent Advances in Geotechnical Earthquake Engineering and Soil Dynamics, St Louis, MO.

[55] Idriss, I.M. (1990). "*Response of soft soil sites during earthquakes*," Proc. Symposium to Honor H. B. Seed, Berkeley, CA, 273-289.

[56] Idriss, I.M. and Seed, H.B. (1968). "*Seismic response of horizontal soil layers*," Soil Mechanics and Foundations, 94, 4, 1003-1029.

[57] Ishibashi, I. and Zhang, X. (1993). "*Unified dynamic shear moduli and damping ratios of sand and clay*," Soils Found. 33, □ 1, 182–191.

[58] Ishihara, K. (1996). "*Soil Behavior in Earthquake Geothechnics*," Oxford engineering science series; Oxford science publications, Oxford; New York.

[59] Ishibashi, I. and Sherif, M.A. (1974). "*Soil liquefaction by torsional simple shear device*," ASCE Journal of Geotech. Engineering. Div. 97, 4, 639-659.

[60] Jamiolkowsky, M., Lancellotta, R. and Lo Presti, D.C.F. (1994). "*Remarks on the stiffness at small strains of six Italian clays*," Proc. Pre-failure Deformation of Geomaterials, Balkema, 2, 817-836.

[61] Jen, L,C.M. and Wen, K.L. (2009). "*Comparison of three different methods in investigating shallow shear-wave velocity structures in Ilan, Taiwan*," Soil Dynamics and Earthquake Engineering, 29, 133–143.

[62] Kawaguchi, T. and Tanaka, H. (2008). "*Formulation of G_{max} from reconstituted clayey soils and its application to G_{max} measured in the field*," Soils and Foundations, Japanese Geotechnical Society, 48, 6, 821-831.

[63] Kjellman, W. (1951). "*Testing the Shear Strength of Clay in Sweden*," Geotechnique, 2, 225-235.

[64] Kokusho, T. (1980). "*Cyclic triaxial test of dynamic soil properties for wide strain range*," Soils Found., 20, 2, 45–60.

[65] Kokusho, T., Yoshida, Y. and Esashi, Y. (1982). "*Dynamic properties of soft clay for wide strain range,*" Soils Found., 22, 4, 1–18.

[66] Koutsoftas, D.C. and Fischer, J.A. (1980). "*Dynamic properties of two marine clays,*" J. Geotech. Engrg. Div. 106, 6, 645-657.

[67] Kramer, S.L. (1996). "*Geotechnical earthquake engineering,*" Prentice-Hall Civil Engineering and Engineering Mechanics Series, Upper Saddle River, New Jersey.

[68] Komazawa, M., Morikawa, H., Nakamura, K., Akamatsu, J., Nishimura, K., Sawada, S., Erken, A. and Onalp, A. (2002). "*Bedrock structure in Adapazarı, Turkey – a possible cause of severe damage by the 1999 Kocaeli earthquake,*" Soil Dynamics and Earthquake Engineering, 22, 829-836.

[69] Kudo, K., Kanno, T., Okada, H., Özel, O., Erdik, M., Sasatani, T., Sadanori, H., Takahashi, M., and Yoshida, K. (2002). "*Site-specific issues for strong ground motion during the Kocaeli, Turkey, earthquake of 17 August 1999, as inferred from array observations of microtremors and aftershocks,*" Bulletin of the Seismological Society of America, 92, 448-465.

[70] Kuo, C.H., Cheng, D.S., Hsieh, H.H., Chang, T.M., Chiang, H.J., LIN, C.M., and WEN, K.L. (2009). "*Comparison of three different methods in investigating shallow shear-wave velocity structures in Ilan, Taiwan,*" Soil dynamics and earthquake engineering, 29, 1, 133-143.

[71] Kurtulus, A. and Stokoe II, K.H. (2008). "*In situ measurement of nonlinear shear modulus of silty soil,*" Journal of Geotechnical and Geoenvironmental Engineering, 134, 10, 1530-1541.

[72] Lambe, T.W. and Whitman, R.V. (1969). "*Soil mechanics, Series in soil engineering,*" John Wiley and Sons, New York, 553 p.

[73] Landon, M.M., DeGroot, D.J. and Sheahan, T.C. (2007). "*Nondestructive sample quality assessment of a soft clay using shear wave velocity,*" Journal of Geotechnical and Geoenvironmental Engineering, ASCE, 133, 4, 424-432.

[74] Lanzo, G. and Vucetic, M. (1999). "*Effect of soil plasticity on damping ratio at small cyclic strains*," Soils and Foundations, 39, 4, 131–141.

[75] Lin, S.Y., Lin, P.S., Luo, H.S. and Juang, C.H. (2000). "*Shear modulus and damping ratio characteristics of gravelly deposits*," Can. Geotech. J. 37, 3, 638–651.

[76] Long, M. and Menkiti, C.O. (2007). "*Geotechnical properties of Dublin Boulder clay,*" Geotechnique, 57, 7, 597-611.

[77] Long, M., El-Hadj, M. and Hagberg, K. (2010). "*Closure to: Quality of Conventional Fixed Piston Samples of Norwegian Soft Clay,*" Journal of Geotechnical and Geoenvironmental Engineering, 135, 2, 185–198.

[78] Lowe, J. and Zaccheo, P.F. (1975). "*Subsurface explorations and sampling: in Winterkorn, H.F., and Fang, H.Y., (eds.), Foundation engineering handbook,*" Van Nostrand Reinhold Company, (New York, New York), 751 p.

[79] Lunne, T., Berre, T., Anderson, K.H., Strandvik, S. and Sjursen, M. (2006). "*Effects of sample disturbance and consolidation procedures on measured shear strength of soft marine Norwegian clays,*" Canadian Geotechnical Journal, 43, 726-750.

[80] Mayoral J.M., Romo M.P. and Osorio, L. (2008). "*Seismic parameters characterization at Texcoco lake, Mexico,*" Soil Dynamics and Earthquake Engineering, 28, 507–521.

[81] NEHRP. (2003). "*NEHRP Recommended Provisions for Seismic Regulations for New Buildings and Other Structures, Part 1: Provisions and Part 2: Commentary (FEMA 450),*" Building Seismic Safety Council, Washington, D.C., 1, 20, 353 p.

[82] Ng C.W., Pun, W.K. and Pang, R.P.L. (2000). "*Small Strain Stiffness of Natural Granitic Saprolite in Hong Kong,*" J. Of Geotechnical & Geoenvironmental Engng. ASCE, 126, 9, 819-833.

[83] Peacock, W.H. and Seed, H.B. (1968). "*Sand liquefaction under cyclic loading simple shear condition,*" ASCE Journal of Soil mechanics. Found Div. 94, 3, 689-703.

[84] Pecker, A. (2007). "*Determination of Soil Characteristics."* Book chapter of "Advanced Earthquake Engineering Analysis," Volum 494. CISM International Centre for Mechanical Sciences, Springer Vienna.

[85] Pekcan, O. (2001). "*Cyclic behavior of Adapazarı clayey silts,*" M.S. thesis, Middle East Technical University, Ankara, Turkey.

[86] Puzrin, A., Frydman, S. and Talsenick, M. (1995). "*Normalized nondegrading behavior of soft clay under cyclic simple shear loading,*" ASCE Journal of Geotechnical engineering. 121, 12, 836-843.

[87] Prasada, K.N., Trivenia, S., Schanzb, T. and Nagaraj, L.T.S. (2007). "*Sample Disturbance in Soft and Sensitive Clays: Analysis and Assessment,*" Marine Georesources and Geotechnology, 25, 181–197.

[88] Özel, O. and Sasatani, T. (2004). "*A site effect study of the Adapazarı basin, Turkey, from strong- and weak-motion data,*" Journal of Seismology, 8, 559-572.

[89] Park, D. and Hashash, Y.M.A. (2004). "*Soil damping formulation in nonlinear time domain site response analysis,*" Journal of Earthquake Engineering, 8, 2, 249-274.

[90] Raymond, G.P., Townsend, D.L. and Lojkasek, M.J. (1971). "*The effect of sampling on the undrained soil properties of Leda soil,*" Canadian Geotechnical Journal, 8, 546.

[91] Rathje, E.M., Rosenblad, B.L., Stokoe, K.H. and Darendeli, M. (2002). "*Shear Wave Velocity Profiling by SASW Method at Selected Strong-Motion Stations from the 1999 Turkey Earthquakes,*" Proceedings, NSF-Tubitak Workshop on Turkey and Taiwan Earthquake Research, Antalya, Turkey.

[92] Richart, F.E., Hall, J.R. and Woods, R.D. (1970). "*Vibrations of soils and foundations,*" Prentice Hall, Englewoods Cliff, N.J.

[93] Roca, A., Ansal, A. and Figueras, S. (2006) "*Local site effect and microzonation,*" Chapter 4, Assessing and managing earthquake risk: geo-scientific and engineering knowledge for earthquake risk mitigation: developments, tools, techniques, Edited by: Oliviera, C.S., Roca, A. and Goula, X. Springer, Netherland.

[94] Roesset, J.M. (1977). "*Soil amplification of earthquakes*," Numerical Methods in Geotechnical Engineering, C. S. Desai and J. T. Christian (ed.), McGraw-Hill, New York, 649-682.

[95] Roscoe, K.H. (1953). "*An apparatus for the application of simple shear to soil samples*," Proc., 3rd Int. Conf. on soil mechanics and foundation engineering. Zurich, Switz. Sess, 2, 186-191.

[96] Rosenblad, B.L., Rathje, E.M. and Stokoe, K.H. (2001). "*Shear Wave Velocity Profiling by SASW Method at Selected Strong-Motion Stations from the 1999 Turkey Earthquakes*," Final Report to Pacific Earthquake Engineering Research Center.

[97] Sancio, R.B., Bray, J.D., Stewart, J.P., Youd, T.L., Durgunoğlu, H.T., Önalp, A., Seed, R.B., Christensen, C., Baturay, B. and Karadayılar, T. (2002). "*Correlation between ground failure and soil conditions in Adapazari, Turkey*," Soil Dynamics and Earthquake Engineering, 22, 1093-1102.

[98] Sancio, R.B., Bray, J.D., Durgunoğlu, H.T. (2003). "*An assessment of the liquefaction susceptibility of Adapazari silt*," Pacific Conference on Earthquake Engineering, paper no. 172.

[99] Sanin, M.V. and Wijewickreme, D. (2005). "*Cyclic shear response of channel-fill Fraser River Delta silt*," Soil Dynamics and Earthquake Engineering, 26, 854-869.

[100] Santagata, M.C. and Gremaine, J.T. (2002). "*Sampling disturbance effects in normally consolidated clays*," Journal of Geotechnical and Geoenvironmental Engineering, ASCE, 128, 12, 997-1006.

[101] Schnabel, P.B., Lysmer, J. and Seed, H.B. (1972). "*SHAKE: A computer program for earthquake response analysis of horizontally layered sites*," Report EERC 72-12, Earthquake Engineering Research Center, University of California, Berkeley, CA.

[102] Seed, H.B. and Idriss, I.M. (1970). "*Soil moduli and damping factors for dynamic response analyses*," Report EERC 70-10, Earthquake Engineering Research Center, University of California, Berkeley.

[103] Seed, H.B. and Peacock, W.H. (1971). "*Test procedure for measuring soil liquefaction characteristics,*" ASCE Journal of Soil mechanics Found Div. 94, 3, 109-119.

[104] Seed, H.B., Wong, R.T., Idriss, I.M. and Tokimatsu, K. (1986). "*Moduli and damping factors for dynamic analyses of cohesionless soils,*" Journal of Geotechnical Engineering, 112, 11, 1016-1032.

[105] Shibata, T. and Soelarno, D.S. (1978). "*Stress-strain characteristics of clays under cyclic loading,*" Journal of Japanese society of civil engineering, 276, 101-110.

[106] Shibuya, S. and Tanaka, H. (1996). "*Estimate of elastic shear modulus in Holocene soil deposits,*" Soils and Foundations, 36, 4, 45-55.

[107] Silva, W., Darragh, R. and Gregor, N. (1998). "*Reassessment of site coefficients and near-fault factors for building code provisions, Element II,*" Pacific engineering and analyses, NEHRP Report No. 98-HQ-GR-1010, El Cerrito, CA.

[108] Silver, M.L. (1977). "*Laboratory triaxial testing procedures to determine the cyclic strength of soils,*" Report No. NUREG-31, U.S. Nuclear Regulatory Commission, Washington DC.

[109] Song, B.W., Yasuhara, K. and Murakami, S. (2004). "*Direct simple shear testing for post cyclic degradation in stiffness of non-plastic silt,*" Geotechnical Testing Journal, 27, 6, 1-7.

[110] Tan, T.S., Lee, F.H., Chong, P.T. and Tanaka, H. (2002). "*Effect of sampling disturbance on properties of Singapore clay,*" Journal of Geotechnical and Geoenvironmental Engineering, ASCE, 128, 11, 898–906.

[111] Tanaka, K., Ogura, K., and Miura, H. (1985). "*Application of Suspension P-S Logging System to high velocity ground,*" 4th ASEG Conference.

[112] Taylor, D.W. (1948). "*Fundamentals of soil mechanics,*" John Wiley and Sons, Inc., New York, 700 p.

[113] Taylor, D.W. (1952). "*A Direct Shear Test with Drainage Control,*" Symposium on Direct Shear Testing of Soils, ASTM STP No. 131, 63-74.

[114] TS 1900-2, (2006). "*İnşaat Mühendisliğinde Zemin Laboratuvar Deneyleri – Bölüm 2: Mekanik Özelliklerin Tayini (Eurocode 7),*" ICS 93.020, Türk Standardları Enstitüsü, Ankara, 63 p.

[115] TS ENV 1997-3, (2004). "*Jeoteknik Tasarım – Bölüm 3: Arazi Deneyleri Yardımıyla Tasarım (Eurocode 7),*" ICS 91.080.01; 93.020, Türk Standardları Enstitüsü, Ankara, 117 p.

[116] TS ENV 1997-2, (2004). "*Jeoteknik Tasarım – Bölüm 2: Laboratuvar Testine Dayanıklı Tasarım (Eurocode 7),*" ICS 91.010.30; 93.020, Türk Standardları Enstitüsü, Ankara.

[117] TUBITAK -The Scientific and Technological Research Council of Turkey (2010). "*Development of Performance Based Design and Evaluation Methhods by Comparison with Observed Earthquake Performance of the Structures in Turkey*," TUBITAK Project No. 108M303, 3rd Progress Report to be delivered to TUBITAK.

[118] USACE, U.S. Army Corps of Engineers. (1996). "*Engineering and Design - Soil Sampling, Manual No EM 1110-1-1906*," Department of Army, U.S. Army Corps of Engineers, Washington DC.

[119] Vucetic, M. (1984). "*An evaluation of laboratory testing techniques in soil mechanics*," Soils and Foundations, 24, 2, 112-117.

[120] Vucetic, M. and Dobry, R. (1991). "*Effect of soil plasticity on cyclic response,*" Journal of Geotechnical Engineering, ASCE, 117, 1, 89-107.

[121] Vucetic, M., Lanzo, G. and Doroudian, M. (1998). "*Damping at small strains in cyclic simple shear test,*" J. Of Geotechnical and Geoenvironmental Enginering, ASCE, 124, 7, 585-594.

[122] Winterkorn, H.F. and Fang, F.Y. (1975). "*Foundation Engineering Handbook,*" Van Nostrand Reinhold Company.

[123] Wang G.X. and Kuwano, J. (1999). "*Modeling of strain dependency of shear modulus and damping of clayey sand,*" Soil Dynamics and Earthquake Engineering, 18, 6, 463-471.

[124] Williams, R.A., Stephenson, W. J., Frankel, A.D., Cranswick, E., Meremonte, M.E. and Odum, J.K. (2000). "*Correlation of 1- to 10-Hz earthquake resonances with surface measurements of S-wave reflections and refractions in the upper 50 m,*" Bulletin of Seismological Society of America, 90, 1323–1331.

[125] Yakut, A., Gülkan, P., Bakır, B.S. and Yılmaz, M.T. (2005). "*Re-examination of damage distribution in Adapazarı: Structural consideration,*" Engineering Structures, 27, 7, 990-1001.

[126] Yamada, S., Hyodo, M., Orense, R.P., Dinesh, S.V. and Hyodo, T. (2008) "*Strain-dependent dynamic properties of remolded sand-clay mixtures,*" Journal of Geotechnical and Geoenvironmental Engineerıng, ASCE, 134, 7, 972–981.

[127] Yasahura, K., Murakami, S., Song, B.W., Yokokawa, S. And Hyde, A.F.L. (2003) "*Postcyclic degradation of strength and stiffness for low plasticity silt,*" Journal of Geotechnical and Geoenvironmental Engineerıng, ASCE, 129, 8, 756–769.

[128] Yılmaz, M.T., Pekcan, O. and Bakır, B.S. (2004) "*Undrained cyclic shear and deformation behavior of silt–clay mixtures of Adapazarı, Turkey,*" Soil Dynamics and Earthquake Engineering, 24, 497–507.

[129] Zen, K., Yamazaki, H. and Umehara, Y. (1987). "*Experimental study on shear modulus and damping ratio of natural deposits for seismic response analyses,*" Report of the Port and Harbour Research Institute, 26, 1, 41-113.

APPENDIX A

BORELOG

Project Name: Development of performance based design and evaluation methods by comparison with observed earthquake performance of the structures in Turkey, 108M303 TUBITAK.
Location: Site 1 - Papuccular Mah. Yeni Cami District, Adapazari
Date: October 30, 2009 to November 21, 2009
Field Log by: Kavah H. Zehtab
Operator: Geoteknik
Drilling Method: Rotary wash and Core Boring
Water Table Elevation: GWT = 6 m checked everyday

Test ID: BH#01
GPS Coordinates:
Elevation:
Drilling Equipment: Custom made
Responsible Engineers: M. T. Yilmaz and K. H. Zehtab
SPT System: Rope, pulley and cathead method. AWJ rods.
Hammer Type: Donut Hammer
Undisturbed Sampler Type: Shelby Tube
Disturbed Sampler Type: Core Tube; SPT

Depth Scale (m)	Lithology	USCS	Sample Type and No.	Recovery (cm) y Length (cm)	SPT Blows/15 cm	Casing Depth (m)	Rod Length (m)	Description	Moisture Content (%)	Liquid Limit	Plastic Limit	Plasticity Index	Gs	% fines <75	< 2 mm (%)	D50 (mm)	D10 (mm)	Remarks
0																		Saturday 2009.10.31
1	Top soils							Top soils										
2	Silty Sand	SM	UD-01	50/50		1.5		loose to medium dense Sands	31			NP	2.66	33	11	100	100	
3			SPT-01	45/45	4-5-7		4		35			NP	2.64	72	13	100	100	
4	Sandy Silt	ML	UD-02	50/50		1.5			35			NP	2.63	65	8	100	100	
			SPT-02	0/45	10-11-12	1.5	5											
5	Silty Sand	SM	UD-03 SPT-03	0/50 40/45	16-36-50/12cm	3	5.5	Very dense sands	16			NP	2.68	9	4	100	100	Sunday 2009.11.01 50 lbs wouldn't push tube in, sample was taken by hand
6			SPT-04	45/45	12-22-28	3	7.5	Dense Sands	24			NP	2.64	3	0	100	100	**Ground water table**
7	Sand	SW																
8			SPT-05	0/45	8-12-8	3	8.5											Monday 2009.11.02 Sample was taken by hand
9	Clay	CH	UD-04	47/50		4.5		Hard Silts and Clays	45	68	25	43	2.63	100		100	100	
10	Silt	ML	SPT-06	45/45	12-33-28		11		28			NP	2.65	70	14	100	100	
	Clay	CH	UD-05	50/50		4.5			52	60	25	35	2.66	94		100	100	
11	Silt	ML	SPT-07	35/45	33-50/14cm		13		27			NP	2.67	53	10	100	100	
12	Sandy silt	ML	UD-06	20/50		4.5			34			NP	2.61	76	20	100	100	
13	Silt	ML	SPT-08	45/45	4-8-21	6	14		31			NP	2.65	56	14	100	100	
	Fat Clay	CH	UD-07	50/50		6			55	86	31	55		99	65	100	100	
14	Clayey Silt	ML	SPT-09	45/45	15-16-21		15		31			NP		68	23	100	100	
15	Silty Clay	CL							38	29	17	12	2.61	52	18	100	100	Tuesday 2009.11.03
			UD-08	50/50		6			38	46	17	29	2.58	82	30	100	100	
16	Clay	CH	SPT-10	45/45	13-14-15		17		40	66	22	44	2.64	99	68	100	100	
			UD-09	50/50		6			45	56	24	32	2.56	77	30	100	100	
17	Silty Clay	CL	SPT-11	45/45	24-18-25		18		37	30	23	7	2.64					

Figure A.1 Borelog of TUBITAK (2010).

Project Name: Development of performance based design and evaluation methods by comparison with observed earthquake performance of the structures in Turkey, 108M303 TUBITAK.
Location: Site 1 - Papuccular Mah. Yeni Cami District, Adapazari
Date: October 30, 2009 to November 21, 2009
Field Log by: Kavah H. Zehtab
Operator: Geoteknik
Drilling Method: Rotary wash and Core Boring
Water Table Elevation: GWT = 6 m checked everyday

Test ID: BH#01
GPS Coordinates:
Elevation:
Drilling Equipment: Custom made
Responsible Engineers: M. T. Yilmaz and K. H. Zehtab
SPT System: Rope, pulley and cathead method. AWJ rods.
Hammer Type: Donut Hammer
Undisturbed Sampler Type: Shelby Tube
Disturbed Sampler Type: Core Tube; SPT

Depth Scale (m)	Lithology	USCS	Sample Type and No.	Recovery (cm) / Length (cm)	SPT Blows/ 15 cm	Casing Depth (m)	Rod Length (m)	Description	Moisture Content (%)	Liquid Limit	Plastic Limit	Plasticity Index	Gs	% fines <75	< 2 mm (%)	D50 (mm)	D10 (mm)	Remarks
18	Clayey Silt	ML	UD-10	50/50		6			35	43	26	17	2.60	100	36	100	100	
19			SPT-12	45/45	9-9-12		20		38	44	23	20	2.64					
			UD-11	50/50		6			39	40	27	13	2.61	100	23	100	100	
20	Silt	ML	SPT-13	45/45	18-26-31		21		36	43	20	24	2.60	97	28	100	100	
21			UD-12	40/50		6			37	42	28	13	2.61	99	24	100	100	
22			SPT-14	45/45	14-14-16		22.5		40	50	22	28	2.59	98	28	100	100	
			UD-13	50/50		6			36	56	20	36	2.57	98	48	100	100	
23			SPT-15	45/45	13-16-22		24		33	64	24	40	2.63					
24	Clay	CH																
			UD-14	35/50		6			34	71	28	43	2.57	99	62	100	100	
25			SPT-16	45/45	9-11-15		25.5	Very stiff Clays	39	70	27	43	2.62					
			UD-15	50/50		6			35	60	23	37	2.58	100	47	100	100	
26			SPT-17	45/45	19-28-39		27	Hard Silts	35 28	33	28	5 NP	2.64 2.59	95 76	17 16	100 100	100 100	Wednesday 2009.11.04
27	Silt	ML																
			UD-16	29/50		6			37			NP	2.59	80	13	100	100	
28			SPT-18	45/45	21-23-22		29		34			NP	2.65					
	Silty Clay	CL	UD-17	30/50		6			31	44	27	18	2.56	93	24	100	100	
29	Silt	ML	SPT-19	45/45	21-35-26		30		27			NP	2.63	79	14	100	100	
30	Sandy Silt	ML																
			UD-18	15/50		6			35			NP	2.65	76	12	100	100	
			SPT-20	45/45	13-14-17		31.5		37	31	28	3		90		100	100	
31	Silt	ML																
32			SPT-21	45/45	25-19-19	6	33		32	29	24	5		65		100	100	
33	Clay	CH	UD-19	36/50		6			41	73	32	41	2.49	99		100	100	
34																		
35	Silt	ML	UD-20 SPT-22	0/50	18-36-50/13cm	6	36		25			NP	2.69	65	8	100	100	

Figure A.1 Continued.

Project Name: Development of performance based design and evaluation methods by comparison with observed earthquake performance of the structures in Turkey, 108M303 TUBITAK.
Location: Site 1 - Papuccular Mah. Yeni Cami District, Adapazari
Date: October 30, 2009 to November 21, 2009
Field Log by: Kaveh H. Zehtab
Operator: Geoteknik
Drilling Method: Rotary wash and Core Boring
Water Table Elevation: GWT = 6 m checked everyday

Test ID: BH#01
GPS Coordinates:
Elevation:
Drilling Equipment: Custom made
Responsible Engineers: M. T. Yilmaz and K. H. Zehtab
SPT System: Rope, pulley and cathead method. AWJ rods.
Hammer Type: Donut Hammer
Undisturbed Sampler Type: Shelby Tube
Disturbed Sampler Type: Core Tube; SPT

Depth Scale (m)	Lithology	USCS	Sample Type and No.	Recovery (cm) / Length (cm)	SPT Blows/15 cm	Casing Depth (m)	Rod Length (m)	Description	Moisture Content (%)	Liquid Limit	Plastic Limit	Plasticity Index	Gs	% fines <75	< 2 mm (%)	D50 (mm)	D10 (mm)	Remarks
36	Silty Clay	CL	SPT-23	45/45	13-14-13	6	37	Very stiff Clays	37	47	21	25	2.59	94	39	100	100	Thursday 2009.11.05
37																		
38			UD-21	0/50		6												Sample was taken by hand
			C-01	25/30					44	59	24	35	2.60	100	52	100	100	
39	Clay	CH	UD-22	0/50		6												
40			C-02	30/30		6			38	60	25	35	2.62	99	38	100	100	
41	Silty Clay	CL																
			C-03	30/30		6			37	39	18	21	2.62	92	36	100	100	
42			SPT-24	12/45	50/12cm		43	Hard Silts	35			NP	2.65	89		100	100	Friday 2009.11.06
43	Silt	ML																
44																		
45																		
46	Clay	CH																
47			C-04	30/30		6			40	73	28	44	2.59	99	62	100	100	
48			SPT-25	45/45	11-15-18	6	49		44	65	21	25		88		100	100	
49	Elastic Silt	ML																
50																		
51																		
52	Silty Clay	CL																
53			C-05	45/45		6			38	39	23	16	2.64	96	23	100	100	

Figure A.1 Continued.

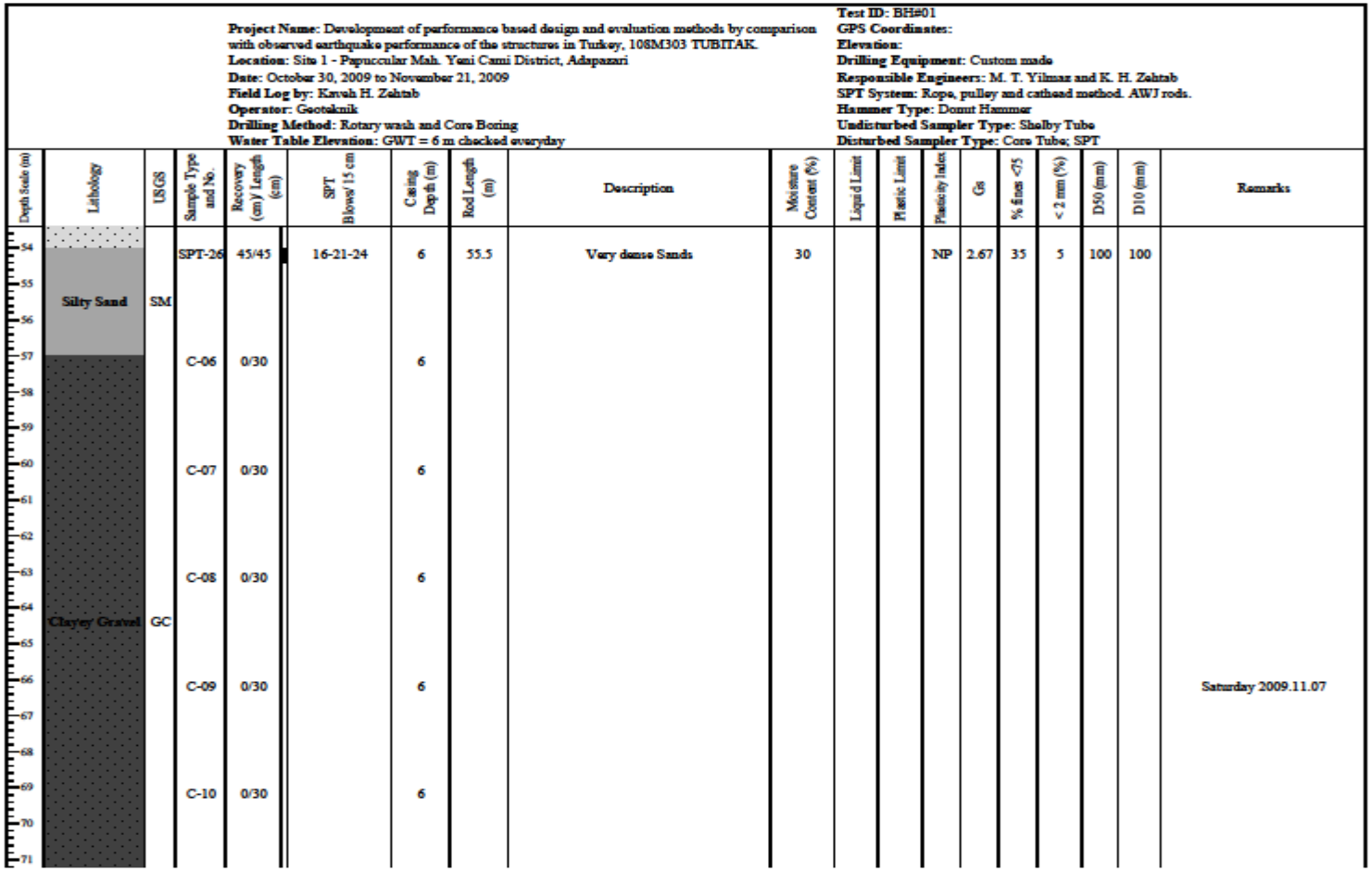

Project Name: Development of performance based design and evaluation methods by comparison with observed earthquake performance of the structures in Turkey, 108M303 TUBITAK.
Location: Site 1 - Papuccular Mah. Yeni Cami District, Adapazari
Date: October 30, 2009 to November 21, 2009
Field Log by: Kavah H. Zehtab
Operator: Geoteknik
Drilling Method: Rotary wash and Core Boring
Water Table Elevation: GWT = 6 m checked everyday

Test ID: BH#01
GPS Coordinates:
Elevation:
Drilling Equipment: Custom made
Responsible Engineers: M. T. Yilmaz and K. H. Zehtab
SPT System: Rope, pulley and cathead method. AWJ rods.
Hammer Type: Donut Hammer
Undisturbed Sampler Type: Shelby Tube
Disturbed Sampler Type: Core Tube; SPT

Depth Scale (m)	Lithology	USCS	Sample Type and No.	Recovery (cm) / Length (cm)	SPT Blows/ 15 cm	Casing Depth (m)	Rod Length (m)	Description	Moisture Content (%)	Liquid Limit	Plastic Limit	Plasticity Index	Gs	% fines <75	< 2 mm (%)	D50 (mm)	D10 (mm)	Remarks
54			SPT-26	45/45	16-21-24	6	55.5	Very dense Sands	30			NP	2.67	35	5	100	100	
55	Silty Sand	SM																
56																		
57			C-06	0/30		6												
58																		
59																		
60			C-07	0/30		6												
61																		
62																		
63			C-08	0/30		6												
64	Clayey Gravel	GC																
65																		
66			C-09	0/30		6												Saturday 2009.11.07
67																		
68																		
69			C-10	0/30		6												
70																		
71																		

Figure A.1 Continued.

Project Name: Development of performance based design and evaluation methods by comparison with observed earthquake performance of the structures in Turkey, 108M303 TUBITAK.
Location: Site 1 - Papuccular Mah. Yeni Cami District, Adapazari
Date: October 30, 2009 to November 21, 2009
Field Log by: Kavah H. Zehtab
Operator: Geoteknik
Drilling Method: Rotary wash and Core Boring
Water Table Elevation: GWT = 6 m checked everyday

Test ID: BH#01
GPS Coordinates:
Elevation:
Drilling Equipment: Custom made
Responsible Engineers: M. T. Yilmaz and K. H. Zehtab
SPT System: Rope, pulley and cathead method. AWJ rods.
Hammer Type: Donut Hammer
Undisturbed Sampler Type: Shelby Tube
Disturbed Sampler Type: Core Tube; SPT

Depth Scale (m)	Lithology	USCS	Sample Type and No.	Recovery (cm) y Length (cm)	SPT Blows/15 cm	Casing Depth (m)	Rod Length (m)	Description	Moisture Content (%)	Liquid Limit	Plastic Limit	Plasticity Index	Gs	% fines <75	< 2 mm (%)	D50 (mm)	D10 (mm)	Remarks
72	Clay																	
73		CH	C-11	30/30		9			39	59	26	33	2.61	97	47	100	100	
74			C-12	30/30		9			41	55	21	34	2.61	94		100	100	
75	Organic Clay	OL	SPT-27	45/45	24-24-33	9	76	Hard Clays	44					98		100	100	Organic
76																		
77																		
78			C-13	0/30		9												Sample was taken by hand
79																		
80																		
81			C-14	0/30		9												
82	Clayey Gravel	GC																
83																		
84																		
85																		
86			C-15	0/30		9												Sunday 2009.11.08
87																		
88																		
89			C-16	0/30		9												Wednesday 2009.11.11

Figure A.1 Continued.

Project Name: Development of performance based design and evaluation methods by comparison with observed earthquake performance of the structures in Turkey, 108M303 TUBITAK.
Location: Site 1 - Papuccular Mah. Yeni Cami District, Adapazari
Date: October 30, 2009 to November 21, 2009
Field Log by: Kavah H. Zehtab
Operator: Geoteknik
Drilling Method: Rotary wash and Core Boring
Water Table Elevation: GWT = 6 m checked everyday

Test ID: BH#01
GPS Coordinates:
Elevation:
Drilling Equipment: Custom made
Responsible Engineers: M. T. Yilmaz and K. H. Zehtab
SPT System: Rope, pulley and cathead method. AWJ rods.
Hammer Type: Donut Hammer
Undisturbed Sampler Type: Shelby Tube
Disturbed Sampler Type: Core Tube; SPT

Depth Scale (m)	Lithology	USCS	Sample Type and No.	Recovery (cm) Length (cm)	SPT Blows/15 cm	Casing Depth (m)	Rod Length (m)	Description	Moisture Content (%)	Liquid Limit	Plastic Limit	Plasticity Index	Gs	% fines <75	< 2 mm (%)	D50 (mm)	D10 (mm)	Remarks
90																		
91																		
92			C-17	0/30		9												
93																		
94																		
95			C-18	0/30		9												
96																		
97																		
98			C-19	0/30		9												
99																		
100																		
101			C-20	0/30		9												
102																		
103	Gravel	GW																
104			C-21	0/30		9												
105																		
106																		

Figure A.1 Continued.

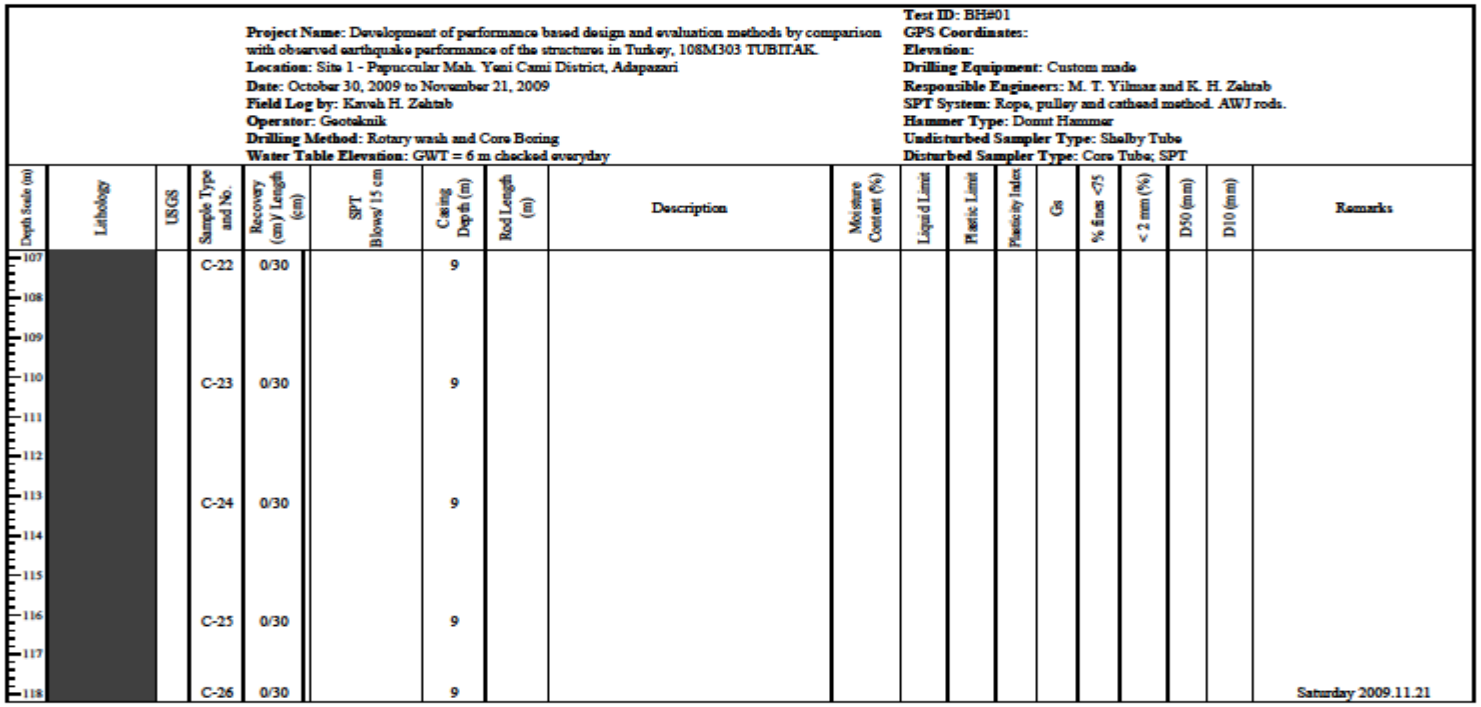

Project Name: Development of performance based design and evaluation methods by comparison with observed earthquake performance of the structures in Turkey, 108M303 TUBITAK.
Location: Site 1 - Papuccular Mah. Yeni Cami District, Adapazari
Date: October 30, 2009 to November 21, 2009
Field Log by: Kavvah H. Zehtab
Operator: Geoteknik
Drilling Method: Rotary wash and Core Boring
Water Table Elevation: GWT = 6 m checked everyday

Test ID: BH#01
GPS Coordinates:
Elevation:
Drilling Equipment: Custom made
Responsible Engineers: M. T. Yilmaz and K. H. Zehtab
SPT System: Rope, pulley and cathead method. AWJ rods.
Hammer Type: Donut Hammer
Undisturbed Sampler Type: Shelby Tube
Disturbed Sampler Type: Core Tube; SPT

Depth Scale (m)	Lithology	USCS	Sample Type and No.	Recovery (cm)/ Length (cm)	SPT Blows/ 15 cm	Casing Depth (m)	Rod Length (m)	Description	Moisture Content (%)	Liquid Limit	Plastic Limit	Plasticity Index	Gs	% finer <75	< 2 mm (%)	D50 (mm)	D10 (mm)	Remarks
107			C-22	0/30		9												
108																		
109																		
110			C-23	0/30		9												
111																		
112																		
113			C-24	0/30		9												
114																		
115																		
116			C-25	0/30		9												
117																		
118			C-26	0/30		9												Saturday 2009.11.21

Figure A.1 Continued.